Spectrum Sharing Systems for Improving Spectral Efficiency in Cognitive Cellular Network

Deepak G.C.

School of Computing and Communications

Lancaster University

A thesis submitted in partial fulfillment for the degree of

Doctor of Philosophy

September 2016

Declaration of Authorship

I, **Deepak G.C.**, declare that this thesis titled "**Spectrum Sharing Systems for Improving Spectral Efficiency in Cognitive Cellular Network**" and the work presented in it are my own. I therefore confirm that:

- Where I have consulted the published work of others, thesis always clearly attributed.
- Where I have quoted from the work of others, the source is always given. With the exceptions of such quotations, this thesis is entirely my own work.
- I have acknowledged all main source of help while preparing this Thesis.
- Where the thesis is based on work done by myself jointly with others, I have made clear what was done by others and what I have contributed myself.
- Detailed breakdown of the publications is presented in the first Chapter of this Thesis.

Signed:

_____

Date:

_____

Acknowledgements

First of all, I would like to show my sincere gratitude to my academic supervisor **Dr. Keivan Navaie** for his care, support and excellent supervision throughout the duration of my PhD. His guidance and immense inspiration have greatly encouraged me in the last four years of my PhD. I wish to express my appreciation to **Prof. Qiang Ni** for his continuous support and engaging in my research works. In addition, the continuous help from the staff at Lancaster University and Infolab21, especially the head of the school **Prof. Jon Whittle** and postgraduate coordinator **Debbie Stubs**, are also highly appreciated. Moreover, I felt so special with everyone in our generous and vibrant Communications System research group at the Lancaster University.

This modest work would not have been possible without the support that I have always been receiving from my family. More precisely, I would like to thank my better half, **Mrs. Mamata Koirala**, whom I have always considered as my infinite source of inspiration in all the battles and endeavours of my life. Her help, care and support in every moment have a special place in my life. I would also like to dedicate this work to my son, **Mr. Bivaan G.C.**, whose presence always motivated me to pursue my aim. I would also like to thank my mother Radha G.C., Mina G.C., father Dhan Bahadur G.C., my brother and sisters, my parents-in-law, who were always behind me with a huge support.

A big thank you to all the British and non-British friends whom I met during my stay at Lancaster, who made my stay here as if I were at my home. At last but not the least, special thanks to European Union Marie Curie grant and my academic supervisor who provided the research funding to become true this personal goal that I have been dreaming for half of my life.

Abstract

Since spectrum is the invisible infrastructure that powers the wireless communication, the demand has been exceptionally increasing in recent years after the implementation of 4G and immense data requirements of 5G due to the applications, such as Internet-of-Things (IoT). Therefore, the effective optimization of the use of spectrum is immediately needed than ever before.

The spectrum sensing is the prerequisite for optimal resource allocation in cognitive radio networks (CRN). Therefore, the spectrum sensing in wireless system with lower latency requirements is proposed first. In such systems with high spatial density of the base stations and users/objects, spectrum sharing enables spectrum reuse across very small regions. The proposed method in this Thesis is a multi-channel cooperative spectrum sensing technique, in which an independent network of sensors, namely, spectrum monitoring network, detects the spectrum availability. The locally aggregated decision in each zone associated with the zone aggregator (ZA) location is then passed to a decision fusion centre (DFC). The secondary base station (SBS) accordingly allocates the available channels to secondary users to maximize the spectral efficiency. The function of the DFC is formulated as an optimization problem with the objective of maximizing the spectral efficiency. The optimal detection threshold is obtained for different cases with various spatial densities of ZAs and SBSs. It is further shown that the proposed method reduces the spectrum sensing latency and results in a higher spectrum efficiency.

Furthermore, a novel power allocation scheme for multicell CRN is proposed where the subchannel power allocation is performed by incorporating network-wide primary system communication activity. A

collaborative subchannel monitoring scheme is proposed to evaluate the aggregated subchannel activity index (ASAI) to indicate the activity levels of primary users. Two utility functions are then defined to characterize the spectral efficiency (SE) and energy efficiency (EE) as a function of ASAI to formulate a utility maximization problem. The optimal transmit power allocation is then obtained with the objective of maximizing the total utility at the SBS, subject to maximum SBS transmit power and collision probability constraint at the primary receivers. Since optimal EE and SE are two contradicting objectives to obtain the transmit power allocation, the design approach to handle both EE and SE as a function of common network parameter, i.e., ASAI, is provided which ultimately proves the quantitative insights on efficient system design. Extensive simulation results confirm the analytical results and indicate a significant improvement in sensing latency and accuracy and a significant gain against the benchmark models on the rate performance, despite the proposed methods perform with lower signalling overhead.

List of Abbreviations

3GPP	third generation partnership project
ASAI	aggregated subchannel activity index
AWGN	additive white Gaussian noise
BPSK	binary phase shift keying
CCT	Charnes-Cooper Transformation
CDF	cumulative distribution function
CoMP	coordinate multipoint
CRN	cognitive radio network
D2D	device to device
dB	decibels
DFC	decision fusion centre
DSA	dynamic spectrum access
ED	energy detection
EE	energy efficiency
EPA	Equal Power Allocation
FFT	fast Fourier transform
GD	Geolocation database
GSM	global system of mobile
IoT	internet of things
KKT	KarushKuhnTucker
LoS	line of sight
LTE-A	long term evolution - advance
M2M	machine to machine
MAC	medium access control
MIMO	multiple input multiple output

MTC	machine type communication
NOMA	non-orthogonal multiple access
OFDMA	orthogonal frequency division multiple access
OSA	opportunistic spectrum access
PDF	probability density function
PBS	primary base station
PCU	Perfect Channel Utilization
PU	primary users
QoS	quality of service
QPSK	quadrature phase shift keying
REM	radio environment mapping
ROC	receiver operating characteristics
SAI	subchannel activity index
SBS	secondary base station
SDR	software defined radio
SE	spectral efficiency
SNIR	signal to noise and interference ratio
SON	self organizing network
SU	secondary users
TDMA	time division multiple access
TDD	time division duplexing
UHF	ulta high frequency
UMTS	Universal Mobile Telecommunications System
VHF	very high frequency
WRAN	wireless regional area networks
WSDB	white space database
ZA	zone aggregator

Contents

List of Tables

List of Figures

Chapter 1

Introduction

We have experienced a substantial wireless data traffic growth in the last decade due to the rapidly growing number of mobile users and data hungry applications, e.g., video streaming, and voice over internet protocol (VoIP). It is expected that the wireless data traffic will increase exponentially until next decade due to the emerging applications of internet of things (IoT) [1], machine-to-machine (M2M) communications [2] in addition to the traditional use of cellular communication for voice and data traffic.

The IP traffic is expected to increase nearly 100-fold from 2005 to 2020 when 11 billion smart devices are connected to the internet virtually creating the information superhighway, according to recent Cisco virtual networking index (VNI) report [3]. Similarly, the smartphone traffic generated by mobile and wireless terminals will account for 66 percent of the total IP traffic by 2020. For instance, M2M devices will have a huge contribution on it with the impressive traffic growth rate by 44 percent during the same period. To manage such a high level of demand, fifth generation (5G) of wireless communication has been recently proposed with the aim of implementing it by 2020 [4].

The aim of 5G is to provide the 1 to 10 Gbps connections to the end users with 1 ms of round trip delay, i.e., latency, on the data packet. Such type of connections are expected to be provided with 100 percent network coverage, however it also targets to reduce the energy consumption by 90 percent simultaneously [5]. A huge technical shift in current wireless protocol stack is necessary to simultaneously achieve the majority of targets put forward by 5G community. As a result,

various new technologies have been proposed in recent years by both industry and academia as possible candidate technologies for 5G, for instance, mmWave communication, non-orthogonal multiple access (NOMA), massive multiple input multiple output (MIMO), cognitive radio networks (CRN) including many others [6], [7].

As a matter of fact, there is no need of a complete generational shift in technologies innovation to achieve the targets set for 5G. One of the views in the research community is that the next generation telecommunication technologies should have a backward compatibility with the existing network infrastructure from economic as well as user experience perspectives. We come to this conclusion just by observing the technology development trends from beginning of mobile communication to the fourth generation (4G) in recent years. Therefore, even in the case of transition from 4G to 5G, many 5G services should be provided through the existing technologies of 4G wireless communication. However, one of the exceptions could be the data transmission with latency in the range of 1 ms. This is a very challenging task in the current telecoms infrastructure, therefore a huge technology transformation may be needed to achieve it [8].

The third generation partnership project (3GPP) Release-11, and subsequent releases, provide the most promising wireless technology platforms, which is referred as long term evolution advanced (LTE-A) [9]. It aims to provide better peak/average spectral efficiency, improved coverage and better cell-edge throughput. The Release-11 introduces new capabilities, e.g., self-organized network (SON), carrier aggregation (CA), machine type communication (MTC), coordinated multi-point (CoMP) transmission and reception, among many other candidate technologies.

As a matter of fact, to achieve the target set by 3GPP, all of the proposed technologies that build a complete LTE-A platform include the ad-on features which ultimately create a complex and large network, which if not properly managed, defeats the benefits of the developed system. Therefore, 3GPP developed SON solutions to handle, for instance, coverage and capacity optimization, handover management, energy saving features, among many other [10]. The functions of SON is divided into three broad categories: self-configuration, self-optimization and self-healing.

The concept of CoMP transmission/reception is to improve the coverage of cellular network, and has been regarded as a key technology of LTE-A. It is easy to maintain the higher system throughput when the user is close to the transmitter, however cell edge users receive a fraction of throughput due to the path loss and channel fading in addition to the interference from neighbour base stations. In CoMP scheme, the transmitters and receivers dynamically coordinate to provide joint scheduling and transmissions as well as joint processing of the received signals. In this way, a user at the edge of a cell is able to be served by two or more base stations to improve signals reception and transmission and increase throughput particularly under cell edge conditions [11]. It mainly focuses on transmission schemes, channel state information reporting, interference measurement, and reference signal design.

The 4G in terms of LTE-A also introduces the MTC enhancements such that the communication involves no or little human interactions among large number of low data rate devices with longer battery life. Here, MTC is also expected to virtually extend the WiFi into the LTE-A and optimize LTE-A for M2M communications [12]. Some of the enhanced features identified by 3GPP for MTC are remote management, congestion control, security, low device cost, and many other features are still being investigated.

The carrier aggregation feature enables a flexible way of frequency-bandwidth allocation to different users to support varying high data rate and wide bandwidth on a different basis [13]. Therefore, CA is the technical solution to overcome the spectrum fragmentation, where up to five carriers can be aggregated, each with a bandwidth of 1.4, 3, 5, 10, 15, or 20 MHz, thereby allowing for overall bandwidth of 100 MHz. For instance, in the UK, two 20 MHz carriers are combined in 1800/2600 MHz band to provide the maximum downlink speed of 300 Mbps [14]. Moreover, CA is supported for both frequency division duplex (FDD) and time division duplex (TDD) with all carriers using the same duplex scheme.

The technique of carrier aggregation is an important contribution from 3GPP in the LTE-A platform to achieve greater capacity from the large number of fragmented spectrum. There have been a number of field tests and commercial implementations of CA to date by various service providers around the globe. Based on its technical aspect and commercial success, it can be argued that CA

is a very first step along the long road to implement cognitive radio networks in future wireless communication system. Spectrum availability in various band is highly variable and may include long idle periods. This fact encouraged spectrum sharing concept which is one of the prominent features of CRN.

In the next section, the detail explanation, opportunities and challenges associated to the CRN will be briefly discussed.

1.1 Cognitive Radio Networks

The Federal Communication Commission (FCC) studied and published a report in 2002 that about one fourth of allocated spectrum in the USA is not fully utilized [15], and similar study was published in the UK by Office of Communication (OfCom). There is also a similar trend in many developed or developing nations around the globe. In the current practice, spectrum for cellular communication is exclusively allocated to licensed users which cannot be accessed by other users or service providers even if the channels are not partially or fully being utilized. When the demand of wireless technologies and services increases dramatically as predicted by Cisco VNI report [3], the static spectrum allocation policy will be obsolete. As a result, there is an immediate need of the dynamic spectrum access (DSA) technologies [16] and new spectrum regulatory policies.

The dynamic nature of the wireless communication has put forward many challenges to the system designers, e.g., inter and intra-cell interference, hidden terminals, path loss and fading effects. Therefore, a reliable and feasible technique has to be developed to exploit the spectrum opportunities in time, space and frequency in such a way that licensed users are always protected from any harmful interference and the possible degradation in quality of service (QoS). Therefore, one of the highly anticipated technologies to solve the spectrum scarcity issue is the cognitive radio [17].

A cognitive radio is defined, in [18], as an intelligent wireless communication system capable of changing its transceiver parameters based on interaction with external environments in which it operates. Therefore, it is intuitive that CRN is an enabling technology to implement the important features of DSA. The ideal DSA approach therefore allocates spectrum, transmit power, and other wireless

communication parameters proportionally to the secondary systems in such a way that every secondary user (SU) not only receives equal share of resources but also sacrifices the QoS equally in cases of system misconfiguration [19]. Therefore, in literature, DSA and CRN are sometimes interchangeably used.

In CRN, unlicensed users of the spectrum, also known as SUs, are allowed to access the licensed bands under the condition that licensed users of the spectrum, also known as primary users (PU), are protected from the harmful interferences [20]. Broadly speaking, two types of CRN have been proposed based on the way SUs access the spectrum [21]. In first case, the CRN adopts opportunistic spectrum access (OSA), where SUs opportunistically operate on the channel which is originally allocated to the PUs. In this case, the SUs must ensure the status of the primary channels are accurately observed. Therefore, in OSA based CRN the accuracy of the observation strategy is exceptionally critical. Secondly, the spectrum sharing (SS) based CRN allows SUs to transmit simultaneously with the PUs over the same spectrum even in cases the PU transmission is active as long as the QoS degradation in primary system due to the SU interference is tolerable. The first type of spectrum sharing is called as overlay spectrum access, whereas the second type is broadly known as underlay spectrum access [22].

1.1.1 Cognitive cycle

It is now very important to understand the cognitive radio cycle to develop the efficient resource allocation methods in CRN. The cycle consists of four fundamental stages, which are spectrum sensing, spectrum decision, spectrum sharing and spectrum handoff, a.k.a, spectrum mobility [23].

- *Spectrum sensing*: The very first stage of CRN is the spectrum sensing which involves the real-time identification of the unused subchannels by the primary systems. Such subchannels, in literature, are also referred as spectrum holes. The details about various sensing methods are found in [24], and some of them will be explained in detail in chapter 3 as well. This stage also includes the identification, with minimum delay, of the arrival

of licensed users on the subchannel(s). Such kind of sensing delay is generally defined by primary systems as a threshold value depending on their interference suppressing capability.

- *Spectrum decision*: The second stage of the cognitive cycle is the spectrum decision based on the spectrum sensing results in the first stage. In this stage, SUs have to select the best available subchannels which must satisfy the minimum throughput requirements on both primary as well as secondary systems. This is achieved by means of spectrum characterization, selection and SU reconfiguration [25]. This, in general, involves the analysis of continuous or discrete statistical information about the primary user activity on the subchannels [26].

- *Spectrum sharing*: The stage of spectrum sharing has gained much attention in the research community right from the beginning of research in cognitive radio. It basically refers the management of coordinated access to the selected (or available) subchannels by the SUs [27], [28]. The access mechanism could be underlay, overlay or combination of them [29]. Therefore, in this stage, it is not only about the spectrum sharing but also involves the transmission power control, time-slot allocation among the SUs.

- *Spectrum handoff*: The spectrum handoff, as a last stage of the cognitive cycle, is the ability of the secondary system to vacate the subchannel(s) as immediately as it is reclaimed by the licensed user and access the new best available subchannel(s) which satisfied the QoS requirements [30]. Although it is very important aspect of CRN, it has gained very limited attention in research community until the recent time. It can be further categorized into proactive handoff and reactive handoff depending on when the handoff process is supposed to be initiated [31].

After introducing the basics of cognitive radio, a brief historical notes on the development of cognitive radio and communication will be presented in the next section.

Table 1.1: The historical development trend of cognitive radio networks

1999	One of the earliest concept paper published in IEEE Communication Magazine
2000	A detail and comprehensive version of cognitive radio published as a PhD dissertation by Joseph Mitola
2002	FCC release the report
2003	Published CRT proceeding (FCC ET Docket No. $03-108$)
2004	One of the pioneering paper published by Simon Haykin in IEEE JSAC
2004	The IEEE 802.22 WRAN standard committee established
2005	IEEE P1900 committee was established
2008/2009	FCC and OfCom opened up the TV white spaces for unlicensed access.
2012	The IEEE802.22 WRAN final report published
2013	Proof-of-concept and experiment testbeds on cognitive radio network appeared
2016	Huge database of research journals in IEEE explorer in spectrum sharing and cognitive radio.

1.1.2 Journey of Cognitive Radio Networks

The adaptability with the dynamic radio environment is one of the important features of spectrum sharing system. This capability was highly discussed in a platform known software-defined radio (SDR) in mid-nineties as a convergence of digital radio and computer software. It is obvious to say that SDR is the turning point to explore the potentials of the cognitive radio as a disruptive technology for next generation of wireless communication. A brief historical development of cognitive radio has been summarized in Table 1.1.

The term *cognitive radio* and *software-defined radio* were firstly framed by J. Mitola in one of his pioneering paper [32] and later in his PhD dissertation [33] in 1999 and 2000, respectively. In fact, the cognitive cycle was described

as a means to enhance the flexibility of future wireless communication, however no solutions and possible applications were proposed by those works. The work published by Simon Haykin [17] in 2004 actually elaborated the signal processing aspect of cognitive radio and opened the window of various research problems and potentials in dynamic spectrum sharing system to apply in the cellular and heterogeneous networks.

Until 2004, the standard committee, in FCC and IEEE, initiated the work towards the dynamic spectrum sharing system. Moreover, a special credit should be given to FCC's Spectrum-Policy Task Force report [15], published in 2002, which concluded that spectrum access is a more significant problem than the actual physical scarcity of spectrum. In addition, the unused and underused portion of spectrum were defined and the concept of spectrum hole was branded for the first time which attracted the attention of wireless communication research community. In 2003, FCC also published the proceeding in cognitive radio for open discussion [18].

To speed up the implementation of dynamic sharing system in reality, a standard protocol was necessary so that the industry, academia and various telecom service providers can work together. In 2004, IEEE established the 802.22 committee to make standards for sharing the unused portion of radio spectrum in very-high frequency (VHF) and ultra-high frequency (UHF) band, i.e., 52 MHz to 862 MHz, which are primarily used for analog and digital TV signal transmission. In 2005, IEEE P1900 Committee[1] was formed to enable the radio and spectrum management for spectrum sharing system. The primary purpose has been defined as to initiate the standardization of cognitive radio for the real-time adjustment of spectrum utilization when the network circumstances and objectives are changed.

The research and innovation activities in cognitive radio was encouraged by various government and regulation agencies. The important decision taken by FCC in the USA in 2009 and OfCom in the UK in 2010 to open up TV white

[1]P1900 committee was later reorganized as Standard Coordinating Committee 41 (SCC 41), which later expanded as dynamic spectrum access network (DySPAN) Standards Committee. Various P1900 committee, which are P1900.1 to P1900.7 Working Group, are actively working for a range of specific research areas in cognitive radio.

spaces, i.e., unused portion of TV band in particular time and location, for unlicensed users implied very long term impact [34]. The final report on medium access control and physical layer specifications for cognitive radio wireless regional area networks (WRAN) was published in 2012 [35]. It defines the operational policies and procedures that allow spectrum sharing where the communications devices may opportunistically operate in the spectrum of the primary services.

Due to enormous potentials in the next generation mobile communication as well as extensive industrial interests, many testbeds are being designed to enhance the research and applicability of cognitive radio. One of the reasons is, of course, WRAN 802.22 standard available which defines various standards for cognitive radio operations. Few examples of such testbeds are Cognitive Radio Experiments World (CREW) project conducted by EU ICT-2009 and Ghent University, Cognitive Radio Network Testbed (CORNET) in Virginia Tech, CorteXLab in France to shape the future IoT, Cognitive Radio Testbed (CoREX) in UCLA among many others. In addition, there are more than 3,000 journal articles and 10,000 conference articles in IEEE database alone until 2016. The immense interests and dedication by academia, industry and government ultimately resulted the cognitive radio communications as one of the important candidate technologies for 5G and beyond [36].

1.2 Research Problems

In the modern cellular systems, one of the scarce resources for wireless data transmission is the radio spectrum. The management of crowded radio spectrum is more important due to the fact that large parts of spectrum are either unused or underused at a given time and geographical location. Therefore, at first hand, the problem domain must be properly identified to find the best strategy of resource allocation. The problem domain, broadly speaking, constitutes spectrum sensing, subchannel allocation and transmission power control in CRN. They are briefly described in this section.

- The spectrum sensing is basically the stage of obtaining the usage pattern of spectrum which significantly embeds the primary users activity on the

subchannels in a given time and geographical locations. There are various methods to achieve this information, e.g., accessing the geolocation database, using beacons and using the local spectrum sensing methods [37]. The geolocation database, which is authorized and administrated by regulatory authorities, is one of the latest prominent works to access the unused subchannels in TV band that can be used for rural broadband access where received SNR at the user terminal is minimum [38].

A number of different techniques of spectrum sensing are being proposed to identify the presence or absence of primary user in the subchannel. Particularly considering the CRN scenario, energy detection, cyclostationary feature detection, matched filter, waveform based sensing along with many other are proposed in recent years [39], [40]. Some of them are also considered to be the candidate technology to enable cognitive communication, e.g., WRAN in TV band using cognitive radio technique. In energy detection, the output of the energy detector is compared with a threshold which heavily depends in the noise floor [41]. Moreover, the cooperative detection methods are also getting a huge attention in research community because it can suppress the effects of noise uncertainty, fading and shadowing in the wireless channels [42].

As a matter of fact, whatever sensing methods are used, the performance of sensing devices improves when high sampling rate, high resolution of analog-to-digital converters(ADC) and high speed processors are provided. In addition, the sensing devices should be able to detect relatively large band of spectrum for identifying the spectrum opportunities. On the other hand, the sensing duration is a very small fraction of the total frame duration. In cases when the sensing duration is maintained higher which ultimately increases the sensing accuracy, the data transmission duration gets smaller which directly affects the throughput performance of the secondary system [43]. This indicates that an stringent tradeoff do always exist in the CRN. Therefore, the spectrum sensing methods need to identify and then solve such a strict tradeoff into more flexible tradeoff for system designers.

- One of the prominent research challenges in CRN is the allocation of the subchannels to the users. The allocated subchannels must be available for longer period of time such that the switching delay can be significantly minimized. However, prediction of subchannel activities in the long term is very difficult to achieve [44]. This subchannel allocation needs the subchannel characterization which involves to estimate various properties of spectrum. The instances are channel switching delay, primary user activity model, statistical QoS, channel holding time etc. [45], [46], [47]. Therefore, the optimal subchannel allocation, on the first hand, needs to estimate the activity level of primary users on the subchannels. However various methods have been proposed to model such activities, e.g., using statistical database, Point Point Process (PPP) model [48], reinforcement learning algorithm [49], a viable solution is still necessary to propose to solve the issues in subchannel allocation.

- When the spectrum sensing is performed and subchannels are assigned, the transmit power must be carefully allocated. In the multichannel and multiuser transmission scenario, the proposed method determines not only the transmit power to each SU but also the power allocation to each subchannel [27]. One of the reasons for such consideration is to protect the primary system from any harmful interferences while sharing the subchannel. Many power allocation methods have been proposed in literature which claim to enhance the system performance in spectrum sharing system. Such power allocation methods consider the maximization of sum-rate [50], spectral efficiency [51] and energy efficiency [52]. In addition, sensing and throughput tradeoff [53] as well as channel handoff and switching delay minimization are also equally considered [30].

- As a matter of fact, all the above mentioned objectives cannot be simultaneously achieved from a single strategy. For instance, when sensing duration is minimized, the sensing accuracy is proportionally compromised whereas the spectral efficiency gets improved. Furthermore, when the energy efficient system is designed, the spectral efficiency may need to be compromised. Similar situation occurs when switching delay is optimized, the

primary users may be highly affected by the higher interference which ultimately forces the SUs to terminate the transmission on cognitive subchannel. Therefore, a new method for CRN must be proposed to put spectrum sensing, spectrum allocation and transmit power control together with a common network parameter such that a better as well as practically achievable tradeoff can be obtained.

1.3 Motivation

The research presented in this thesis is highly motivated by the issues raised in the previous section. Furthermore, the research in the field of spectrum sensing and resource allocation, a low complexoty but highly efficient methods are immediately required. The objective of my research is to bridge the gap in this area.

With the revolution in wireless communication technologies and the cost of wireless devices as well as services falling down dramatically in last two decades, radio spectrum has become the extremely scarce resource for wireless networks to provide the required QoS to the end users. The current static spectrum allocation policy is one of the barriers to increase the spectrum utilization efficiency. Cognitive radio, in parallel, emerged into the wireless communication framework as a tool to solve the spectrum shortage and underutilization problems. Moreover, to fulfil the requirements of 5G such as low latency, high throughput, high spectral and energy efficiency, a very intelligent wireless communication technique is needed. Therefore, the main motivation for this research emerged form finding the best possible techniques which help to achieve the goals with minimum system complexity and lower implementation cost.

The spectrum sensing methods in the literature, whether cooperative or non-cooperative, deal with the tradeoff between sensing and transmission duration. However, a few sensing methods do not work under low signal to noise ratio (SNR), e.g., energy detection, or they are vulnerable to interference due to the sampling clock offset, i.e., cyclostationary detection. Similarly, cooperative spectrum sensing method needs higher computational complexity to achieve an accurate sensing information, whereas wideband sensing increases the hardware design

complexity. Therefore, the research works presented in this thesis are highly motivated to find a low complexity but high sensing accuracy tradeoff in spectrum sensing in CRN.

Similarly, various schemes have been proposed in subchannel allocation and transmit power control in CRN. Many of the proposed methods tend to optimize one network parameter, such as spectral efficiency, energy efficiency and switching delay considering other parameters in the ideal range. In practice however, such flexibility is not always possible to achieve. Therefore, the combined framework was immediately realized to optimize the spectral efficiency, energy efficiency and the primary user activities in which the sensing parameters can be tuned at secondary system to control them. The research presented in this thesis also got motivation from such requirement.

As a motivational work at the beginning of the research, a spectrum sensing tasks were performed at various spectrum range to study the diversity of spectrum usage and availability which will be discussed next.

1.3.1 Spectrum Sensing in Practice: Observation in Lancaster Area

Once spectrum sensing techniques and issues of cognitive radio communication have been discussed, it is very important to elaborate how the idle as well as under-utilized portion of the spectrum are distributed in real wireless communication scenario. For instance, the observation of primary signals in some cellular and TV band in Lancaster City area have been presented in this section to further understand the general concept of cognitive radio for cellular communication.

Depending on the nature of the available subchannel, i.e., both the unused as well as under-utilized, different accessing modes can be used, for instance, overlay and underlay mode of spectrum access. The recent announcement by Ofcom assures the creation of White Spaces Databases (WSDBs) on UHF TV band which is operated by selected organizations that have been qualified by Ofcom to operate in the United Kingdom and they provide the WSDB Services to white space devices (WSDs) [54]. However, similar concept is not feasible in

the cellular communication due to the dynamic nature of users. Therefore, a real time spectrum sensing result is needed to exploit the available subchannels.

As mentioned previously, cognitive radio concept can be implemented within the TV band in VHF and UHF spectrum, typically in 54 MHz to 790 MHz [55], to cellular communication in 900/1600 MHz, LTE in 800 MHz, UMTS in 2100 MHz [56] and even most recently proposed in mmWave band. In this section, the field based spectrum sensing results are presented showing the TV white spaces, various cellular bands including 3G and 4G/LTE signals.

The software defined radio platform is used to find the spectrum availability map using the device originally designed as a receiver for digital video broadcasting-terrestrial (DVB-T). The frequency tuner uses the micro coaxial antenna port with omnidirectional antenna. The received radio frequency signal at the tuner are down-converted to intermediate frequency and then to the baseband signal. The sampling rate in this spectrum sensing is set to 2.4 MHz and antenna gain is 40.

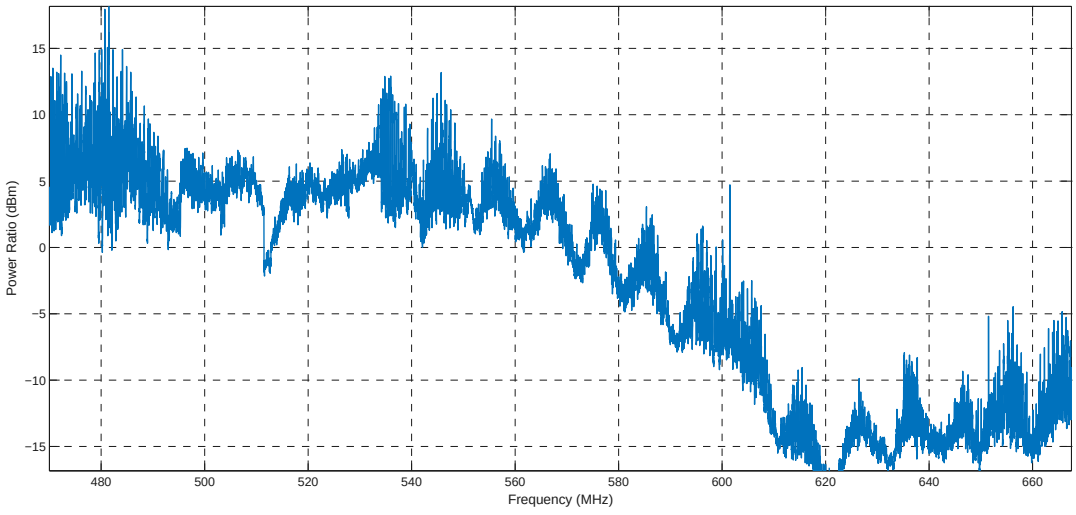

Figure 1.1: The received signal power in dBm in the radio spectrum of 400 MHz to 670 MHz.

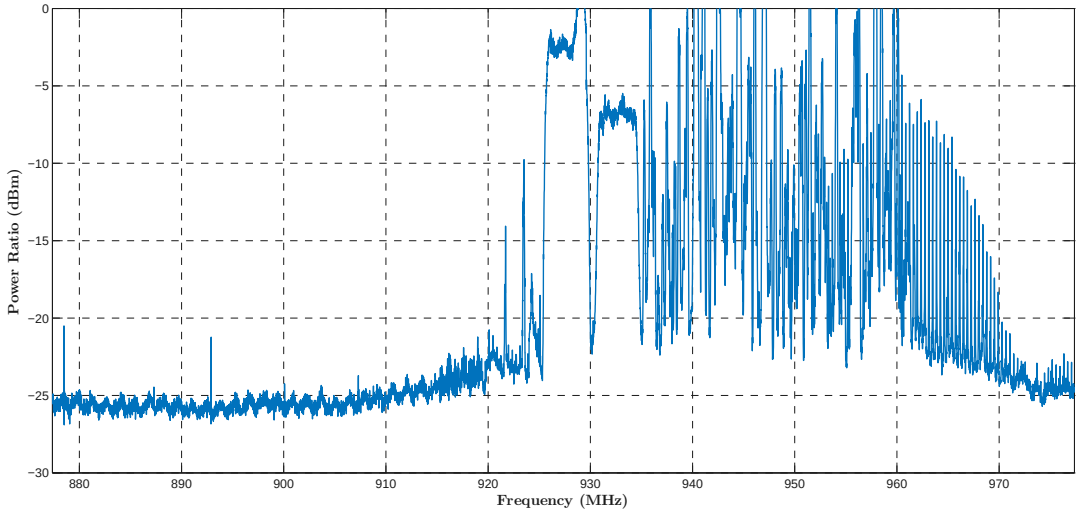

Figure 1.2: The received signal power in dBm in the radio spectrum of GSM.

The received signal strength at the spectrum sensors between 400 to 670 MHz is shown in Fig. 1.1. The sensing result shows how non-uniformly the spectrum is utilized at any instant of time and location in which a robust cognitive radio technology is required to increase the spectrum utilization. It can be observed that the spectrum above 600 MHz can be used for WRAN for broadband access in which large portion of spectrum is below -15 dBm signal strength. It must be noted that the secondary system must maintain the interference to the primary system below the threshold of -15 dBm. For TV white space applications, such information is maintained as database which can be accessed by WSDs.

The received signal strength in the GSM and LTE band are shown in Fig. 1.2. The spectrum below 910 MHz is available to access at the time of sensing which can be shared among the secondary users. However, it is not possible to use a database concept in this case due to the fact that the spectrum access pattern is highly dynamic. Therefore, a robust spectrum sensing method is needed in this case. Above the 910 MHz, the spectrum are being accessed quite frequently, however there are many subchannels in the idle state which could be shared because the received signal strength is relatively low, i.e., less than -20 dBm. A small

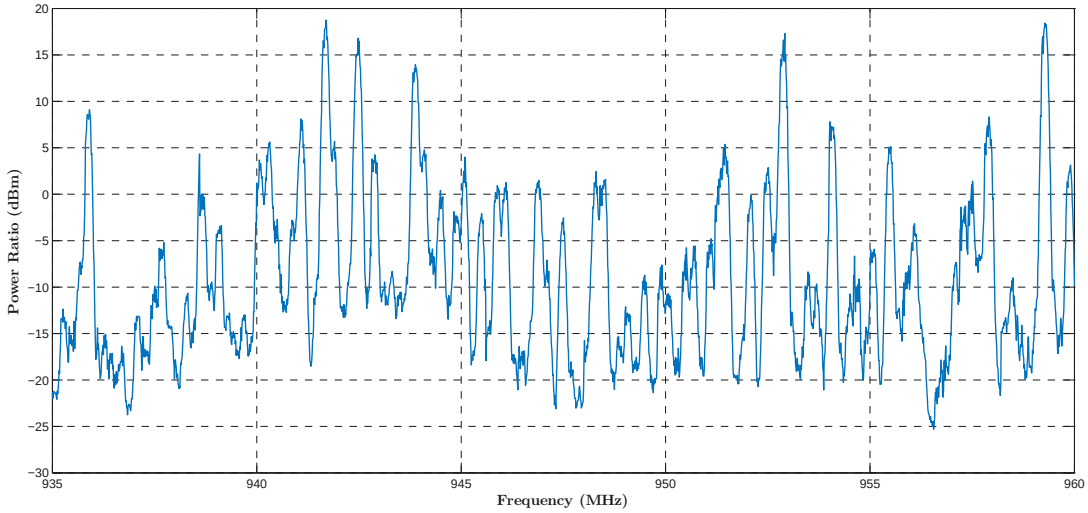

Figure 1.3: The received signal power in dBm in the radio spectrum of 900 MHz.

portion of 900 MHz band is shown in Fig. 1.3. The spectrum is usually averaged over many samples, the observed sequences are just an instantaneous observation. However it has been observed similar distribution of spectrum access, it can

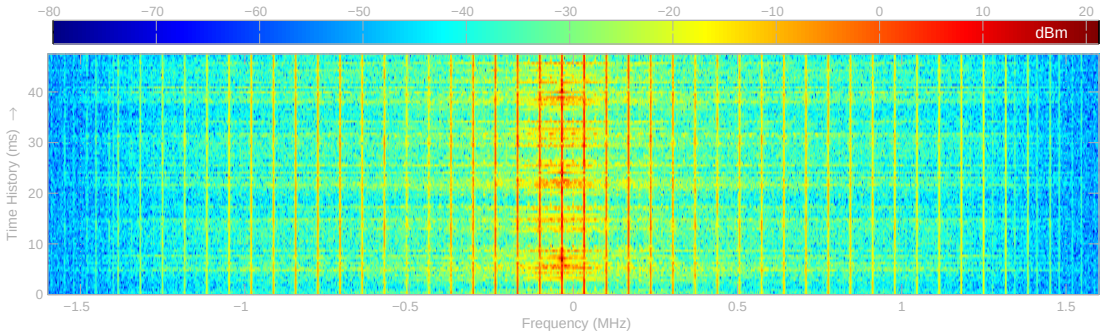

Figure 1.4: The OFDM subcarriers of LTE signal captured at the central frequency 891 MHz in time and frequency axis.

be argued that channel access distribution will follow similar pattern in average. When closely observed the spectrum, subchannels are available to be accessed by the secondary system, under strict interference constraint, even though they are not contiguous.

In Fig. 1.4, the individual subcarrier have been identified at the baseband central frequency 891 MHz and the bandwidth is 2.8 MHz. The red and yellow vertical lines indicate the individual OFDM subcarrier where red line indicates the higher received signal strength. Therefore, OFDM is considered as a ideal candidate for multiplexing in CRN because the subcarriers allocation to users can be done adaptively.

1.4 Thesis Outline

This thesis is organized into six different chapters, which covers spectrum sensing and resource allocation strategies for cognitive radio networks.

In **Chapter 2**, various aspects of spectrum sensing for cognitive radio communication will be presented. It will firstly describe the requirements of spectrum sensing in cognitive radio along with the very important tradeoff between sensing and transmission duration. Secondly, various spectrum sensing methods are described that are available in the literature as a foundation of the proposed spectrum sensing methods later in the thesis. The cooperative and non-cooperative spectrum sensing are also described with their respective advantages and disadvantages. The challenges of spectrum sensing methods for cognitive radio will also be described. Thirdly, the spectrum sensing results obtained from the specially designed spectrum sensors for TV band and GSM band, i.e., 500 MHz, 800 MHz and 1600 MHz will be presented to show the nature of spectrum availability in real network.

In **Chapter 3**, the considered system model will be described in detail. The multi-cellular and multi-carrier system with primary and secondary service providers collocated in the same geographical region for spectrum sharing system will be presented. The subchannel division, orthogonal frequency division multiple access (OFDMA) as modulation scheme and various channel and interference

models are described to justify their usage in the considered system of spectrum sensing and resource management.

In **Chapter 4**, the proposed spectrum sensing scheme will be exclusively described. It is basically the sensor-enabled cognitive radio system where the dedicated sensing devices replace the spectrum sensing task from the secondary system. As a result, the secondary users can have more slot duration to transmit the data packets in addition to the lower power consumption due to skipping the sensing task. This chapter will also present design criteria of sensing devices such that the tradeoff among the sensing accuracy, system throughput and sensing network cost can be explained both mathematically and through the simulation results. The detail communication protocol among secondary system and the sensing devices will also be presented.

In **Chapter 5**, the proposed resource allocation method will be presented. Firstly, a reliable method of estimating the activities of primary users on the subchannels are explained defining a parameter called subchannel activity index. This parameter will be later obtained in the multiple cell scenario which indicates the best possible subchannel in the vicinity of the cell at a particular time and location. Furthermore, the transmit power allocation problem is defined and solved to find the optimal transmit power. While formulating the optimization problem, both spectral efficiency and energy efficiency will be considered. Later in the chapter, the integrated method of analysis is presented which shows a better system design approach to maintain the balanced energy and spectral efficiency by changing the sensing parameters in the secondary system.

Finally, **Chapter 6** presents the conclusions of the thesis by briefly reviewing the contributions of the proposed methods and associated challenges while implementing them in real network scenario. Based on the recent research activities, the future directions of resource allocation in cognitive radio in terms of 5G and its standardization are also discussed.

1.5 List of Publications

Deepak, G.C., Keivan Navaie, and Qiang Ni, "Power allocation in multicell collaborative cognitive radio networks," *Under review on IEEE Transaction*

(The content presented in Chapter 5 is based on this paper.)

Deepak G.C., and Keivan Navaie, "A low latency zone-based cooperative spectrum sensing," *IEEE Sensor Journal*, vol. 16, no. 15, pp. 6028-6042, Aug. 2016.
(The content presented in Chapter 4 is based on this paper.)

Deepak G.C., and Keivan Navaie, "On the collaborative cognitive radio networks," *IEEE InfoCom Student Seminar*, San Francisco, USA, 10-15 April, 2016.
(The content presented in Chapter 5 is based on this paper.)

Diky Siswonto, Li Zhang, Keivan Navaie, and Deepak G.C., "Weighted Sum Throughput Maximization in Heterogeneous OFDMA Networks," *IEEE VTC-Spring conference*, Nanjing, China, 15-18 May, 2016.
(The content presented in Chapter 4 is based on this paper.)

Deepak, G.C., Keivan Navaie, and Qiang Ni "Inter-cell collaborative spectrum monitoring for cognitive cellular networks in fading environment," *Proc of IEEE Int. Conf. on Comm. (ICC)*, IEEE pp. 7498-7503, 2015.
(The content presented in Chapter 5 is based on this paper.)

Deepak G.C., and Keivan Navaie "On the sensing time and achievable throughput in sensor-enabled cognitive radio networks," *Proc. of Tenth Int. Symp. on Wireless Commun. Systems (ISWCS)*, IEEE, pp. 1-5, 2013.
(The content presented in Chapter 4 is based on this paper.)

Chapter 2

Spectrum Sensing for Cognitive Radio

Spectrum sensing is the mechanism to identify the fully or partially unoccupied spectrum by primary users at a particular time and geographical location. The fully unoccupied spectrum are also defined as the spectrum holes. In more general cognitive radio term, spectrum sensing techniques result the spectrum usage characteristics in terms of multiple dimension of frequency, time and space [24]. Spectrum sensing has been considered to be the fundamental requirement for spectrum sharing in cognitive radio framework.

The primary users (or primary systems) and secondary users (or secondary systems) are frequently used while discussing the cognitive radio and spectrum sensing. Primary users are the mobile terminals who have the exclusive right to access the specific part of the spectrum as soon as there is data packet to transmit. It means, in cellular system, the primary users are the incumbent licensee of the spectrum for which they pay the cost to get access. On the other hand, secondary users have the lower right to access the same spectrum which they have to exploit in such a way that they do not cause any harmful interference to the primary system.

The spectrum sensing task is generally performed by the secondary users. As a result, the secondary users must have a reliable and accurate cognitive radio capabilities to exploit the unused part of radio spectrum. However, in some latest advancements, the database service provider may disseminate the accurate

status of the target frequency band. One of the examples is the geolocation database (GD) of TV white spaces to be used for broadband access when the TV transmitter is not using a particular band [57]. This has been proposed in the IEEE 802.22 standard and it is partially implemented with wireless regional area network (WRAN) in practice. The basic information about this standard will be discussed in the next chapter.

The wideband spectrum sensing is necessary in some cognitive radio applications where large band of spectrum is to be opportunistically accessed. However, wideband spectrum sensing requires higher power consumption for analog-to-digital conversation in addition to high sampling rate [40]. To avoid such problems, the wideband can be divided into the narrowband subchannels which is also known as the multiband spectrum sensing. They can be sensed either sequentially or in parallel depending on the availability of number of sensing antennas. The advantage of multiband sensing is that the subchannels are assumed to be independent and the narrowband spectrum problems becomes a binary hypothesis test. In the following section, we will present various multiband spectrum sensing techniques that are in practice.

2.1 Spectrum Sensing Techniques

The output of spectrum sensing decides whether a particular subchannel is available or being occupied. Therefore, the problem, in its simplest form, can be modelled as binary hypothesis test at the secondary users, or spectrum sensors if sensing is done at the separate entity. The null hypothesis is denoted by H_0 when a particular subchannel is idle. In this case, the received signal is of course only the random channel noise. In contrast, the alternative hypothesis is denoted by H_1 when a particular subchannel is occupied by primary users. In this case, the received signal is both the noise and signal transmitted by primary system.

To define the spectral sensing techniques, various discrete signals are defined from mathematical and signal processing perspectives. Let the received signal at the secondary users receiving antenna is denoted by $\boldsymbol{y} = [y[0], y[1], \ldots, y[K-1]$. Here $y[k]$ denotes the k^{th} sample in the sequence for $k = 0, 1, \ldots, K-1$. The sampled signal is $y[k] \triangleq y(kT_s)$ where $f_s = \frac{1}{T_s}$ is the sampling rate. The digitally

modulated signal samples transmitted by the primary system is represented by $\boldsymbol{x} = [x[0], x[1], \ldots, x[K-1]$, where k^{th} element of the sequence is denoted by $x[k] \triangleq x(kT_s)$. The noise vector is denoted by $\boldsymbol{w} = [w[0], w[1], \ldots, w[K-1]$ where the k^{th} sample in the sequence is denoted by $w[k] \triangleq w(kT_s)$. For mathematical tractability, the channel gain between primary transmitter and secondary receiver is considered to be unit, though this assumption is practically not feasible. This channel gain will be considered in the next chapter onwards when more advance form of spectrum sensing and resource allocation methods are presented.

The spectrum sensing technique should be able to differentiate between the following two contrast hypotheses.

$$y[k] = \begin{cases} w[k], & : H_0, \\ x[k] + w[k], & : H_1, \end{cases} \tag{2.1}$$

where, $w(k)$ is considered to be circulatory symmetric zero mean complex Gaussian random variables with variance σ^2.

2.1.1 Energy detection

The energy detection, also known as radiometer, is one of the well known spectrum sensing methods due to its low computational complexity and easy to implement [58], [59]. This is due to the fact that it does not involve any complex signal processing techniques. The energy detectors, i.e., secondary users unless otherwise stated, measures the energy received during the finite sensing duration which is then compared against the predetermined threshold which depends on the noise floor [60]. This is a popular spectrum sensing technique because the detectors do not need a priori knowledge of signal transmitted by the primary system, but it is assumed that large number of signal samples are available at the detector.

The energy detection spectrum sensing method comes with various challenges, for instance, selection of the energy detection threshold. If the detection threshold is not properly obtained, the spectrum sensing efficiency needs to be highly compromised. In addition, energy detectors are also unable to differentiate between

the channel noise and the interference signal from primary users. Therefore, this method provides relatively poor performance when received SNR is very low [61].

In order to identify whether particular subchannel is idle or busy, the test statistics in the form of decision metric, i.e., $\Lambda[\boldsymbol{y}]$, is first calculated by averaging the energy received over a period of N observed samples as following.

$$\Lambda[\boldsymbol{y}] = \frac{1}{K} \sum_{k=0}^{K-1} |y[k]|^2. \tag{2.2}$$

In the next stage, the decision metric is compared against the detection threshold ε_{th} to make the decision about whether the subchannel is idle, i.e., in favour of hypothesis H_0, or occupied, i.e., in favour of hypothesis H_1. Therefore, the energy detector decides that H_1 is true under the condition $\Lambda[\boldsymbol{y}] > \varepsilon_{\text{th}}$ and secondary users are not allowed to use the subchannel. Similarly, H_0 is true in all other cases in which the subchannel is allowed to be accessed by secondary users to transmit their data.

Two parameters are very important to measure the performance of energy detection method, which are probability of false alarm, denoted by P_{f}, and probability of detection, denoted by P_{d}. Moreover, the probability of miss detection, P_{m}, refers to the case when detection of subchannel is failed and they are related as $P_{\text{d}} + P_{\text{m}} = 1$. The P_{f} is the probability that the spectrum sensors incorrectly decide that a particular subchannel is occupied by primary users when actually the hypothesis H_0 is true, i.e., the subchannel is idle. The probability of false alarm is then formulated as below.

$$P_{\text{f}} = \Pr\{\Lambda[\boldsymbol{y}] > \varepsilon_{\text{th}} | H_0\}. \tag{2.3}$$

Similarly, the P_{d} is the probability that the spectrum sensors correctly decide that a particular subchannel is occupied by primary users when actually the hypothesis H_1 is true, i.e., the subchannel is busy. The probability of detection is then formulated as below.

$$P_{\text{d}} = \Pr\{\Lambda[\boldsymbol{y}] > \varepsilon_{\text{th}} | H_1\}. \tag{2.4}$$

From the very basic definition of P_{f} and P_{d}, it is easy to say that the larger P_{d} is always expected whereas P_{f} is expected to be smaller. When P_{d} is lower,

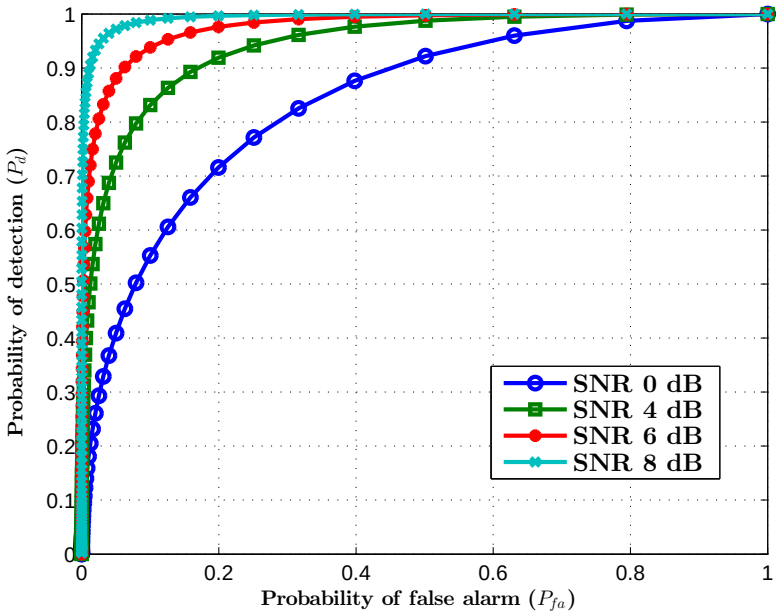

Figure 2.1: Receiver operating characteristics curve for energy detection method through AWGN channel for various received SNR.

the primary user transmission in the subchannel is missed which ultimately cause undesired interference to the primary users. Similarly, when P_{f} is higher, many opportunistic spectrum accesses on the subchannels are missed which causes lower spectrum utilization. Therefore, it is very important to restrict them within a acceptable values. The general concept on the spectrum sensing design is to minimize the P_{f} while P_{d} is kept above the minimum level to protect the primary system from the interference. However, various advanced methods have been proposed in the literature to achieve this tradeoff.

When P_{d} is plotted against the P_{f}, the resulting plot is known as the receiver operating characteristics (ROC) curve. At a particular instance of sensing, a pair of $(P_{\mathrm{f}}, P_{\mathrm{d}})$ can be obtained which lies in the ROC curve as shown in Fig. 2.1. It shown how P_{f} and P_{d} are achieved for various received signal SNR from 0 dB to 8 dB. It can be observed that when P_{f} is relaxed to the higher value, the detection accuracy can be improved with higher P_{d}. Moreover, when the received SNR is

higher, the better $(P_\mathrm{f}, P_\mathrm{d})$ pair is achieved.

The performance of energy detection varies according to the fading channels. This method highly depends on the sensing threshold which merely depends on the noise variance. In practice however, such noise variance cannot be predicted in advance. Due to this uncertainties, accurate subchannel detection is impossible below certain SNR, which is also known as SNR wall [61].

2.1.2 Matched Filter Detection

The matched filter technique to obtain the subchannel information requires perfect knowledge of signalling features on the data transmitted by the primary systems [62], [63]. The features include the operating frequency, bandwidth, modulation type, frame format or pulse shaping. Therefore, for a known deterministic signal, matched filter detector acts as a replica correlator. The test statistic simply correlates the n^{th} sample of the observed sequence $y[n]$ at the receiver of the spectrum sensors to the replica of primary user signal $x[n]$. The null hypothesis (H_0) and alternative hypothesis (H_1) are then tested as following.

$$\begin{aligned} \Lambda[\boldsymbol{y}] &= \mathbb{R}\left[\sum_{n=0}^{N-1} y[n]x^*[n]\right] > \varepsilon_\mathrm{th} : H_1, \\ \Lambda[\boldsymbol{y}] &= \mathbb{R}\left[\sum_{n=0}^{N-1} y[n]x^*[n]\right] \leq \varepsilon_\mathrm{th} : H_0, \end{aligned} \tag{2.5}$$

where ε_th is the detection threshold[1], $\mathbb{R}[\cdot]$ denotes the real part of complex number whereas $()^*$ denotes the complex conjugate.

The advantage of using the matched filter is that it takes low sensing duration to meet the P_f and P_d requirements set by primary system [64]. It is due to the fact that the smaller number of samples are required to detect the subchannel in comparison to the energy detection. As a result, the matched filter detector may acquire the higher transmission duration, and therefore improved system throughput. In this method, the required number of samples grows according to

[1] Just for simplicity, the same threshold symbol is used as in the energy detection, however they are characteristically different parameters.

$O(1/\text{SNR})$ which indicates that higher the variance of channel noise, larger number of samples must be processed to meet the required level of P_f. However, the beauty of matched filter detection cannot be achieved without sacrificing something. firstly, secondary users may require to demodulate or decode the signal transmitted from primary system which consumes more energy while sensing the subchannels. Secondly, the implementation complexity is relatively higher due to the requirements of dedicated receiver for every known signal type [59].

2.1.3 Cyclostationary Detection

The information bearing signal in communication system exhibit a form of periodicity, for instance, symbol rate, chip rate, channel code or cyclic prefix [65], [66]. The noise presents no correlation due to the wide sense stationary whereas the modulated signals exhibit the correlation due to the redundancy of signal periodicities. This feature of periodic pattern on the transmitted signal can be exploited for spectrum sensing by cyclostationary detection. One of the features that make cyclostationary detection method a very attractive option is that it has ability to differentiate the primary user signal not only from the channel noise but also from another primary user signal or interference [67].

The orthogonal frequency division multiplexing (OFDM) signals can be considered which are embedded with the cyclic prefix to protect the signals from intersymbol interference. The cyclic prefix basically means each OFDM symbol preceded by replica of end part of the same symbol. Therefore cyclic prefix can be easily exploited for spectrum sensing using cyclostationary detection. When the cyclic frequency is considered to be α, the cyclic spectral density (CSD) function of received signal $y[n]$ is calculated as following [68].

$$S(f,\alpha) = \sum_{l=-\infty}^{\infty} R_y^\alpha(l) e^{-j2\pi fl}, \tag{2.6}$$

where,

$$R_y^\alpha(l) = E[y[k+l]y^*[k-l]e^{2\pi\alpha k}]. \tag{2.7}$$

The peak value of CSD is attained when the fundamental frequency and cyclic frequency of $y[k]$ are matched which merely indicates the hypothesis H_1 is correct.

In all other cases, the hypothesis H_0 is correct. If the cyclic frequency is unknown, it can be easily extracted from the received signal. The drawbacks of this detection technique is that it reduces the system capacity due to signalling overhead because the same information has to transmit twice within a frame. Moreover, the computational complexity is very high in comparison to the matched filter and energy detector because it has to cope with the effect of sampling frequency offset in the system.

Many other spectrum sensing techniques have been proposed in the literature, for instance, blind sensing, filter-bank based sensing, multi-taper sensing, compressive sensing. All of them have a set of advantages and disadvantages and the choice depends on the network scenario and the sensing hardware available.

2.2 Cooperative Spectrum Sensing

The primary and secondary systems may not be in the line-of-sight (LoS) communication due to the mobility of the users. This results the noise uncertainty, path loss, channel fading and shadowing on the received signal. Therefore, the spectrum sensors receive very low primary signal and may incorrectly detect the presence or absence of primary users on subchannels. This condition is also referred as hidden terminal problem of spectrum sensing. On the other hand, the secondary users must sense the channels as correctly as possible to maintain the sensing reliability even in worst fading scenario to mange the interference to primary system below the predefined threshold.

To improve the sensing accuracy, i.e., sensitivity, of cognitive radio spectrum sensors and to make it more robust against the hidden terminal problem and channel fading irrespective of the sensing methods in use, cooperative spectrum sensing has been considered as an appropriate solution [69]. The concept of spectrum sensing with cooperation is to use multiple sensors distributed across the coverage area and combine their individual measurements into one common decision. The probability of miss detection and probability of false alarm would be considerably minimized when cooperative sensing technique is used [70] in addition to solve the hidden primary terminal problem and it may also lower the sensing duration [71].

Table 2.1: The comparison and summary of three spectrum sensing methods.

	Energy Detector	Matched Filter	Cyclostationary Detector
Test statistics	The total energy of received signal at the CR receivers	Correlation with the received signal at CR receiver and a replica of the signal	The cyclic spectrum density function of the received signal
Sensing accuracy	Low with no prior information of the PUs	High: It is optimum detection method with a short sensing time (It needs a prior information of the PU's signal).	Medium: It can differentiate between different PU signals.
Implementation complexity	Low: It is simple and easier to implement in practice.	High if the SU receivers need to estimate different types of PU signals, however pre-stored information can be used to reduce this complexity.	High but in less extent to that of the Matched Filter
Robustness against low SNR	low: The energy detector is very sensitive to noise power mismatch.	High: It offers good detection in very noisy scenarios.	Medium: Its performance in the low SNR is better than the energy detector.

When the cooperative sensing is performed among large number of secondary users or cooperative sensors, the sensing performance as well as the sensing reliability are significantly improved. In contrast, the complexity of the system

design also increases simultaneously due to the flooding of large number of control signals. Such control signals are possibly transmitted through the ISM band, dedicated band or even an underlay system such as ultra wide band. Therefore, an efficient information sharing algorithm is required to achieve the maximum benefits of the cooperation in cognitive radio enabled wireless communication.

When the distributed sensing devices detect the subchannel state, they are either shared among them or forwarded to the central processing unit depending on the mode of operation. Once the final decision is made, the spectrum sensing as well as channel sharing information are shared among the multiple users through the control channel. In many cooperative sensing method, the cognitive radio network is divided into the clusters and the decision information is transmitted to the cluster head in an assigned frame/slot [72]. While executing this task, the coordination algorithm should be designed such that the minimum delay is achieved [46]. The cooperative sensing is performed either centrally or in distributed fashion depending on where the sensing results are processed.

2.2.1 Centralized Sensing

In centralized spectrum sensing, individual spectrum sensors or secondary users sense the subchannel in its geographical location which are then collected at the central processing unit, also known as decision fusion centre (DFC). The available subchannels are identified at the DFC using various decision fusion rules which are being proposed in literature with their own pros and cons. The information is then multicasted through the dedicated control channel to the secondary users [73]. The obstructions in between primary and secondary systems may cause multipath fading and shadowing, however another user in its vicinity may have good channel condition which helps the cooperative detection process to be more robust than the case when single user is sensing the subchannel. Even the control channel could be under deep fading, however they are assumed to be a perfect channel in the network design.

Depending on the nature of sensing results obtained at the local sensors and the processing of information at the DFC, centralized sensing method are categorised as the soft combining and hard combining methods.

2.2.1.1 Soft Combining

In soft combining method, the locally sensed subchannel information is forwarded to the DFC without taking any local decision or hypothesis test [74]. The decision is made at the DFC by combining those unprocessed data using the appropriate methods. One of the conventionally used rule is the square law combining of received data from the individual sensing data. In this method, the estimated energy level is reported back to the DFC and all energy levels from secondary users are combined with square law which is then compared against the threshold value to decide the status of the subchannel. However, there are various methods to combine soft data together, such as correlation based soft combining [75].

Let us consider that there are $z = 1 \dots Z$ sensors or secondary users to cooperatively sense the subchannels. By assuming the noise vector $\boldsymbol{w}_{\mathrm{z}}$ and signal vector $\boldsymbol{x}_{\mathrm{z}}$ are independent for each sensors, the received signal vector from z sensors is obtained as $\boldsymbol{y} = [\boldsymbol{y}_1^T, \boldsymbol{y}_{\mathrm{z}}^T \dots \boldsymbol{y}_{\mathrm{Z}}^T]$. The log-likelihood ratio provides the test statistics as following.

$$\log\left(\frac{\Pr(\boldsymbol{y}|H_1)}{\Pr(\boldsymbol{y}|H_0)}\right) = \sum_{z=1}^{Z} \frac{||\boldsymbol{y}_z||^2}{\sigma_z^2} = \sum_{z=1}^{Z} \boldsymbol{\Lambda}_z, \tag{2.8}$$

where, $\boldsymbol{\Lambda}_z$ is the log-likelihood ratio from the z^{th} sensor. The statistics $\frac{||\boldsymbol{y}_z||^2}{\sigma_z^2}$ is the soft decision from z secondary users. The weighted sum in (2.8) is then compared against the threshold value to decide the status of the subchannels.

The soft combining cooperative technique provides accurate estimation of the subchannel status, however it need a relatively huge bandwidth due to embedding much information in control packets. On the other hand, if one of Z number of the secondary users is untrustworthy, it severely degrades the cooperative gain and therefore the spectrum sensing efficiency [76].

2.2.1.2 Hard Combining

The soft combining potentially require the complex structure of signal processing hardware because DFC may receive large amount of data to process. The best alternative of this technique is that the sensing devices take decision from the locally sensing data and quantize the decision in binary format, which are, in

general terms, known as hard decision bits. Therefore, in hard combining, the DFC is just to process the received bits and take the decision using various logic fusion rules; for instance, AND-logic rule, OR-logic rule, majority-count-login rule amongst others are proposed in literature [77].

When the individual sensing device z take local decision, the individual test statistics are quantized into a single bit such that $\Lambda_{(z)} \in \{0, 1\}$ are the hard decision bits. It indicates that when local test statistics is greater than the predefined threshold, the decision is taken as 1 which indicates the subchannel is busy. In other cases, the decision is taken as 0 which indicates the subchannel is idle. When there are Z number of sensors, the test statistic at the DFC using simple voting rule decides in favour of the hypothesis H_1 when the following condition is satisfied.

$$\sum_{z=0}^{Z-1} \Lambda_{(z)} \geq C, \tag{2.9}$$

where, $1 \leq C \leq Z$. The fusion AND, OR and majority count rules are the special cases when C is fixed at a particular value [40]. In cases when $C = Z$, the fusion rule is known as AND fusion rule in which all the local sensors must unanimously agree on the status of the subchannel. When $C = 1$, the fusion rule is known as OR-logic where even one of the sensing devices decides the channel to be idle, the channel is declared to be available to use by cognitive users. Finally, when $C = Z/2$, the decisions are fused using majority count rule where majority of the sensing devices must agree on the channel status. The detail of each method is skipped here, however they will be briefly described when they are used in the following chapters.

2.2.2 Distributed Sensing

When the number of secondary users are increased in centralized cooperation, the cooperation complexity is simultaneously increased. In the distributed cooperative sensing method, the sensing devices act as relay and share the subchannel status information with each other rather than sensing to the centralized DFC [78]. In this case, the secondary users according to their detection performance

may form a logical cluster on a temporary basis. Such cluster may be dynamically forming depending on the distribution of the sensing devices. However in some cases, the secondary users may share subchannel information to each other on an ad hoc manner where information is forwarded to its one hop neighbour using the amplify-and-forward technique.

The obvious advantage of distributed sensing is that no deployment of DFC is needed which reduces the implementation cost. However, the signalling overhead could be higher than in centralized system due to flooding of control signal among the sensors if the cluster is not perfectly formed. The sensing and reporting time is significantly reduced due to the decentralized decision taking procedure which helps to increase the system throughput [79]. The detail of this method will also be explained in next chapters when the proposed methods are presented in detail.

2.3 Challenges in Spectrum Sensing

Despite the spectrum sharing system is the solution to solve the spectrum scarcity problem, there are many impediments to achieve a balance tradeoff. The factors, for instance, interference protection, spectrum efficiency, energy efficiency, sensing duration, implementation cost etc., depend among each other and finding the optimal operating point is a challenging task in CRN.

The probabilities of false alarm and miss detection always maintain a fundamental tradeoff in spectrum sensing. The false alarm probability is related to the implementation cost in CRN whereas probability of miss detection is responsible for the performance of the sensing system. The higher the false alarm, the lesser is the spectrum opportunity, whereas, higher miss detection increases the interference to the primary system. In practice, unfortunately, both of them cannot be minimized simultaneously with a single detection algorithm or hardware. In the recently proposed methods, one probability is kept fixed and another probability is minimized. From primary system point of view, probability of miss detection is expected to be minimum, whereas from secondary system point of view, the probability of false alarm should be kept minimum. Therefore, the balance of both of them is an interesting as well as a challenging task.

The management of sensing accuracy and data transmission duration tradeoff is another challenging task in spectrum sensing. As a matter of fact, when the large number of samples are received at the secondary system receiver, the higher accuracy in spectrum sensing is achieved. However, in doing so, secondary users have to spend more slot duration to the sensing task which causes the shorter duration for data transmission [80]. As a result, the achievable spectral efficiency at the secondary system is minimized. Some solutions have been proposed in [81], [82] where the optimal sensing duration is possible to obtain which maximizes the secondary user throughput and, at the same time, the interference to primary system can be kept at minimum. However, a perfect tradeoff between sensing duration and throughput is very difficult to handle in practice.

When the cooperative method of spectrum sensing is used, irrespective of the decision fusion methods, the energy consumption of the secondary system increases when the number of cooperative users grows. Therefore, the energy efficient design of cooperative sensing method is always a challenging task. The methods such as censoring [83], sleeping [84], clustering [85], amongst others, have been proposed to solve energy consumption problems, however optimal sensing and energy tradeoff is difficult to achieve in cooperative CRN.

2.4 Conclusions

In this chapter, the spectrum sensing techniques for cognitive radio were described considering both advantages and disadvantages of predominant spectrum sensing methods. The energy detection method has been concluded to be the simplest one from the system design point of view, however it does not perform well under low receive SNR. The cyclostationary and matched filter based sensing have better sensing efficiency but they have higher system complexity due to the requirements of advance digital signal processors. The cooperative sensing method and various decision fusion methods have also been presented along with their merits and challenges. The cooperative sensing can reduce the probabilities of miss detection and false alarm while sensing the subchannels but the system complexity increases due to large number of control signals. The associated hard combining and soft combining methods were also discussed in detail.

The spectrum sensing for real signals in various radio spectrum, ranging from TV transmission in UHF and VHF to cellular and LTE bands, have also been discussed. The results demonstrated that the unused and under-utilized spectrum can be exploited to build a complete spectrum sharing system. The OFDMA subcarriers were also captured to show how OFDMA subcarriers can be allocated to the secondary users to realize the cognitive radio communication.

The fundamental limitations with non-cooperative sensing, which at the end when it comes to the sensing accuracy, could be addressed by means of cooperation among sensing devices. However in this case the sensing complexity needs to be addressed simultaneously. The problem with the current spectrum sensing method is that they do not exploit the network structure to reduce the signalling overhead without compromising the sensing accuracy of secondary system. This highly motivates to investigate a sensing method by means of distributed sensing network which would balance the tradeoff between sensing accuracy and signalling overhead.

Chapter 3

System Model

The generic system model is presented in this chapter which is going to be referred in the subsequent chapters with the required add-on features and functions where it is necessary. The system model in general accommodates the cellular network structure, channel model, frame structure in addition to other physical (PHY) and medium access control (MAC) layer technologies.

3.1 Network Modelling

The considered system model consists of a cellular network that is enabled with the cognitive radio functionality. The specific reason to focus on the cellular system for dynamic spectrum allocation is that cellular systems are in use throughout the world and many devices and data applications for the spectrum used for cellular communication are comprehensively researched, understood and implemented. On the other hand, the usage pattern of cellular spectrum is much more dynamic in comparison to the recently developed cognitive radio in TV spectrum for rural broadband in which spectrum identification is relatively simple because the spectrum is idle over the longer period of time [86]. Therefore, a robust, efficient and less complex system must be designed for cellular systems to efficiently utilize the idle or under-utilized portion of scarce cellular spectrum.

The reference system model is an autonomous cellular network where each secondary user (or distributed and independent sensing device) performs the spectrum sensing task and the subchannels are accessed if and only if the received

power on the channel is less than the threshold value. The considered cellular network is characterized by the fact that the intercell interference is inevitable due to the universal frequency reuse scheme. Therefore, the identical frequency bands can be allocated between two adjacent cells. As a result, a dynamic transmit power control at each base station is required in such systems to minimize the interference.

The cellular cognitive radio network can possibly be represented as an autonomous cellular network where primary system and secondary system are considered into the same geographical location sharing the common set of resources. Therefore, in a such autonomous cellular system, the role of adaptation in efficient resource allocation becomes increasingly important [87].

The considered system model is an infrastructure-based cellular CRN, also referred to as the secondary system, collocated with a legacy primary cellular network. The schematic of the considered network scenario is shown in Fig. 3.1. The primary users communicate with the primary base station and secondary users communicate with the cognitive radio base stations on the allocated time slots and frequency subchannels. The primary and secondary users are served by a single primary and secondary base station, respectively as considered in [88].

The transmit power control algorithm is executed in the secondary system and the primary system's transmit power is considered to be fixed, i.e., no power control mechanism is considered on the primary transmitter. Without loss of generality, all the transmitters and receivers in the system are equipped with the single omnidirectional antenna unless otherwise stated. The analysis however can be easily extended into sectorized cell by considering each sector as a cell with a single antenna. There is no direct signalling between the primary system and the secondary system.

3.2 Channel Modelling

The total frequency band of B Hz is licensed to the primary system which serves primary users for voice and data communications. The primary users are indexed by $j \in \{1, \ldots, J\}$. The spectrum of the primary system is shared with a secondary system for downlink transmission. The CRN is a multicell network with M

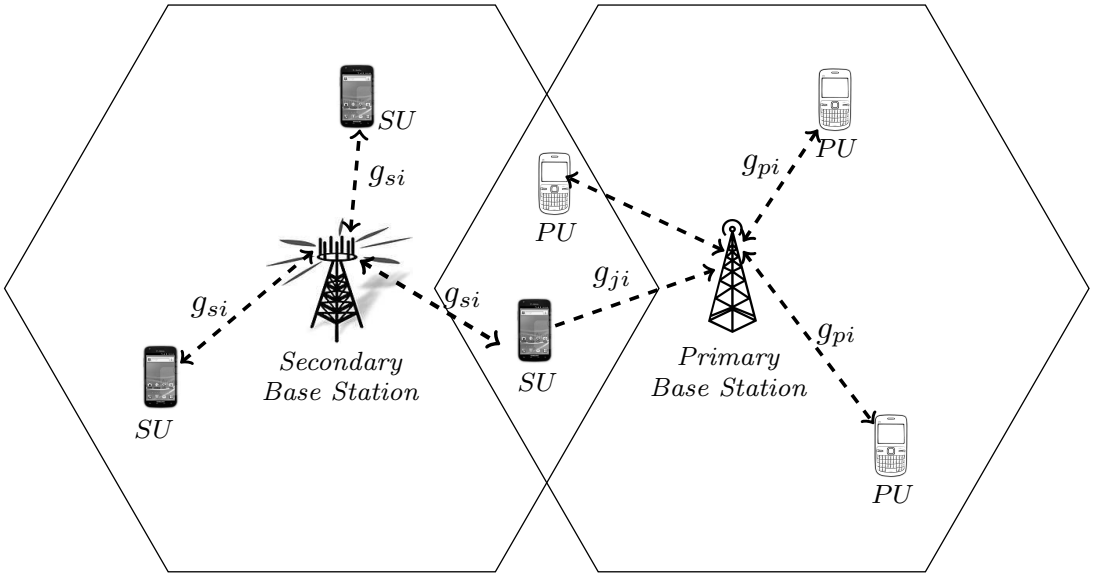

Figure 3.1: The considered cellular cognitive raido network as a reference system model.

secondary base stations (SBSs). In the central cell, SBS serves secondary users indexed by $s \in \{1, \ldots, S\}$. In addition, the radio spectrum is divided into N non-overlapping $B_i = B/N$ Hz subchannels which are indexed by $i \in \{1, \ldots, N\}$.

The communication link between the secondary transmitter to the secondary receivers, for subchannel $i \in \{1, \ldots, N\}$, referred to as secondary channel which is denoted by $g_{si}(\nu)$. Similarly, the secondary transmitter to the primary receivers, for subchannel $i \in \{1, \ldots, N\}$, is referred to as interference channel which is denoted by $g_{ji}(\nu)$. The parameter ν denotes the joint fading state which is dropped hereafter for brevity. Due to the small-scale frequency-dependent multipath propagation characteristics, each SU may experience different channel gains across different subchannels, $i = \{1, \ldots, N\}$, each with bandwidth of B_i Hz. Depending on the PU activity and its required QoS at a specific time and location, secondary users may have access to x number of subchannels where $0 \leq x \leq N$.

To sense the subchannels by secondary users and dynamically adjust their operating parameters, the physical layer of the secondary system needs to be highly

flexible as well as adaptable. The method of accessing the subchannels in multi-carrier transmission, also known as orthogonal frequency division multiple access (OFDMA), has the potential to fulfil the requirements [89]. Therefore, OFDMA has been highly anticipated to realize the cognitive radio concept to provide an scalable and adaptive technology for air interface. In the considered system model, the secondary system utilizes OFDMA to access N non-overlapping sub-channels.

When OFDMA is used, the subcarriers are grouped together into a cluster which are assigned to the individual user. This flexibility and adaptability makes this the best candidate transmission technology for cognitive radio. Such applications of OFDMA in cognitive radio have been considered in significant number of previous works as in [90], [91], [92]. The advantages of OFDMA in cognitive radio as summarized below.

- Since the spectrum sensing may be required to achieve the benefits of cognitive radio communication, the computational complexity of sensing algorithm is significantly lowered when OFDMA is implemented. It is due to the fact that the received signal is passed through the fast Fourier transform (FFT) circuitry in OFDMA system to convert time domain signal into the frequency domain. The primary signal detection can be performed on the received signal in frequency domain since the signal of primary system is spread over a group of range of FFT output samples.

- The improvement in spectrum utilization using the waveform shaping technique where some subcarriers can be turned off depending on the existence of primary users.

- The interoperability associated with OFDMA makes it a good choice for cognitive radio. Since OFDMA has been used in both long-range as well as short-range communication systems, cognitive radio networks equipped with OFDMA can be used with various technologies including WiMAX, IEEE 802.11x, IEEE 802.22, amongst others.

- Its adaptability to the changing environment is very good. For instance, it can adaptively change the transmit power, channel coding or modulation order based on the channel quality as well as the user requirements.

The objective in this system model is to maximize the parameters such as spectral efficiency or energy efficiency. The optimization problem is thus in the form of a utility function in terms of secondary system throughput and weighting factor, which, in its simplest form, could be formed as a linear combination as shown below:

$$\max \sum_{s \in \mathcal{S}} \sum_{i \in \mathcal{N}} \alpha_{si} R_{si}, \tag{3.1}$$

where R_{si} is the average rate for user s while accessing subchannel i. Also, $\mathcal{S}$ is the set of secondary users which access the available subchannels $\mathcal{N}$ whereas $\boldsymbol{\alpha}$ is the weighting factor which maintains fairness among the primary and secondary users due to the fact that the gain at secondary system comes at the expense of primary throughput because the interference is introduced at primary receivers [93]. Here, $\boldsymbol{\alpha}$ is the set of weights which is based on predefined QoS requirements and the primary users activity. The total transmit power and maximum interference to primary system constraints will also be considered in the proposed spectrum sensing and resource allocation methods.

3.3 Frame Structures

The frame structure of the considered spectrum sensing and sharing model is depicted in Fig. 3.2. Each frame consists of the sensing time slot which is followed by the data transmission slot. The secondary users have to sense a set of subchannels within the sensing duration using the energy detection as mentioned in chapter 2. The decisions are then shared among other cellular base stations or clusters within a cell depending on the system design. The information then provides whether the subchannel is idle or occupied by the primary users at particular time and location. If a particular subchannel is found to be idle, the secondary base station allows particular user to access the subchannel with

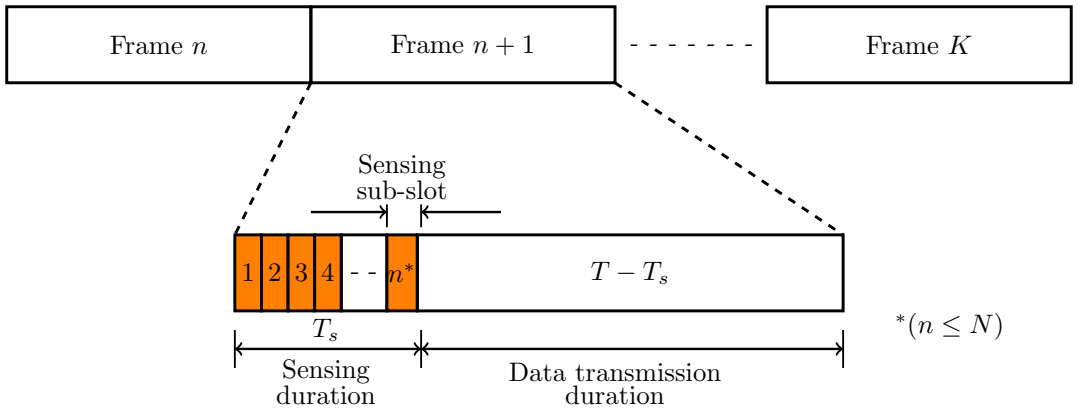

Figure 3.2: The frame structure of the considered reference system model with distinct sensing sub-slots and data transmission duration.

allocated maximum transmit power. When the subchannel is found to be busy due to possible arrival of primary user, a new subchannel is provided if one is currently available. The secondary user will have to immediately trigger the channel switching algorithm. If the subchannel is busy, the spectrum sensing technique is repeated again.

The sensing slot is allocated for the spectrum sensing in addition to execute many other cognitive radio related functions, for instance, decision taking, subchannel allocation and subchannel handoff whenever they are necessary. The frame duration is denoted as T out of which T_s, where $T_s \leq T$, is the sensing duration. Therefore, the data transmission duration is $T - T_s$. The secondary systems may be able to sense the multiple subchannels within the sensing duration in which case sensing duration is divided into the sub-slots. One sensing sub-slot is considered as the duration to sense a single subchannel. Therefore, there are maximum of N sensing sub-slots in which case the sensing slot is denoted as $T_s = \{T_{s1}, T_{s2}, \ldots, T_{sk}\}_{k \leq N}$.

In the considered system model, a very important tradeoff appears between the sensing duration and the data transmission duration, thus the throughput on the secondary system. In cases the Shannon capacity of the channel is considered as $R_c = \log_2(1+\text{SNIR})$ where SNIR is the received signal to noise and interference ratio, the effective throughput on the data transmission duration is achieved to

be $(T - T_s)R_c$. When the sensing duration is increased to enhance the sensing accuracy by receiving the larger number of samples for energy detection (or for any other detection methods), the transmission duration is significantly reduced which directly degrades the secondary system throughput. In other words, for any two sensing durations T_s^1 and T_s^2 such that $T_s^1 < T_s^2$, then $(T-T_s^1)R_c > (T-T_s^2)R_c$ which is described as a sensing-throughput tradeoff in CRN.

There have been series of proposed methods to find the optimal sensing time and transmit power allocation scheme with the aim of achieving maximum throughput. The CRN framework in [82] demonstrated that better achievable throughput is achieved when average power constraint, instead of instantaneous power constraint, is taken. Similarly, the design of optimal sensing time and ergodic throughput on secondary system in wideband sensing based spectrum sharing is presented in [53]. The auction based spectrum sensing and subchannel allocation is also presented in [94] with the underlay and overlay spectrum accessing schemes. However, the spectrum accuracy and the achievable throughput in CRN can never be attained simultaneously with any of the proposed methods. This is due to the fundamental limits of the available spectrum sensing mechanisms. To solve this issue, a fundamental change is necessary to design the spectrum sensing and throughput tradeoff from a unique and different perspective of system design. The instance considered here, which is described in the next chapter, is the independent sensing network model to achieve both with reduced signalling overhead.

3.4 Cognitive Radio Standard: IEEE 802.22

The discussion of spectrum sensing and resource allocation in cognitive radio enabled cellular network becomes incomplete without describing the IEEE 802.22 WRAN standard. It is also important to briefly mention it here because the standard will be frequently used in the subsequent chapters when the cellular CRN parameters have to be chosen while proposing new methods of spectrum sensing and resource allocation as well as for the comparison purpose.

The first worldwide wireless standard to realize the cognitive radio communication in practice is IEEE 802.22 which was released in July 2011. Therefore,

Table 3.1: The physical and medium access control layer parameters set for IEEE 802.22 WRAN standard.

FFT size	1024, 2048, 4096
Cyclic Prefix size	Variable
Bits per symbol	2, 4, 6
Pilots	96, 192, 384
Bandwidth	6, 7 and 8 MHz
Multiple access	OFDMA/TDMA
Code rate	$\frac{1}{2}$, $\frac{2}{3}$, $\frac{3}{4}$, $\frac{5}{6}$
Modulation schemes	BPSK, QPSK, 16-QAM, 64-QAM
Duplex	TDD
Frame size	Super-frame: 160 ms, frame: 10 ms

this is the milestone for future CRN technology because it employs a number of cognitive features such as spectrum sensing, subchannels allocation and transmit power control. It provides network access for users within a cell by sharing a vacant TV white spaces (TVWS) which has excellent radio propagation characteristics to improve the wireless broadband connectivity in rural areas [95]. Various technologies in PHY and MAC layers are considered in this standard, which defines the typical operating range of 17 to 30 km and up to maximum of 100 km is targeted in a particular geographical location with a maximum data rate up to 22Mbps [96]. All other PHY and MAC layer parameters set for IEEE 802.22 WRAN standard are shown in Table 3.1.

The PHY layer of this standard is based on the OFDMA in which 1680 subcarriers are grouped into the 60 subchannels. The modulation schemes are defined as binary phase shift keying (BPSK), quaternary phase shift keying (QPSK), 16-quadrature amplitude modulation (16-QAM) and 64-QAM. The MAC layer is responsible for the resource allocation in IEEE 802.22 standard in which a point-to-multipoint mode is adopted. Therefore, the proposed cellular topology consists

Table 3.2: The secondary users spectrum sensing sensitivity requirements for IEEE 802.22 standard.

	Analog TV	Digital TV	Wireless Microphone
Sensitivity	-94 dBm/6 MHz	-116 dBm/6 MHz	-107 dBm/6 MHz
SNR	1 dB	-21 dB	-12 dB
P_{d}	0.9		
P_{f}	0.1		
T_s	2 sec		

of a single secondary base station[1] communicate with many white-space-enabled user devices.

The IEEE 802.22 supports two different methods to detect the primary users on the subchannels. The first one is spectrum sensing methods and the second one is geolocation database (GD) approach. There are some technical difficulties to achieve the strict requirements set for spectrum sensing in TV band. The required sensing sensitivity and other parameters are summarized in Table 3.2. It can now be observed that some of the primary signals, e.g., digital TV, must be sensed at a very low SNR as well the devices must be able to sense the signal below the noise level. Furthermore, the probability of detection must be strictly maintained at or above 0.9 whereas the false alarm probability should be maintained below 0.1. All of the defined parameters ultimately results that the spectrum sensing in TVWS is a primary challenge.

In cases the spectrum sensing is not a reliable option for TVWS, the GD approach has also been considered to determine the presence or absence of primary services in the subchannels within the area of interest. The GD, in its basic form, stores and updates the channel availability information within TV band in certain area which is managed by spectrum management regulators[2]. Such database

[1]TV transmitters are obviously the primary system in this model.

[2]The GD based TV white spaces have been considered by regulators such as FCC and Ofcom. The FCC approved ten companies including Google, Spectrum Bridge, Telcordia etc.

information contains operating channels, duration of use, device transmit power, user location and such other relevant information. In this scheme, the secondary devices first send a query to the database server to know the available frequency channels in TV band within their location. It is obvious that such devices must be equipped with global positioning system (GPS) to find the precise location of the user. The devices then receive the list of unoccupied subchannels before initiating the communication [97].

The further step taken to enable GD is the radio environment mapping (REM) which can be considered as advance knowledge base which keeps record of multi-domain information about the subchannels and networks as well as the historical information. The optimal scheme to access such database information is still in the early research phase. However, recently proposed methods to choose the database access strategy are the probabilistic decision process [98] and Markov decision process [99], amongst others. In any accessing method, the existing rules must be properly addressed and at the same time they have to maximize the overall communication opportunities through the on-demand access.

3.5 Conclusions

In this chapter, the reference system model has been highlighted such that it will be easier in the next two chapters where system model is discussed with some add-on features. The network architecture is considered as infrastructure based multi-cellular network where independent primary and secondary cellular systems share the scarce radio spectrum. The network design has also been considered keeping in mind the multi-tier small cell network, i.e., heterogeneous network, as a network scenario for 5G and beyond. Therefore, the considered system model and the proposed methods of spectrum sensing and resource allocation in the next chapters are equally applicable to the next generation networks with minimum level of modification.

Since there are primary and secondary cellular systems, there are communication links, i.e. secondary transmitter to secondary receivers and primary transmitter to primary receivers, as well as interference links, i.e., from secondary

as a GD administrator and some of them have already completed the tests by 2015.

transmitter to primary receivers. The stochastic behaviour of such channel gains plays a vital role in system performance because they are random in nature and difficult to predict in real time. Therefore, assumptions are frequently made about the channel gains, such as channel reciprocity and probability distribution function with known parameters when they have to be modelled in practice. The basic channel property as well as some physical layer technologies have been also discussed in this chapter. In addition, OFDMA plays vital role to realize CRN which makes spectrum sensing task less computationally complex due to the FFT circuitry available in OFDMA. It also maintains higher spectrum utilization and is compatible with many existing systems and hardware.

The frame structure of the proposed system model is also discussed in this chapter. The sensing duration and data transmission duration together form a strict tradeoff in practice, also known as sensing and throughout tradeoff. Therefore, it is very important to implement the optimal sensing method to find the optimal sensing duration which maximizes the secondary system throughput by keeping interference to the primary system below the threshold level. The current work is highly inspired with this requirement by designing a novel technique of spectrum sensing to realize the cognitive radio in practice. Moreover, a brief working principle of first cognitive radio standard, i.e., IEEE 802.22, has been also discussed which is available in the TV band where the spectrum holes can be exploited to provide the remote broadband services.

Chapter 4

Low-Latency Zone-Based Cooperative Multichannel Spectrum Sensing

In wireless communications, data is often transmitted within the allocated time frames. The number of data bits transmitted in each time frame is directly related to the the system throughput. To enable the dynamic spectrum access (DSA) in cognitive radio communication, part of each time frame is allocated to spectrum sensing thus no transmission is allowed in this duration [22]. By increasing the sensing duration the sensing accuracy is also increased, however the remaining time for transmission thus the system throughput is also correspondingly decreased. This results in a fundamental trade-off between sensing accuracy and system throughput [43]. As a consequence, choosing the optimal value of sensing duration is a challenging task [53]. Therefore, a unique method of spectrum sensing is needed in CRN to achieve the better sensing-throughput tradeoff deal without increasing the sensing complexity and signalling overhead. In this chapter, the details of such spectrum sensing technique will be presented as one of the proposed methods.

Conventionally, the spectrum availability is sensed at the SUs which are randomly distributed over space and time. Fundamental characteristics of multiuser wireless environment including multipath fading, user mobility and hidden terminal problem, as well as limited sensing duration result in reducing the spectrum

sensing accuracy. Therefore, in such environments conventional sensing mechanisms are not able to efficiently sense the spectrum availability with an acceptable level of accuracy required for protecting the PUs from inevitable interference [100].

To address the sensing accuracy issue, cooperative spectrum sensing techniques have been introduced in literature, e.g., [101], [102], [103], [104]. In cooperative spectrum sensing, SUs sense the spectrum availability and share this information with other network entities. Spectrum availability decision is then made by combining the collected sensing information based on a rule, e.g., AND, OR or K-out-of-N[1] [43]. The advantages and challenges associated with the cooperative spectrum sensing are already discussed in Section 2.2 and Section 2.3. In such methods, the spectrum availability information obtained from multiple SUs can also be processed using more sophisticated techniques. Instances include weighting [41], multidimensional correlation [42] and minimizing the collision probability at the PUs [100]. In weighting, the share of the provided information by each sensor in the final decision is determined by a weighting vector which is a system design parameter. Further, [42] leverages the spatio-temporal correlations between spectral observations among various nodes and across different time instants to minimize the sensing cost and maximize its accuracy.

Various settings have been proposed for implementing cooperative spectrum sensing, e.g., [105] and references therein present the detail survey. The cooperative spectrum sensing proposed in [103] divides the coverage area into clusters, where the SUs perform spectrum sensing and base station acts as a decision fusion centre. The users considered as the cluster heads then make spectrum availability decisions. In such a cooperative sensing model, a higher sensing duration results in a shorter data transmission duration which results degradation in achievable data rate. In addition, the signalling overhead is also higher in the secondary system and the performance is highly sensitive to the reporting channel conditions.

The logical cluster formation proposed in [106] has been designed to tackle the issues due to the imperfect reporting channel conditions. In [107], the cluster formation is proposed based on the heterogeneous characteristics of primary and

[1]K-out-of-N rule is also mentioned as majority count rule in literature when $K \leq N/2$, however both can be used interchangeably in theory.

secondary users such that users in the same cluster sense the identical set of channels to increase the sensing accuracy. The cluster heads however act locally therefore unable to incorporate their location information into the network wide channel allocation. In addition, various decentralized cooperative schemes are proposed, e.g., [108], where no decision fusion entity exists and therefore the SUs themselves diffuse the received decisions.

In addition to the centralized and decentralized cooperative schemes, a relay-based multiple hops cooperative sensing is proposed in [109], where source to destination spectrum information is forwarded by the relay nodes, where either amplify-and-forward or decode-and-forward method is implemented. This tackles the issues of erroneous report channel by increasing the cooperation footprint.

A two channel sensing technique under imperfect spectrum sensing based on the independent set of access and backup subchannels is also proposed in [110], where both subchannels are sensed in a single time slot to improve the system performance by jointly considering spectrum sensing and spectrum access. Although cooperative sensing often improves the sensing accuracy, the corresponding signalling overhead further reduces the overall system throughput.

As a matter of fact, whether it is centralized, decentralized or relay-assisted cooperative model mentioned in [101]-[109], the formation of clusters is very challenging due to the time varying nature of the wireless channels and mobility of users. The merits of incorporating the location information are recognized in conventional cognitive radio [111] as well as in advance cooperative communication [105]. However, embedding the location information in the CRN design might increase the signalling overhead. The dynamic cluster formation algorithm also causes very high signalling overhead. Therefore, an independent spectrum monitoring network has been proposed in this chapter to improve the cooperative sensing efficiency with reduced complexity.

In majority of the available cluster based cooperative sensing approaches, in addition to the signalling overhead due to the cluster head selection, cooperative spectrum sensing also introduces extra spectrum sensing latency. This is due to the fact that the SUs need to allocate an extra part of their fixed time frame to transmit the sensing information to a fusion centre and then wait for the sensing decision to be made and received back. To address this issue, the sensor selection

algorithms have been proposed in [112], [113]. However, cooperative sensing fails to provide required low-latency access which is of an immense importance in use cases including M2M communications [114]. Also, M2M plays an important role in the structure of the Internet-of-Things (IoT) which will be mainly connected through wireless communications.

4.1 Sensor Network Enabled Spectrum Sensing

The framework to offload the cooperative sensing to an independent monitoring network has been proposed in [115] to tackle the latency issues due to the sensing durations. It comprises of sensors deployed within the coverage area of cellular network and continuously monitor the spectrum availability. The sensing information is then communicated by the sensors to a central entity on separate signalling channels. In this setting, by careful design of system parameters, the same level of accuracy is achieved without reducing the system throughput. There is, of course, cost associated with building the monitoring network, which is justified in [115] considering extraordinary price of radio spectrum in mobile communication bands. An independent network of sensors is further considered in [116],[117] for nomadic cognitive networks in urban and sub-urban areas. The advantages of considering a separate monitoring network are twofold. Firstly, it lowers the corresponding sensing latency due to the reduced sensing duration, thus the spectral efficiency is increased by offloading the spectrum sensing task to an independent monitoring network. Secondly, the spectrum sensing accuracy is significantly improved due to cooperative sensing.

The above mentioned techniques improve the sensing accuracy and the associated latency, however they ignore the location information of sensors. Due to very high number of objects in the coverage area, incorporating the location information into sensing is capable of enabling spectrum reuse across very small regions in the network coverage area which is, in the proposed method, is referred as *micro-spectrum-reuse*. Incorporating the exact location of the sensors however might introduce a new dimension to the spectrum sensing complexity and increases its associated costs. Instead in this chapter a simple *Zone-Based Cooperative Spectrum Sensing* will be proposed. The sensing architecture in the

proposed method is based on dividing the coverage area into zones and defining a zone aggregator (ZA) as an intermediate entity. A general case is considered here in which the spectrum is divided into number of channels (i.e., subchannels in multicarrier systems). The ZAs then process the sensing outcome of the sensors for each subchannel located in their corresponding zone. The aggregated decision for each zone is then passed to a fusion centre. In the proposed scheme, to address the overhead issue it is further devised a one-bit-per-subchannel signalling scheme between the ZAs and the fusion centre.

In the proposed method, a central decision fusion centre located, e.g., in the secondary base station then utilizes the aggregated sensing information in the network zones. The SBS accordingly allocates the available subchannels to maximize the spectral efficiency and keep the interference at the PUs below the system required threshold. The corresponding function of the DFC is formulated as an optimization problem and show that it is a convex optimization problem. The optimal detection threshold is then obtained for different cases with various spatial densities of ZAs and SBSs. We further obtain a close form for the optimal sensing threshold based on a weight-based approach.

Various factors are involved in the efficiency of the proposed method in this chapter, including number of zones and base stations, the spatial distribution of the sensing devices and the zone size. The impacts of these factors are deeply investigated on the system performance and propose techniques for efficient design of the corresponding parameters. This provides extra degrees of freedom in designing the spectrum monitoring network and provides quantitative insight on deployment of such networks. In the analysis of the proposed method, it is focused on energy detection as the main spectrum sensing method at the sensors. The analysis presented here can be extended to design the parameters for cases where other spectrum sensing techniques are utilized in the sensors.

In the proposed method, the latency associated with the spectrum sensing is the time required for signalling between the SUs and the DFC. For a given required spectrum sensing accuracy, it is also shown that the the proposed method ultimately provides a lower latency in comparison with conventional sensing meth-

ods[1]. Therefore, the proposed method provides enabling techniques and protocols for adopting DSA in low latency M2M communications.

The analyses presented here are unique as they provide quantitative insight on the achievable gain on the spectral efficiency using cooperative sensing based on an independent monitoring network.

Using simulations the investigation on the accuracy of spectrum sensing in the proposed method is performed as a function of the distributed sensing information. The achieved throughput gains of the proposed method for various network parameters, e.g., sensing duration, detection threshold, primary user activities, are also investigated. In addition, the proposed zone-based cooperative spectrum sensing method is compared against the reference model where there is no cooperation among the clusters or SBS. Moreover, the comparisons are also made with the cases where the spectrum sensing information is combined using only OR/AND method.

The contributions presented in this chapter are summarized as following.

1. A novel spectrum sensing method is proposed based on an independent spectrum monitoring network and devise the associated system, algorithms and signalling protocols which incorporate zone location information in the spectrum sensing. The proposed method in this chapter enables *micro-spectrum-reuse* and results in higher spectral efficiency, lower signalling overhead, and thus the lower latency in comparison to the cases where no subchannel monitoring network is implemented.

2. An analytical framework is developed with the objective of maximizing system throughput under various monitoring network scenarios subject to spectrum sensing accuracy and maximum tolerable imposed interference at the primary systems.

3. Extensive simulations confirm the analytical results and indicate the throughput performance and sensing latency improvement using the proposed sensing method. The simulation results also outline the parameter design ex-

[1]Hereafter, conventional sensing is referred to any spectrum sensing technique in SUs in which the time frames are divided into sensing, and transmission durations.

plain the role of various factors including spatial density of ZAs, and SBSs, primary system activity, and sensing threshold on the sensing performance.

4.2 Network Model

The general concepts of the system model, which consists of multi-cellular multi-carrier CRN, has been already presented in chapter 3 and further details and add-on features associated with the proposed techniques will be discussed in this chapter. A schematic of the system is shown in Fig. 4.1 in which a primary base station (PBS) provides service to the PUs which are randomly distributed within the coverage area. The secondary system is also a cellular network which utilizes OFDMA, where the frequency spectrum is divided into N non-overlapping channels. The detail of OFDMA in terms of cellular CRN is described in Section 3.2. The channel model and the frame format are also the same as described previously. The add-on components in this case are the distributed sensing devices for spectrum sensing purpose. Therefore, in addition to the cellular architecture, the concept of clusters is also designed for sensing purpose as shown in Fig. 4.1.

4.2.1 Spectrum Monitoring Network

The spectrum sensors are distributed uniformly within the coverage area. In practice, their locations can be engineered by the service providers. For simplicity, a homogeneous network of sensors is further assumed, where sensing parameters of all the sensor nodes are the same. Unlike the conventional sensing methods, where SUs sense the subchannels sequentially before accessing them, in the proposed method, the sensing task is offloaded to a spectrum monitoring network. In this setting, each sensing device detects the primary spectrum activity on a subset of channels, $i \in \{1, \ldots, N\}$, within a circular region with radius, r_{sen} and reports their availability to the SBS. As a result of the proposed independent sensing network, the sensing order of multiple subchannels becomes irrelevant due to the sufficiently longer sensing duration available. During transmitting the subchannel availability reports to the zone aggregators, the sensing function is stopped. The

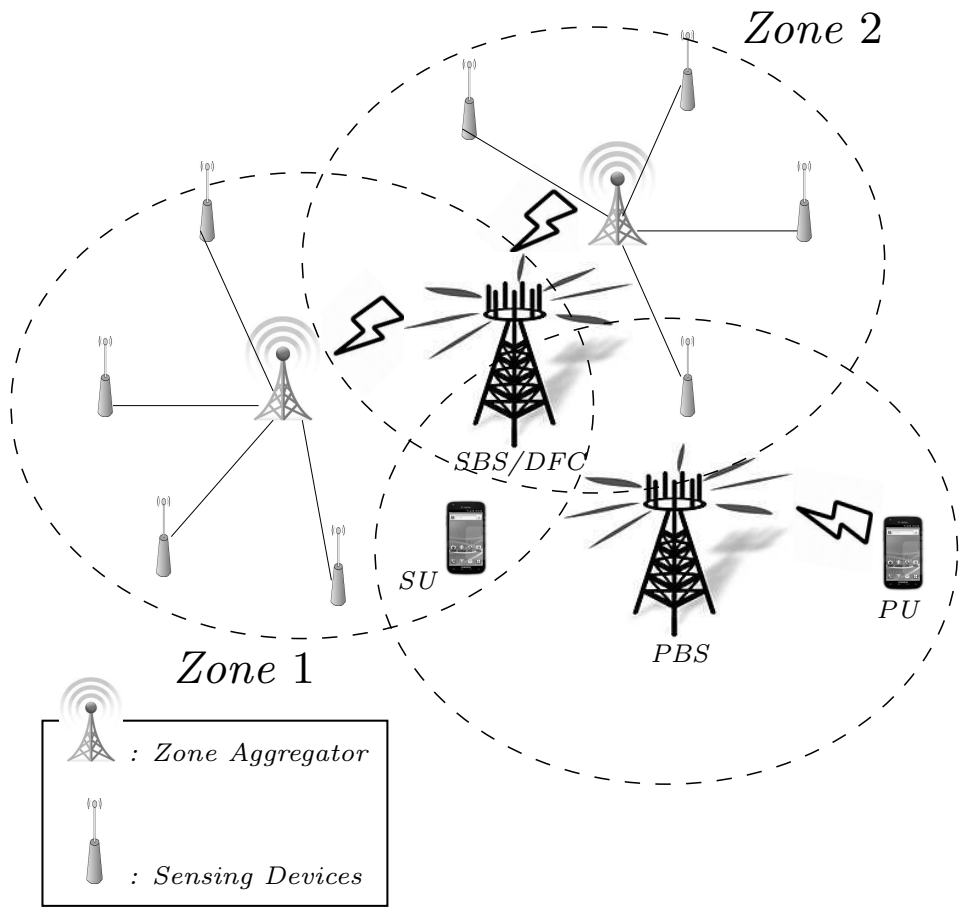

Figure 4.1: The system model for zone-based cooperative spectrum sensing technique.

connectivity of the sensing network therefore depends on r_{sen} and distribution of sensing devices.

To associate the sensing information with the location, the coverage area is then divided into the overlapped zones. The zones are chosen assuming a uniform distribution of sensing devices. In each zone, there is a zone aggregator (ZA) which receives the sensing information from sensors located in its circular sensing zone with radius r_{ZA}. The sensing devices and ZAs collectively form a monitoring network which is designed for cooperative spectrum sensing in the secondary network. Each ZA is associated to the location of its covered zone and

broadcast a pilot signal including a zone identification (ZID). Monitoring network utilizes a narrow band pre-allocated spectrum independent from the primary and secondary systems.

The received information in the ZAs is then processed and forwarded to the DFC located, e.g., in the SBS indexed by $m = 1, \ldots, M$. Based on the sensing information provided by the corresponding ZAs, DFC then decides the availability of each channels in that particular zone. Here, ZAs are indexed by $z = 1, \ldots, Z$, where Z is the number of zone aggregators in the system.

4.2.2 Sensing Devices

Sensors utilize energy detection technique for detecting the availability of the channels. Energy sensing has been considered here due to its simplicity and tractability as it does not need a priori channel information [84], [118] as explained in chapter 2.

The sampled signals received at the sensor during the sensing duration are $y_i[k] = w_i[k]$, and $y_i[k] = g_i[k]x_i[k] + w_i[k]$, under hypothesis H_0 and H_1, respectively, where H_0 (H_1) represents the absence (presence) of the primary signals. In addition, $y_i[k]$ is the k-th received sample over subchannel i and $g_i[k]$ is the channel gain from primary transmitter to the secondary receiver, i.e., the interference link, which is assumed to be fixed during the signalling period. Noise signal, $w_i(k)$, is independent and identically distributed circularly symmetric complex Gaussian with zero mean and variance of $\mathrm{E}[|w_i[k]|^2] = \sigma_w^2$. The detail of energy detection is same as explained in Section 2.1.1.

Time is slotted into frames in which the frame duration and the sensing duration for each sensing device are denoted by T, and $T_{s,i}$, respectively. The sampling frequency is f_s, thus the number of samples during the sensing duration is $K = T_{s,i} f_s$. The received signal energy is

$$\mathscr{E}_i[\mathbf{y}] = \frac{1}{K} \sum_{k=1}^{K} |y_i[k]|^2. \tag{4.1}$$

In cases where the PUs are communicating with the PBS, the transmitted signal is also being received by the sensing devices which are located within the

transmission range of the PU. Therefore, the sensors periodically sense subchannel i and obtain the corresponding test statistics, i.e., energy levels, and the hypothesis test is then performed based on the measured parameters and the system defined parameters. The performance of the spectrum sensing techniques, similar as mentioned previously, is characterized by false alarm and miss detection probabilities. For a subchannel i, the probability of false alarm, and miss detection are represented by $\mathcal{P}_{\mathrm{f,i}}$, and $\mathcal{P}_{\mathrm{m,i}}$, respectively, and detection probability is defined as $\mathcal{P}_{\mathrm{d,i}} = 1 - \mathcal{P}_{\mathrm{m,i}}$. The lower the detection probability, the higher is the chance of collision between PU and SU transmission; thus lower is the the system spectral efficiency. Similarly, having a higher false alarm results in under-utilization of the practically available primary spectrum by the SUs [22].

The miss detection and false alarm probabilities are obtained as Chi-squared distribution with $2K$ degrees of freedom, however it is shown, according to the central limit theorem, that for a large number of independent and identically distributed (i.i.d) samples ($K > 40$) obtained from primary transmitter, the cumulative density function (CDF) of the estimated energy can also be approximated by a normal distribution, see, e.g., [119]. In such cases, the false alarm and detection probabilities are as following [43].

$$\begin{aligned} \mathcal{P}_{\mathrm{f,i}}(\varepsilon_i, T_{s,i}) &= \Pr(\mathscr{E}_i[\mathbf{y}] > \varepsilon_i | H_0) \\ &\triangleq \mathrm{Q}\left(\left(\frac{\varepsilon_i}{\sigma_w^2} - 1\right)\sqrt{T_{s,i} f_s}\right), \end{aligned} \tag{4.2}$$

and

$$\begin{aligned} \mathcal{P}_{\mathrm{d,i}}(\varepsilon_i, T_{s,i}) &= \Pr(\mathscr{E}_i[\mathbf{y}] > \varepsilon_i | H_1) \\ &\triangleq \mathrm{Q}\left(\left(\frac{\varepsilon_i}{\sigma_w^2} - \gamma_i - 1\right)\sqrt{\frac{T_{s,i} f_s}{2\gamma_i + 1}}\right), \end{aligned} \tag{4.3}$$

where

$$\gamma_i = \frac{\mathrm{E}[|x_i|^2]|g_i|^2}{\sigma_w^2}$$

is the average received SNR of the PUs signal on subchannel i. Here, ε_i and $T_{s,i}$ are the energy detection threshold and sensing duration for the sensing devices.

Moreover, ε_i and $T_{s,i}$ are the design parameters and they represent the trade-off between $\mathcal{P}_{\mathrm{f,i}}(\varepsilon_i, T_{s,i})$, and $\mathcal{P}_{\mathrm{m,i}}(\varepsilon_i, T_{s,i}) = 1 - \mathcal{P}_{\mathrm{d,i}}(\varepsilon_i, T_{s,i})$ which is often referred to as receiver operating characteristics (ROC) curve [120]. One of the instances of ROC curve is described in Fig. 2.1. The sensing results and therefore the $\mathcal{P}_{\mathrm{f,i}}(\varepsilon_i, T_{s,i})$, and $\mathcal{P}_{\mathrm{m,i}}(\varepsilon_i, T_{s,i})$ are obtained from the individual ROC curve for each subchannel, therefore the subscript i can also be removed in this chapter for brevity to subsequently represent them as $\mathcal{P}_{\mathrm{f}}(\varepsilon_i, T_{s,i})$, $\mathcal{P}_{\mathrm{d}}(\varepsilon_i, T_{s,i})$ and $\mathcal{P}_{\mathrm{m}}(\varepsilon_i, T_{s,i})$, respectively.

4.3 Zone-Based Cooperative Spectrum Sensing

In the proposed method, spectrum sensors report the locally sensed subchannel decisions to their corresponding ZAs. ZAs then transmit their aggregated decision to the SBS. In cases when the SUs request for the new channel, an available subchannel from $\{1, \ldots, N\}$ is granted to the SU. Therefore, the efficiency of the proposed method depends on the accurate detection of the PU activity on each subchannel rather than sensing duration, since in the proposed method, sensors are, in fact, independent from the secondary network.

The logical AND rule is implemented at the ZAs which is applied on the sensing information collected from individual sensors in its corresponding zone. Based on AND rule, for a subchannel to be available in a zone all sensors located in a zone must unanimously agree on the subchannel availability. In other words, if any sensor in a given zone observes subchannel i as busy, then subchannel i is considered busy thus the SUs located in that zone are not granted access to subchannel i by the SBS. This rather pessimistic strategy is designed to best protect the active PUs within the zone. As a result, the achievable spectral efficiency in this case acts as a lower bound to the maximum achievable spectral efficiency. Other techniques, e.g., k-out-of-N, can be applied depending on the interference suppression capability of the primary system. In addition, using this fusion method maintains the mathematical tractability to obtain the sensing thresholds later in the paper. Here, SBS may also act as ZA in cases where the cell size is small such that sensors have direct communication with the SBS.

Corresponding to each subchannel, one bit information is generated by each sensor, where 0 indicates the subchannel is available and, 1 otherwise. For instance, if there are 10 sensors in a zone monitoring a total of 128 subchannels, for each sensing period, a total 1280 bits of signalling is transmitted in that zone. ZA then feeds back the subchannel availability to the DFC as a binary vector, where each entry shows the availability of the corresponding subchannel in that zone. DFC then allocates channels to maximize *micro-spectrum-reuse*.

The signalling diagram for the proposed zone-based cooperative sensing techniques is shown in Fig. 4.2. The sensing devices are synchronized and they sense the subchannels periodically. Therefore, every sensing device is programmed to sense the spectrum and reports its sensing decisions back to its corresponding ZA. The proposed protocol in this chapter is based on providing best-effort service to the SUs. The SU which requires access to the subchannel transmits a request message (REQ) to the SBS including its required bandwidth (B) as well as its corresponding ZIDs (Z_k). The received ZIDs by each SU act as a location pointer by enabling location pointer in the channel information field.

The DFC then allocates subchannels, $i \in \{1, \ldots, N\}$, to the SU in that zone (if any) as well as corresponding thresholds, I_{th}. Here, I_{th} is a system defined parameter and it is set by primary system according to their capacity to suppress the inter-zone interference, via a response message (RES). Furthermore, the DFC is able to incorporate other information in its decision making, such as subchannel and traffic variations. Thus DFC has a potential to act as a knowledge-based/expert entity which keeps record of relevant primary channel information such as traffic activities and load variations, transmission power, and subchannel power gain.

The SUs then start communicating on the allocated subchannels while constantly checking the ZIDs. Here, the coexistence beacon protocol is adopted as in [35] in which the subchannel information is embedded in the transmission. In the proposed method and later in the simulations, a unique identity is set for the PUs and SUs which is also embedded in their transmitted signal. As soon as a PU starts transmission, then using this unique identity field, the sensing devises are capable of recognizing that the detected signal is in fact from a PU transmitter. The monitoring network continuously senses the subchannels. Therefore, if

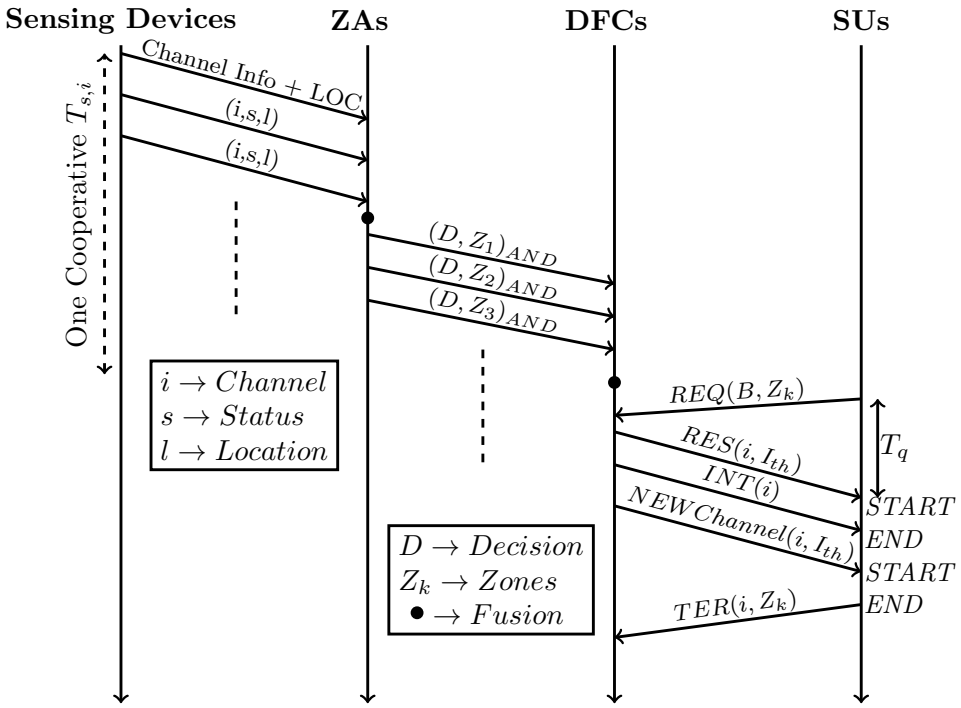

Figure 4.2: The signalling diagram of the proposed zone-based cooperative spectrum sensing technique.

a PU starts transmitting on a given subchannel, the SUs transmission on that subchannel is immediately stopped and other available subchannels, if any, will be allocated to that SU. Similarly, if a SU moves into another zone, i.e., its corresponding ZID is changed, the allocated subchannel in its original zone is released and a new subchannel, if available, is allocated to the SU in its new zone. Alternatively, to identify whether a detected signal is from a PU transmitter, inter-frame quiet period (IFQP) protocol [35] can also be implemented. In such cases, the DFC sends an interrupt message (INT) to the SU to immediately release the allocated subchannel(s). If SU still requires access and previously allocated subchannels are no longer available, a NEW message is sent by the DFC allocating new subchannel(s) (if available), where NEW message has same parameters as RES message. In cases, where the SU does not require access anymore, a terminating message (TER) is sent to the DFC to release the corresponding subchannels $i \in \{1, \ldots, N\}$ within zone Z_k.

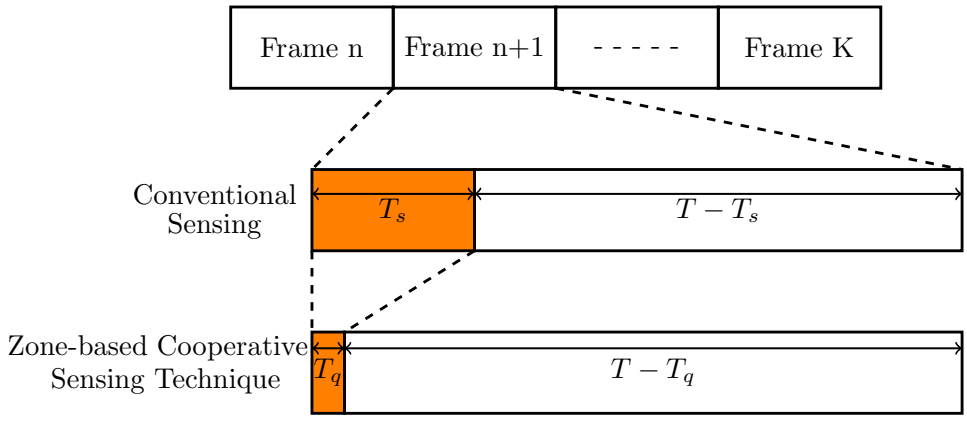

Figure 4.3: The time frame in the proposed method consists of the query duration (T_q), and transmission duration ($T - T_q$). In the conventional sensing, a frames consists of the sensing duration, $T_{s,i}$, and transmission duration ($T - T_{s,i}$).

In the proposed protocol for the zone-based cooperative spectrum sensing, the required signalling between the sensors and the ZAs, and similarly ZA and the DFC is designed to be very limited to reduce the spectrum resources allocated to the monitoring network. Note that a given subchannel might be available in more than one zones thus based on the proposed method in this chapter, *micro-spectrum-reuse* is expected to enable multiple zones inside the SBS coverage.

4.3.1 Offloading and Sensing Latency

The offloading technique of spectrum sensing activities to the independent sensing devices has a direct implication on the latency, and thus on the system throughput. Due to a separate sensing network which maintains almost real-time primary subchannel availability status, the corresponding subchannel allocation latency in the secondary user is significantly reduced comparing to the cases without the spectrum monitoring network. This has been investigated in detail which is presented in next section and finally the analysis is validated through the simulations.

The time frames structure of the proposed method and that of the conventional sensing are shown in Fig. 4.3. Here, $T_{s,i}$ is the sensing duration for the

conventional spectrum sensing and T_q is the duration of the required communication between the secondary system and the secondary base station. Hereafter, we refer to T_q as the query time, where $T_q << T_{s,i}$. The low latency of the proposed signalling method is due to substituting the sensing duration $T_{s,i}$ with T_q. The extra transmission time, $T_{s,i} - T_q$, results in increasing the total system spectral efficiency and its corresponding cost is deploying the spectrum monitoring network. Therefore, careful analysis is required to evaluate whether the gain on the spectral efficiency dominates the costs of deploying the monitoring network.

Without sensing devices, a portion of the frame duration, i.e., $T_{s,i}$, must be sacrificed for spectrum sensing by the SUs. As a result, a shorter time is available to the SUs for data transmission. Therefore, offloading the sensing task to the sensing devices significantly increases transmission durations without reducing the sensing accuracy. The optimal sensing duration, $T_{s,i}$ is not defined in WRAN standard [35], however it is shown in [43] that the optimal $\frac{T_{s,i}}{T}$ is 4% to 5%. In the proposed method, $\frac{T_q}{T_{s,i}}$ is chosen to be less than 1%.

Because of the independent spectrum sensing network, the sensing devices are able to sense the subchannel throughout the frame duration. Therefore, using the zone-based cooperative sensing protocol enables simultaneous sensing, in the monitoring network, and data transmission at the secondary system. In this case, the only time interval required for obtaining the availability of the subchannel is T_q which is the duration of signalling between REQ messages sent by the SU and RES message sent by the DFC. The signalling duration in the proposed method is a very small fraction of sensing duration of the conventional approach of spectrum sensing.

4.4 Sensing Design

4.4.1 Spectrum Sensing Accuracy

Inaccurate sensing either negatively affects the primary system performance through creating interference (in cases of miss detection), or results in a lower spectral efficiency in the secondary network by missing an actual access opportunity (in cases

of false alarm). To investigate the sensing accuracy, here it is simply assumed that the sensors are uniformly distributed in the network coverage area.

Lemma 4.1. *In a monitoring network with Z ZAs/cell indexed by $z = 1, \ldots, Z$ and M cooperative SBS indexed by $m = 1, \ldots, M$, the probability of accurate sensing for equiprobable hypotheses subchannels [121], $i \in \{1, \ldots, N\}$, at the SBS is:*

$$\mathcal{P}_{cs,i}^{(SBS)} \triangleq 1 - \left[\left\{ 1 - \mathcal{P}_d(\varepsilon_i, T_{s,i}) \right\}^Z + \left\{ \mathcal{P}_f(\varepsilon_i, T_{s,i}) \right\}^Z \right]^M, \forall i. \tag{4.4}$$

Proof. See Appendix A.

Remark 4.1. *The probabilities for hypotheses H_0, and H_1 are denoted by P_{H_0}, and P_{H_1}, respectively. Equiprobable subchannel assumption indicates that half of the channels are busy at any observation window. However, the analytical and simulation results in the next sections in this paper are equally credible for other scenarios, for instance, unutilized, i.e., $P_{H_0} << 0.5$, underutilized, i.e., $P_{H_0} > 0.5$, and crowded, i.e., $P_{H_0} > 0.9$ subchannels. This assists obtaining analytical solutions in terms of detection threshold, and normalized throughput later in this Thesis.*

Here, Lemma 1 indicates that $\mathcal{P}_{cs,i}$ depends on probabilities of miss detection and false alarm, as well as the number of ZAs and sensors in each zone. This provides two new degrees of freedom which could be exploited to improve the sensing accuracy. In practical systems, the summation of the two terms inside the bracket in (4.4) constitutes a small value for a given sensing device. This is due to the fact that miss detection and false alarm probabilities cannot independently adopt arbitrary values as they follow the corresponding sensors' ROC.

Note that in (4.4), $\mathcal{P}_{cs,i} \in [0, 1]$ which can be obtained by varying the operating points in ROC curve within the limits, i.e., $\mathcal{P}_{\mathrm{m}}(\varepsilon_i, T_{s,i}) \leq 0.5$, and $P_{\mathrm{f}}(\varepsilon_i, T_{s,i}) \leq 0.5$. These cases will be considered as constraints while formulating the optimization problem $\mathcal{P}_1$. By applying these constraints, it is assured that the probability of correctly sensing the subchannel stays within the feasible range and therefore

value of $\mathcal{P}_{cs,i}$ stays within 0 and 1. This also ensures the protection from system failure due to the bad detectors. Therefore, the worst detection cases, e.g., $\mathcal{P}_{\mathrm{f}}(\varepsilon_i, T_{s,i}) \geq 0.5$ and $\mathcal{P}_{\mathrm{m}}(\varepsilon_i, T_{s,i}) \geq 0.5$, are excluded in the proposed method. As a result, if a subchannel is badly detected, the resources will not be allocated by the SBS to any user to protect the primary users from probable interference.

4.4.2 Optimal Sensing to Improve Spectral Efficiency

Here, the system function as an optimization problem is formulated with the objective of maximizing the spectral efficiency at the secondary system. In addition, R_i^{00}, and R_i^{01} are the SUs' throughput conditioned over hypotheses H_0, and H_1, respectively. Therefore, based on conditional probability of correctly sensing the subchannel and [43], [53], the achievable throughput is obtained as $\frac{T-T_{s,i}}{T}\left(\mathcal{P}_{cs,i|H_0}P_{H_0}R_i^{00} + \mathcal{P}_{cs,i|H_1}P_{H_1}R_i^{01}\right)$. Assuming equiprobable hypothesis in which $P_{H_0} = P_{H_1}$ as in [121], the secondary system throughput for subchannel i is reduced as following.

$$R(\varepsilon_i, T_{s,i}) = \frac{T - T_{s,i}}{T} P_{H_1}\left[\mathcal{P}_{cs,i}R_i^{00} + \mathcal{P}_{cs,i}R_i^{01}\right], \forall i. \tag{4.5}$$

Here, $\mathcal{P}_{cs,i}$ represents the measure of spectral efficiency of the secondary system. A higher sensing accuracy contributes towards a higher spectral efficiency thus improves the system throughput.

For a special case of $Z = M = 1$, using (4.4) and (4.5) the total secondary system throughput, $R(\varepsilon_i, T_{s,i})$, is

$$\frac{T - T_{s,i}}{T} P_{H_1}\left[(1-\mathcal{P}_{\mathrm{f}})R_i^{00} + (1-\mathcal{P}_{\mathrm{f}})R_i^{01} - K_L\right], \tag{4.6}$$

where, $K_L = P_{H_1}\left[(1-\mathcal{P}_{\mathrm{d}})R_i^{00} + (1-\mathcal{P}_{\mathrm{d}})R_i^{01})\right]$ is the throughput loss due to the miss detection ($\mathcal{P}_{\mathrm{m}} > 0$). Note that if $\mathcal{P}_{\mathrm{m}} \to 0$, then $K_L \to 0$.

For given values of Z and M, the optimal sensing parameters are obtained via the following optimization problem.

Problem $\mathcal{P}_1$**:**

$$\max_{\varepsilon_i, T_{s,i}} \quad R(\varepsilon_i, T_{s,i}), \tag{4.7a}$$

$$\text{s.t.} \quad I_p(\varepsilon_i, T_{s,i}) \leq \bar{I}_{th}, \tag{4.7b}$$

$$\mathcal{P}_{\mathrm{m}}(\varepsilon_i, T_{s,i}) \leq \bar{\mathcal{P}}_{\mathrm{m}}, \tag{4.7c}$$

$$\mathcal{P}_{\mathrm{f}}(\varepsilon_i, T_{s,i}) \leq \bar{\mathcal{P}}_{\mathrm{f}}, \ \forall i, \tag{4.7d}$$

where

$$I_p(\varepsilon_i, T_{s,i}) = \sum_i \mathcal{P}_{\mathrm{m,i}}(\varepsilon_i, T_{s,i}) P_{t,s} \ g_i \tag{4.8}$$

is the aggregated interference received at the PUs. For subchannel i, (4.7b) ensures that the received interference remains below the given threshold level, $\bar{I}_{th}$. This will protect the PUs against the potential sensing errors [122]. In addition, the minimum detection probability of "spectrum holes" is enforced by (4.7c) and (5.17a). In $\mathcal{P}_1$, $P_{t,s}$ is the SU's maximum transmit power, g_i is the channel gain between the secondary transmitter and the primary receiver, and $\bar{\mathcal{P}}_{\mathrm{m}}$, and $\bar{\mathcal{P}}_{\mathrm{f}}$ are the maximum miss detection, and false alarm probabilities, respectively. These parameters are provided by the related communication standards, see, e.g., [35].

In $\mathcal{P}_1$, $P_{H_0} R_i^{00} + P_{H_1} R_i^{01}$ is constant during a time frame duration, T. Moreover, in the proposed method, $T_{s,i} = T_q \ll T$, therefore $\frac{T - T_{s,i}}{T}$ is almost constant (See Fig. 4.3) which is referred to as T_{Tx} throughout this Thesis. Consequently, the only optimization parameter in $\mathcal{P}_1$ is $\mathcal{P}_{cs,i}$, which is a function of ε_i, and $T_{s,i}$.

Based on the above, $\mathcal{P}_1$ is then reduced to the following optimization problem.

Problem $\mathcal{P}_2$**:**

$$\max_{\varepsilon_i, T_{s,i}} \quad 1 - \left[\left\{ 1 - \mathcal{P}_d(\varepsilon_i, T_{s,i}) \right\}^Z + \left\{ \mathcal{P}_{\mathrm{f}}(\varepsilon_i, T_{s,i}) \right\}^Z \right]^M, \tag{4.9a}$$

$$\text{s.t.} \quad \sum_i \mathcal{P}_{\mathrm{m}}(\varepsilon_i, T_{s,i}) P_{t,s} g_i \leq \bar{I}_{th}, \tag{4.9b}$$

$$\mathcal{P}_{\mathrm{m}}(\varepsilon_i, T_{s,i}) \leq \bar{\mathcal{P}}_m, \tag{4.9c}$$

$$\mathcal{P}_{\mathrm{f}}(\varepsilon_i, T_{s,i}) \leq \bar{\mathcal{P}}_f, \ \forall i. \tag{4.9d}$$

The following set of Lemmas are needed for further analysis to obtain the solutions of $\mathcal{P}_2$. It is also due to the fact that (4.9c) and (5.17b) are the probabilistic constraints which make the optimization problem difficult to handle, thus

difficult to obtain the closed form solution. Therefore, it is necessary to find the equivalent approximation with the deterministic nature with the help of following Lemmas.

Lemma 4.2. *If* $\mathcal{P}_m(\varepsilon_i, T_{s,i}) \leq 0.5$, *and* $\mathcal{P}_f(\varepsilon_i, T_{s,i}) \leq 0.5$, *then* $\sigma_w^2 \leq \varepsilon_i \leq (1 + \gamma_i)\sigma_w^2$.

Proof. See Appendix B.

Here, the necessary conditions to maximize the system throughput are therefore $\mathcal{P}_{\mathrm{d}}(\varepsilon_i, T_{s,i}) \geq 0.5$ and $\mathcal{P}_{\mathrm{m}}(\varepsilon_i, T_{s,i}) \leq 0.5$ must be maintained at the cognitive radio system. Moreover, they also exactly follow the requirements of one of the cognitive radio standards, i.e., IEEE 802.22, in practice.

Lemma 4.3. *For a fixed,* $T_{s,i}$, *and* $\varepsilon_i \geq \sigma_w^2$, $\mathcal{P}_f(\varepsilon_i, T_{s,i})$ *is a decreasing and convex function of* ε_i.

Proof. See Appendix C.

Lemma 4.4. *For a fixed* $T_{s,i}$, $\varepsilon_i \leq (1 + \gamma_i)\sigma_w^2$, $\mathcal{P}_m(\varepsilon_i, T_{s,i})$ *is an increasing and convex function of* ε_i.

Proof. See Appendix D.

Using Lemmas 4.2 - 4.4, the probabilistic constraints in (5.17b) and (4.9c) are approximated by $\sigma_w^2 \leq \varepsilon_i \leq (1 + \gamma_i)\sigma_w^2$.

Using Lemmas 4.2, 4.3 and 4.4 it is straightforward to prove the following Lemma.

Lemma 4.5. *For a given* $T_{s,i}$, *if* $\mathcal{P}_m(\varepsilon_i, T_{s,i}) \leq 0.5$, *and* $\mathcal{P}_f(\varepsilon_i, T_{s,i}) \leq 0.5$, *then* $\mathcal{P}_m(\varepsilon_i, T_{s,i})$, *and* $\mathcal{P}_f(\varepsilon_i, T_{s,i})$ *are both convex functions of* ε_i.

It is now important to examine the convexity of the constraints defined in $\mathcal{P}_2$ to further generalize the problem [123]. Therefore, the following Lemma is also needed for further simplification of $\mathcal{P}_2$.

Lemma 4.6. Lemma 6: *For* $\sigma_w^2 \leq \varepsilon_i \leq (1+\gamma_i)\sigma_w^2$, $\mathcal{P}_m(\varepsilon_i, T_{s,i})$ *and* $\mathcal{P}_f(\varepsilon_i, T_{s,i})$ *are decreasing convex functions of* $T_{s,i}$.

Based on Lemmas 4.2 - 4.5, it can be easily concluded that both $\mathcal{P}_{\mathrm{m}}(\varepsilon_i, \overline{T}_{s,i})$ and $\mathcal{P}_{\mathrm{f}}(\varepsilon_i, \overline{T}_{s,i})$ are convex functions of ε_i, where sensing duration is fixed at $\overline{T}_{s,i}$ under the conditions to protect the PUs. Here, the conditions to maximize the throughput are: $\mathcal{P}_{\mathrm{d}}(\varepsilon_i, T_{s,i}) \geq 0.5$, and $\mathcal{P}_{\mathrm{m}}(\varepsilon_i, T_{s,i}) \leq 0.5$, which are the requirements of IEEE 802.22 standards [35].

Based on the above, $\mathcal{P}_2$ is approximated as the following.

Problem $\mathcal{P}_3$**:**

$$\max_{\varepsilon_i} \quad 1 - \left[\left\{ 1 - \mathcal{P}_{\mathrm{d}}(\varepsilon_i) \right\}^Z + \left\{ \mathcal{P}_{\mathrm{f}}(\varepsilon_i) \right\}^Z \right]^S, \tag{4.10a}$$

$$\text{s.t.} \quad \sum_i \mathcal{P}_{\mathrm{m}}(\varepsilon_i, T_{s,i}) P_{t,s} g_i \leq \bar{I}_{th}, \tag{4.10b}$$

$$\sigma_w^2 \leq \varepsilon_i \leq (1+\gamma_i)\sigma_w^2, \ \forall i. \tag{4.10c}$$

In $\mathcal{P}_3$, (4.10c) is convex under the stated conditions in Lemmas presented above. The interference constraint at the PU, (4.10b), is due to the imperfect channel sensing, where $|g_i|^2$ is the gain of subchannel i. Here, $P_{t,s} > 0$ is the transmission power of the SU and $\mathcal{P}_{\mathrm{m,i}}(\varepsilon_i, \overline{T}_{s,i})$ is a convex function of ε_i under the condition given in Lemma 4.2. Since non-negative sum of convex functions is a convex function in the same domain, the interference constraint is also a convex function of ε_i. To show the convexity of $\mathcal{P}_3$, it is further needed to investigate (4.10a). Note that throughout this chapter $\mathcal{P}_{\mathrm{m(f)}}(\varepsilon_i, \overline{T}_{s,i})$ and $\mathcal{P}_{\mathrm{m(f)}}(\varepsilon_i)$ are interchangeably used for brevity.

Corollary 4.1. *In the zone-based cooperative spectrum sensing, for any combination of* M *and* Z*, the throughput, (4.10a), is a concave function of* ε_i .

Proof. See Appendix E.

Based on the above, $\mathcal{P}_3$ is a convex optimization problem.

4.4.3 Optimal Detection Threshold

When the spectrum sensing problem is a linear programming problem, several established methodologies to solve such problems, such as simplex and interior point methods, do exist. However, even when the optimization problem is non-linear but its convexity could be established, as explained in the previous sections for the current system model, several known methods can be employed to solve such problems. One of the examples is of course to use the Lagrangian duality method, where local optimal is also the global optimal solution, usually with the application of Karush-Kuhn-Tucker (KKT) conditions [124]. Therefore, the Lagrangian method is implemented here to find the solutions of $\mathcal{P}_3$ and the Lagrange duality property is applied as described in [125]. The Lagrangian function corresponding to $\mathcal{P}_3$ is

$$\begin{aligned}\mathcal{L}(\varepsilon_i, \lambda_1, \boldsymbol{\lambda_2}, \boldsymbol{\lambda_3}) =& 1 - \left[\left\{1 - \mathcal{P}_{\mathrm{d}}(\varepsilon_i)\right\}^Z + \left\{\mathcal{P}_{\mathrm{f}}(\varepsilon_i)\right\}^Z\right]^M \\ &+ \lambda_1(I_{th} - \sum_{i=1}^{N} \mathcal{P}_{\mathrm{m}} P_{t,s}\ g_i) + \sum_{i=1}^{N} \lambda_{2i}(\varepsilon_{max} - \varepsilon_i) \\ &+ \sum_{i=1}^{N} \lambda_{3i}(\varepsilon_i - \varepsilon_{min}),\end{aligned} \tag{4.11}$$

where, $\varepsilon_{max} = (1+\gamma_i)\sigma_w^2$, $\varepsilon_{min} = \sigma_w^2$, and λ_1, $\boldsymbol{\lambda_2}$, $\boldsymbol{\lambda_3}$ are non-negative Lagrangian dual variables corresponding to the constraints. Here, λ_1 is scalar because subchannel i accessed exclusively by only one PU. The interference constraint protects the PUs on subchannel $i = 1, \ldots, N$ in case of miss detection. Similarly, $\boldsymbol{\lambda_2}$ and $\boldsymbol{\lambda_3}$ are the Lagrangian multipliers associated with detection threshold constraints. Throughput this Thesis, vectors are presented using bold fonts.

The corresponding duality gap is expected to be zero as $\mathcal{P}_3$ is convex and the Slater's condition [125] is satisfied. The KKT conditions for any set of ε_i^*, λ_1, $\boldsymbol{\lambda_2}$,

$\boldsymbol{\lambda_3}$ are [125]:

$$\nabla \mathcal{L}(\varepsilon_i^*, \lambda_1^*, \boldsymbol{\lambda_2^*}, \boldsymbol{\lambda_3^*}) = \mathbf{0}, \tag{4.12a}$$

$$I(\varepsilon_i^*) \leq I_{th}, \tag{4.12b}$$

$$\lambda_1^* > 0, \boldsymbol{\lambda_2^*} \succ \mathbf{0}, \boldsymbol{\lambda_3^*} \succ \mathbf{0}, \tag{4.12c}$$

$$\lambda_1^*(I_{th} - \sum_{i=1}^{N} \mathcal{P}_{\mathrm{m,i}} P_{tx}\ g_i) = 0, \tag{4.12d}$$

$$\sum_{i=1}^{N} \lambda_{2i}(\varepsilon_{max} - \varepsilon_i^*) = 0, \tag{4.12e}$$

$$\sum_{i=1}^{N} \lambda_{3i}(\varepsilon_i^* - \varepsilon_{min}) = 0, \quad \forall i. \tag{4.12f}$$

Here, a similar approach as in [122] is followed to obtain the solutions. If the condition $\sigma_w^2 < \varepsilon_i < (1+\gamma_i)\sigma_w^2$ holds, the constraint (4.12b) becomes linear, i.e., $I(\varepsilon_i^*) = I_{th}$. Therefore, for any $\lambda_1^* \geq 0$, $\lambda_1^*(I_{th} - I(\varepsilon_i^*)) = 0$.

The complementary slackness conditions in (4.12e) and (4.12f) are further analysed. From (4.12e), for $\lambda_{2i}^* > 0$ for any subchannel, $\varepsilon_{max} - \varepsilon_i^* = 0$, the optimal detection value, ε_i^*, is equal to ε_{max}. For cases where $\lambda_{2i}^* = 0$ for any subchannel i, then $(\varepsilon_{max} - \varepsilon_i^*) > 0$, therefore $\varepsilon_i^* < \varepsilon_{max}$. Similar observation on (4.12f) results in $\varepsilon_i^* > \varepsilon_{min}$. Under the same condition, $\lambda_{3i}^* = 0$ for any channel, $i = \{1, \ldots, N\}$. However, this assumption may not be correct anymore in case of $\varepsilon^* \notin [\varepsilon_{min}, \varepsilon_{max}]$, since the optimization problem is exclusively convex within this interval.

In the considered multi-channel scenario, it is now assumed that the subchannels are identically distributed and sensed similarly, thus the results obtained are valid for all subchannels, $i \in \{1, \ldots, N\}$. Therefore, the subchannel index i is dropped hereafter for brevity. From the Lagrangian stationary point, (4.12a), is

$$\frac{\partial \mathcal{L}(\varepsilon^*, \lambda_1^*, \boldsymbol{\lambda_2^*}, \boldsymbol{\lambda_3^*})}{\partial \varepsilon} = 0. \tag{4.13}$$

If both Z and M vary, then it is not easy to obtain a closed form solution for $\mathcal{P}_3$. Instead, this problem is solve separately for different numbers of Z and M

Table 4.1: The optimal SNR threshold for different scenarios

Scenario 1 $(Z=1,\ M=1)$	$\varepsilon_X = \frac{\sigma_w^2}{2\gamma}\left[\gamma_c + \frac{2}{f_s T_s}\ln\left(\frac{T_{Tx}}{T_{Tx}+\lambda_1 P_{t,s}\ g}\right)\right]$
Scenario 2 $(Z=2,\ M=1)$	$\varepsilon_X = \frac{\sigma_w^2}{2\gamma}\left[\gamma_c + \frac{2}{f_s T_s}\ln\left(\frac{2\overline{\mathcal{P}}_{\mathrm{f}} T_{Tx}}{2\overline{\mathcal{P}}_{\mathrm{m}} T_{Tx}+\lambda_1 P_{t,s}\ g}\right)\right]$
Scenario 3 $(Z=3,\ M=1)$	$\varepsilon_X = \frac{\sigma_w^2}{2\gamma}\left[\gamma_c + \frac{2}{f_s T_s}\ln\left(\frac{3\overline{\mathcal{P}}_{f}^2 T_{Tx}}{3\overline{\mathcal{P}}_{\mathrm{m}}^2 T_{Tx}+\lambda_1 P_{t,s}\ g}\right)\right]$
Scenario 4 $(Z=1,\ M=2)$	$\varepsilon_X = \frac{\sigma_w^2}{2\gamma}\left[(\gamma+1)^2 - 1 + \frac{2}{f_s T_s}\times\ln\left(\frac{2(\overline{\mathcal{P}}_{\mathrm{m}}+\overline{\mathcal{P}}_{\mathrm{f}}) T_{Tx}}{2(\overline{\mathcal{P}}_{\mathrm{m}}+\overline{\mathcal{P}}_{\mathrm{f}}) T_{Tx}+\lambda_1 P_{t,s}\ g}\right)\right]$
Scenario 5 $(Z=1,\ M=3)$	$\varepsilon_X = \frac{\sigma_w^2}{2\gamma}\left[(\gamma+1)^2 - 1 + \frac{2}{f_s T_s}\times\ln\left(\frac{3(\overline{\mathcal{P}}_{\mathrm{m}}+\overline{\mathcal{P}}_{\mathrm{f}})^2 T_{Tx}}{3(\overline{\mathcal{P}}_{\mathrm{m}}+\overline{\mathcal{P}}_{\mathrm{f}})^2 T_{Tx}+\lambda_1 P_{t,s}\ g}\right)\right]$

similar to the approach used in proving Corollary 4.1. Here, ε_M is obtained which is defined as sensing detection threshold for all subchannels, where M is constant. Similarly, ε_Z is then obtained which is defined as sensing detection threshold for all subchannels, where Z is constant. The optimal detection threshold will be shown to be a linear combination of ε_M and ε_Z.

The optimal detection threshold for various design scenario has been summarized in Table 4.1 where ε_X is either ε_Z or ε_M. In the following, each scenario shown in the table will be investigate in detail for further analysis and to obtain the closed form optimal solution.

4.4.3.1 Scenario 1 ($Z = 1, M = 1$)

In this case, (4.13) is rewritten as

$$\begin{aligned}\frac{\partial \mathcal{L}_1(\varepsilon^*, \lambda_1^*)}{\partial \varepsilon} =& \frac{\partial}{\partial \varepsilon}\Bigg(T_{Tx}\Big[1 - (\mathcal{P}_{\mathrm{m}}(\varepsilon) + \mathcal{P}_{\mathrm{f}}(\varepsilon))\Big] \\ &+ \lambda_1(I_{th} - \mathcal{P}_{\mathrm{m}}(\varepsilon)P_{t,s}\ g)\Bigg) = 0,\end{aligned} \tag{4.14}$$

which results in the following equation.

$$T_{Tx}\frac{\partial \mathcal{P}_{\mathrm{d}}(\varepsilon)}{\partial \varepsilon} + \lambda_1 P_{t,s}\frac{\partial \mathcal{P}_{\mathrm{d}}(\varepsilon)}{\partial \varepsilon} = T_{Tx}\frac{\partial \mathcal{P}_{\mathrm{f}}(\varepsilon)}{\partial \varepsilon}. \tag{4.15}$$

To derive the solution in terms of detection threshold, $\frac{\partial \mathcal{P}_{\mathrm{d}}(\varepsilon)}{\partial \varepsilon}$ and $\frac{\partial \mathcal{P}_{\mathrm{f}}(\varepsilon)}{\partial \varepsilon}$ are utilized which have been obtained in Lemma 4.3, and Lemma 4.4, respectively. For a given T_s, straightforward mathematical derivations result in a closed form expression for the optimal SNR threshold for all subchannels.

$$\varepsilon^*_{M(Z)} = \frac{\sigma_w^2}{2\gamma}\left[\gamma_c + \frac{2}{f_s T_s}\ln\left(\frac{T_{Tx}}{T_{Tx} + \lambda_1 P_{t,s}\ g}\right)\right], \tag{4.16}$$

where $\gamma_c = (\gamma + 1)^2 - 1$.

4.4.3.2 Scenario 2 ($Z = 2, M = 1$)

In this case, similar to (4.14) and (4.15) and straight mathematical derivation, following is easily obtained.

$$\frac{\partial \mathcal{L}_2(\varepsilon_i^*, \lambda_1^*)}{\partial \varepsilon_i} = \frac{\partial}{\partial \varepsilon_i}\Big(T_{Tx}\big[1 - (\mathcal{P}^2_{\mathrm{m}}(\varepsilon_i) + \mathcal{P}^2_{\mathrm{f}}(\varepsilon_i))\big] + \lambda_1(I_{th} - \mathcal{P}_{\mathrm{m}}(\varepsilon_i)P_{t,s}\ g_i)\Big) = 0, \tag{4.17}$$

$$\begin{aligned}\frac{\partial \mathcal{L}_2(\varepsilon^*, \lambda^*)}{\partial \varepsilon} =& \frac{\partial}{\partial \varepsilon}\Bigg(T_{Tx}\big[1 - (\mathcal{P}^2_{\mathrm{m}}(\varepsilon) + \mathcal{P}^2_{\mathrm{f}}(\varepsilon))\big] \\ &+ \lambda_1(I_{th} - \mathcal{P}_{\mathrm{m}}(\varepsilon)P_{t,s}\ g)\Bigg) = 0,\end{aligned} \tag{4.18}$$

$$\varepsilon_M^* = \frac{\sigma_w^2}{2\gamma}\left[(\gamma+1)^2 - 1 + \frac{2}{f_s T_s}\ln\left(\frac{Z\bar{\mathcal{P}}_f^{Z-1}T_{Tx}}{Z\bar{\mathcal{P}}_m^{Z-1}T_{Tx} + \lambda_1 P_{t,s}\ g}\right)\right]. \tag{4.17}$$

$$\varepsilon_Z^* = \frac{\sigma_w^2}{2\gamma}\left[(\gamma+1)^2 - 1 + \frac{2}{f_s T_s}\ln\left(\frac{M(\bar{\mathcal{P}}_m + \bar{\mathcal{P}}_{\mathrm{f}})^{M-1}T_{Tx}}{M(\bar{\mathcal{P}}_{\mathrm{m}} + \bar{\mathcal{P}}_{\mathrm{f}})^{M-1}T_{Tx} + \lambda_1 P_{t,s}\ g}\right)\right]. \tag{4.18}$$

which results in the following equation.

$$T_{Tx}\left[-2\bar{\mathcal{P}}_{\mathrm{m}}\frac{\partial\mathcal{P}_{\mathrm{d}}(\varepsilon)}{\partial\varepsilon} + 2\bar{\mathcal{P}}_{\mathrm{f}}\frac{\partial\mathcal{P}_{\mathrm{f}}(\varepsilon)}{\partial\varepsilon}\right] = \lambda_1 P_{t,s}\ g\frac{\partial\mathcal{P}_{\mathrm{f}}(\varepsilon)}{\partial\varepsilon}. \tag{4.19}$$

Following the same line of argument as in deriving (4.16), the optimum SNR threshold is then obtained for any subchannel as following.

$$\varepsilon_M^* = \frac{\sigma_w^2}{2\gamma}\left[\gamma_c + \frac{2}{f_s T_s}\ln\left(\frac{2\bar{\mathcal{P}}_{\mathrm{f}}T_{Tx}}{2\bar{\mathcal{P}}_{\mathrm{m}}T_{Tx} + \lambda_1 P_{t,s}\ g}\right)\right]. \tag{4.20}$$

Here, ε_M^* is the optimum SNR threshold valid for the frame duration T.

4.4.3.3 Scenario 3 ($Z = 3, M = 1$)

Similar to the above, it can be obtained as

$$\varepsilon_M^* = \frac{\sigma_w^2}{2\gamma}\left[\gamma_c + \frac{2}{f_s T_s}\ln\left(\frac{3\bar{\mathcal{P}}_{\mathrm{f}}^2 T_{Tx}}{3\bar{\mathcal{P}}_{\mathrm{m}}^2 T_{Tx} + \lambda_1 P_{t,s}\ g}\right)\right]. \tag{4.21}$$

Finally based on the results above, and following the same line of argument as in Corollary 4.1, for a fixed M and any number of ZAs, i.e., $z = 1, \ldots, Z$, the optimal SNR threshold can be generalized as shown in (4.17).

4.4.3.4 Scenario 4 ($Z = 1, M = 2$)

In this case, at a particular time and location, a SBS may receive sensing information from more than one ZAs. In this scenario, similar to the case where

Z is variable, Lagrangian stationary point is used as mentioned in (4.12a). For $M = 2$, it is simple to show that

$$\varepsilon_Z^* = \frac{\sigma_w^2}{2\gamma_i}\left[(\gamma+1)^2 - 1 + \frac{2}{f_s T_s} \times \ln\left(\frac{2(\overline{\mathcal{P}}_{\mathrm{m}} + \overline{\mathcal{P}}_{\mathrm{f}})T_{Tx}}{2(\overline{\mathcal{P}}_{\mathrm{m}} + \overline{\mathcal{P}}_{\mathrm{f}})T_{Tx} + \lambda_1 P_{t,s}\ g}\right)\right]. \tag{4.19}$$

4.4.3.5 Scenario 5 ($Z = 1, M = 3$)

Similar to the previous cases, the optimal threshold can be obtained for different values of M, for instance $M = 3$. Finally, following the same steps as in obtaining (4.17), the generalized optimal solution for any number of SBSs as shown in (4.18).

Note that in (4.16)-(4.19), the miss detection and false alarm maximum tolerable values are selected such that $\overline{\mathcal{P}}_{\mathrm{m}} < 0.5$, and $\overline{\mathcal{P}}_{\mathrm{f}} < 0.5$ as described in the previous Section.

4.4.4 Unified Detection Threshold

As it is seen above, the optimal values of detection thresholds, ε_M^* and ε_Z^*, both depend on Z and M. In addition, due to the random nature of wireless channel the exact number of sensing devices that their sensing information received at ZA cannot be considered fixed. For instance, some sensing devices may fail to communicate with the ZAs and apparently with SBS. In some cases, the communication channel between sensing devices may also undergo deep fading in which the sensing network scenario is changed. Therefore, a unified detection mode is necessary so that the proposed technique works for any possible scenario and various combinations of Z and M. Here, a linear combination of ε_M^* and ε_Z^* is proposed as described below.

$$\varepsilon^* = \alpha\varepsilon_M^* + (1-\alpha)\varepsilon_Z^*, \tag{4.20}$$

where α is directly related to the network structure, i.e., Z and M: if $Z < M$ then α is $0 < \alpha < 0.5$ to emphasize on the contribution of ε_Z^* comparing to ε_M^* in (4.20). This is simply because ε_Z^* is the detection threshold for cases, where $Z < M$. In contrast, where $Z > M$, system sets $0.5 < \alpha < 1$, so ε_M^* contributes more than ε_Z^* in ε^*. However, in cases where Z and M are equal, system sets $\alpha = 0.5$ and

apparently ε_M^* and ε_Z^* contribute equally in (4.20). In the simulations presented later in this chapter, system selects α within the ranges mentioned above based on the densities of Z and M, for instance, when $Z \gg M$, α is selected on the lower range of $0.5 < \alpha < 1$. For the cases where $M = 0$, and $Z = 0$, the system sets $\alpha = 1$, and $\alpha = 0$, respectively.

In cases where due to the random time varying nature of wireless communication, such as channel fading, interference, hidden terminal problem, etc., either or both of Z and M are equal to zero, then the optimal detection threshold is undefined because ε_M^* and ε_Z^* are $-\infty$. As a matter of fact, this situation does not normally occur in the proposed model of zone-based cooperative spectrum sensing but should be considered as a special case to avoid singularities. Here the proposed method has a specific treatment to tackle such issues as described in the following.

According to (4.17) and (4.18), $M = 0$, and $Z = 0$ indicate $\varepsilon_Z^* \to -\infty$, and $\varepsilon_M^* \to -\infty$, respectively. At the same time, the sensing system controls α to avoid such a condition. Therefore, for $M \to 0$, sensing system sets $\alpha \approx 1$. Therefore,

$$\lim_{M \to 0} \varepsilon_Z^*(M).(1 - \alpha) \approx 0, \tag{4.21}$$

which indicates that optimal detection threshold solely depends on the ε_M^* in (4.20). Similarly, if $Z \to 0$, the sensing system selects $\alpha \approx 0$, thus,

$$\lim_{Z \to 0} \varepsilon_M^*(Z).(\alpha) \approx 0, \tag{4.22}$$

i.e., the optimal detection threshold solely depends on the ε_Z^* in (4.20). Using this method, it is now possible to obtain a unified version of optimal spectrum sensing threshold.

In the next section, a step by step algorithm is discussed for obtaining an estimation for ε^* based on the above analysis. In obtaining the optimal detection threshold which maximizes the system throughput, the bisection method is implemented.

Algorithm 1 : ε^* Estimation for Zone-Based Cooperative Spectrum Sensing

Input: $\overline{T}_{s,i}$,$\overline{\mathcal{P}}_{\mathrm{f}}(\overline{T}_{s,i})$, $\overline{\mathcal{P}}_{\mathrm{d}}(\overline{T}_{s,i})$, f_s, γ_i, $\varepsilon_{1,min}$, $\varepsilon_{1,max}$, δ, I_{th}

Output: ε_i^*, λ_i^*, $\forall i$

find the value of α from control packets of SBS and ZAs
calculate $\lambda_{1,min}$, and $\lambda_{1,max}$ from $\varepsilon_{1,min}$, and $\varepsilon_{1,max}$, respectively using (4.20)
for $i = 1, \ldots, N$ **do**
    while $I_{th} - I_c < \delta$ **do**
        find the effective λ_1 using bisection method:
        $\lambda_1 = \frac{\lambda_{1,min}+\lambda_{1,max}}{2}$
        calculate optimal SNR threshold, ε_i^*, from
        (4.17), (4.18), (4.20)
        obtain $P_m(\varepsilon_i^*)$ and interference at the PUs, i.e.,
        $I_c = P_{t,s}\ g_i \mathcal{P}_{\mathrm{m}}(\varepsilon_i^*)$
        if $I_c > I_{th}$ **then** $\lambda_1 \leftarrow \lambda_{1,min}$
        else $\lambda_1 \leftarrow \lambda_{1,max}$
        end if
    end while
end for
obtain ε^* and λ_1^* and throughput gain $R(\varepsilon^*)$, for all subchannels

4.4.5 An Algorithm for Estimating ε^*

The proposed method to estimate ε^* is presented in Algorithm 3, where γ, $\mathcal{P}_{\mathrm{d}}(\varepsilon)$, and $\mathcal{P}_{\mathrm{f}}(\varepsilon)$ are subchannel dependent parameters which are different for each subchannel. Here, the channel independent parameters are adjusted to obtain the optimal channel detection threshold such that the system throughput is maximized while the constraints are also satisfied by the spectrum sharing system.

In the proposed method, $T_s \ll T$ is a given system parameter thus the optimization variable for each subchannel is the detection threshold, ε_i. It is to note that (4.20) is a monotonically decreasing function of λ_1, i.e., for every $\lambda_1^a < \lambda_1^b$, we get $\varepsilon(\lambda_1^a) > \varepsilon(\lambda_1^b)$. Therefore, bisection method is adopted to find the detection threshold by solving the $\mathcal{P}_3$ subject to the constraints in (4.10b) and (4.10c).

4.5 Simulation Results and Analysis

In this section, the performance of the proposed zone-based cooperative spectrum sensing is evaluated under various network settings and parameters with the help of the simulation tools. Further comparisons will be presented regarding the performance of the proposed method against the benchmark systems. The first benchmark model is the case where there is no cooperation among the clusters/SBS, and the second benchmark network setting is when the decisions are diffused at the central entity using the OR/AND rule. The corresponding resource allocation framework in terms of latency, detection probability, communication activity of primary systems etc. are then compared. The considered system is a cognitive radio system, where $N = 16$ and $T = 100$ ms. The mean signalling duration for each SU, $\mathrm{E}[T_{s,i}]$, is maintained at 2 ms. The sampling rate is $f_s = 20$ kSample/Second and therefore the sampling overhead is $f_s T_{s,i} = 60$ and $\sigma_w^2 = 1$ is also considered.

It is further assumed that the subchannels are equiprobable such that $P_{H_0} = 0.5$. The traffic on the subchannels is randomly generated and SUs always have data packets ready to be transmitted unless otherwise stated. The subchannels between primary and secondary systems are modelled as Rayleigh fading with scale parameter of 1. The primary channel protection and spectrum utilization level are defined according to the IEEE 802.22 standard [35] as $\overline{\mathcal{P}}_{\mathrm{d}} \geq 0.9$, and $\overline{\mathcal{P}}_{\mathrm{f}} \leq 0.1$, respectively. The parameters have been chosen following the available standards for cognitive radio standard as explained in Section 3.4.

4.5.1 Comparative Study of Sensing Accuracy

The proposed zone-based cooperative spectrum sensing, as defined in (4.4), is validated by considering the appropriate value of probability of detection which fulfils the requirement of constraint (4.7c) as well as the cognitive radio standard for WRAN, i.e., IEEE 802.22. Moreover, the false alarm probability is obtained from the corresponding ROC curve which is the basis of the performance indicator in spectrum sensing. Therefore, the instantaneous $\mathcal{P}_{\mathrm{d}}$ and $\mathcal{P}_{\mathrm{f}}$ pair is chosen for

a given combination of M and Z to test the spectrum sensing accuracy of the proposed method.

For comparison, $Z = 1$ is considered as the conventional cooperative spectrum sensing based on Lemma 4.1 at the SBSs and therefore there is no subchannel reusability. The case of higher Z represents the special scenario that the multiple antennas are transmitting at the BSs and the cell is divided into sectors. In this case, each sector can be considered as a single antenna cell and therefore number of ZAs and SBSs are increased. The case $Z = 1$ will be considered as a benchmarking scenario for comparison. In Fig. 4.4, the normalized system throughput, which is directly related to the system spectral efficiency, is plotted versus the number of zone aggregators for different number of SBSs. Here, it is seen for the case $Z = 1$ that the normalized throughput is 0.6 whereas in a zone-based cooperative spectrum sensing method as indicated by $Z \geq 2$, it is significantly improved from 0.9 to 0.96 when ZAs are set to 2 and 3, respectively. This is due to the fact that the proposed method has better spectrum sensing accuracy due to the higher number of locally sensing decisions obtained from distributed spectrum sensors than majority of the conventional cooperative channel sensing techniques.

The higher sensing accuracy ensures that no access to that particular subchannel is granted by the SBS to protect the PUs. The result also provides insight on the rate of spectral efficiency increased by increasing M as a result of the proposed *micro-spectrum-reuse* technique. Here, it is also confirmed in Fig. 4.4 that the increase of normalized throughout from 0.9 to 0.96 when cooperative SBSs are increased from 2 to 3.

As it is further observed, in cases where there are larger number of ZAs, the spectral efficiency is relatively higher. It is due to the fact that the number of spectrum sensors per ZA becomes lower in this scenario. As a result, the probability of unanimous agreement of subchannels to be available in a zone is higher due to the implementation of AND rule among less number sensing devices. It can also be concluded from Fig. 4.4 that when higher number of ZAs are installed, the number of cooperative SBS does not necessarily need to increase to achieve better system throughput. This helps to find the optimal number of zones and SBS to set up within the cell to achieve the objective.

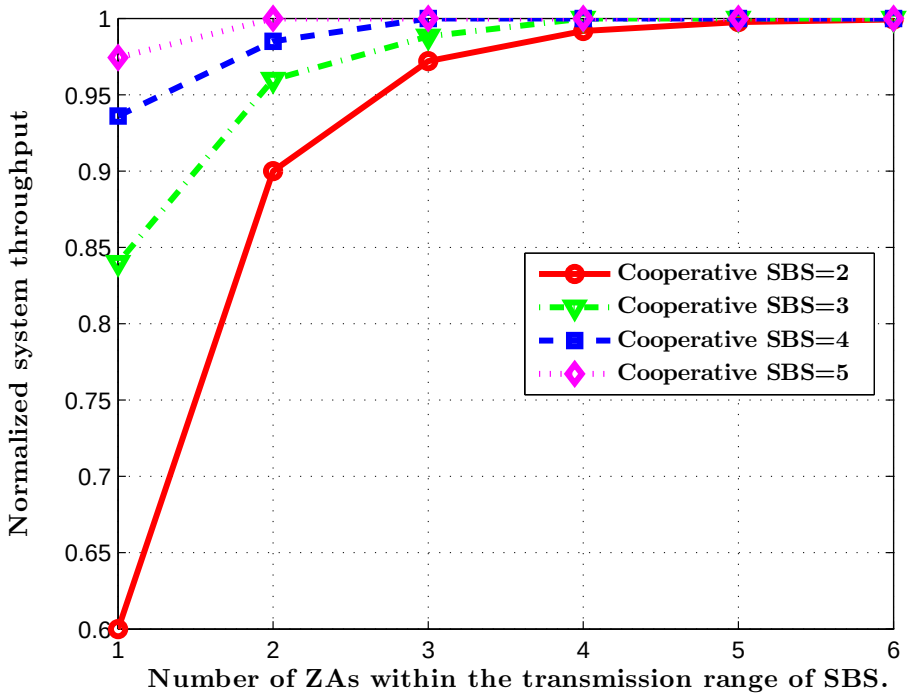

Figure 4.4: Normalized throughput *vs.* different values of Z and M.

Fig. 4.5 compares the spectrum sensing accuracy of the proposed method against the non-cooperative technique as well as the subchannel assignment with cooperative sensing [126] in which the OR fusion method is implemented for various received SNR. It is obvious that the performance gain in terms of the sensing accuracy is achieved with the expense of installing new sensing infrastructure, however it brings multiple advantages in the proposed network scenario. In addition to sensing accuracy as shown in Fig 4.5, it also increases the transmission duration for the SUs which contributes to achieve higher aggregated throughput at the secondary system with reduced system complexity.

In this particular case, the simulation is performed for AWGN channel using QPSK modulation with sampling overhead $T_{s,i}f_s = 100$ and $\mathcal{P}_\mathrm{f}$ is no more than 0.1. The sensing network has been created by setting $Z = 3$ and $M = 2$ for the proposed method. In addition, there are 3 cooperative sensors installed for OR

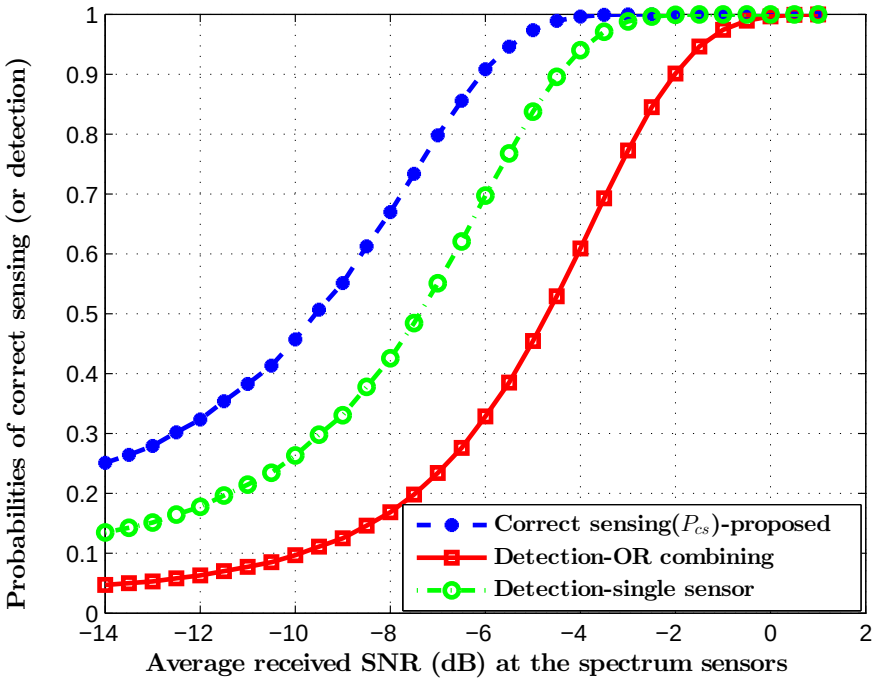

Figure 4.5: Probability of correctly detecting the subchannels *vs.* average received SNR when false alarm rate is fixed.

fusion method. It can be observed in figure that the correctly sensing probability of the proposed method is improved to 0.99 in comparison to 0.6 in case of non-cooperation sensing technique and 0.85 in case of hard decisions are aggregated with OR fusion method at -4 dB received SNR.

However the sensing performance at higher SNR, i.e., greater than 0 dB in the considered scenario, is observed to be similar in all three cases, this situation cannot be guaranteed in wireless communication due to the severe fading and hidden terminal problems. Moreover, energy detection performs better in such ideal case of higher SNR. Therefore, the sensing efficiency of the proposed method is higher than other two references cases in low received SNR regimes.

4.5.2 Tradeoff Between Sensing Latency and Detection Threshold

In Fig. 4.6, the optimal spectrum detection threshold, ε^*, is plotted versus sensing duration at the spectrum sensors for different values of maximum acceptable miss detection probability, where one ZA aggregates subchannel availability information from four spectrum sensing devices. The threshold in fact determines the $\mathcal{P}_{\mathrm{m}}$ and $\mathcal{P}_{\mathrm{f}}$ pair for the proposed sensing method and thus the system performance.

As it is seen, for long sensing duration in the secondary system, obtaining the optimal detection threshold deems irrelevant and not related to the maximum acceptable miss detection probability. However in the proposed method, the sensing duration is represented by the short signalling duration, i.e., less than 2 ms in Fig. 4.6, the optimal detection threshold must be obtained to improve the system throughput. Therefore, the length of transmission duration does not need to be compromised whilst latency is significantly reduced.

The obvious tradeoff is to relax the sensing duration ($T_s > 2$ ms) in which the transmission duration is shorter, but higher will be the latency associated with the spectrum sensing. In contrast, the sensing duration, thus the latency, can be reduced ($T_s < 2$ ms), where a higher complexity is expected as the appropriate sensing threshold must be evaluated through the proposed algorithm. Note that in the proposed method the latency associated with the sensing is very small and the cost is limited to the corresponding computational complexity required for evaluating the optimal detection threshold.

4.5.3 Performance Evaluation with Optimal Detection

Here, the performance of the proposed cooperative spectrum sensing method in terms of probabilities of false alarm and miss detection, thus probability of correct sensing, is further examined as a function of sensing duration, T_s, i.e., equivalently T_q in the proposed method. In the simulation settings, the conditions in Lemma 4.2 to Lemma 4.5 are strictly held. This means that for the simulated system, optimization problem $\mathcal{P}_3$ is convex thus (4.17) and (4.18) are the optimal solutions.

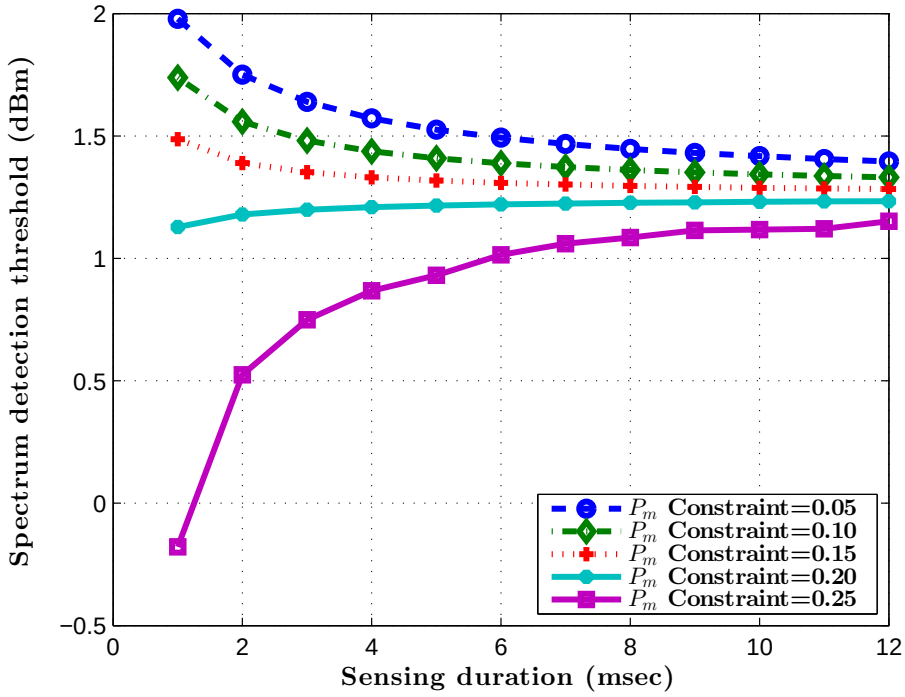

Figure 4.6: Optimal spectrum detection threshold *vs.* sensing duration (latency) for various miss detection constraints.

In the proposed method, the sensing duration, T_s, is significantly smaller compared to the frame duration, T, therefore it is independent of the optimization procedure. However, in the conventional spectrum sharing methods, where SUs sense and utilize the ideal subchannels, optimal choice of T_s is crucial. Under the scenario mentioned above, $\mathcal{P}_{\mathrm{m}}(\varepsilon^*)$, and $\mathcal{P}_{\mathrm{f}}(\varepsilon^*)$ for an optimal value of detection threshold have been obtained as shown in Fig. 4.7. While obtaining $\mathcal{P}_m(\varepsilon^*)$ for an optimal detection threshold, $\mathcal{P}_{\mathrm{f}}(\varepsilon_i^*)$ is kept fixed and vice versa. As expected, the longer the signalling duration, the lower will be the miss detection and false alarm probabilities. In addition, lowering $T_{s,i}$ from 9 ms to 6 ms significantly reduces $\mathcal{P}_{\mathrm{m}}(\varepsilon^*)$ and $\mathcal{P}_f(\varepsilon^*)$ for all subchannels. On the other hand, reduction of T_s from 6 ms to 3 ms does not reduce sensing accuracy in the same proportion. This suggests a way to adjust the signalling duration based on the required spectrum

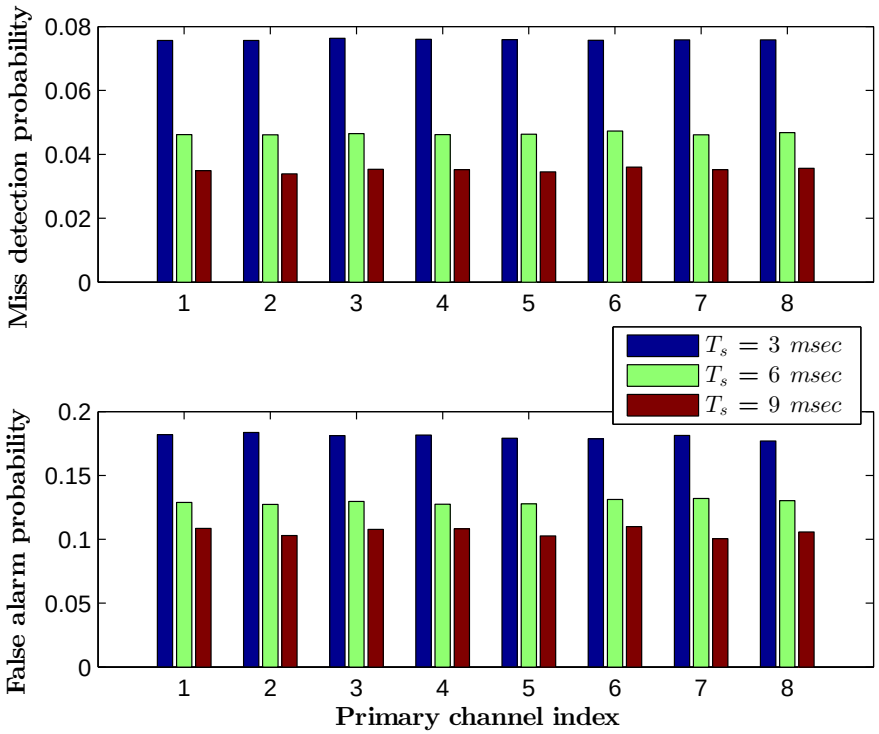

Figure 4.7: Probability of miss detection and false alarm of the first eight subchannels for different values of T_s.

detection accuracy at the secondary system.

4.5.4 System Throughput Analysis

Here, the performance of the proposed cooperative spectrum sensing method to maximize the system throughput is examined in which the aggregated interference to the PU is considered to be less than the threshold. The conditions in Lemma 4.2 to Lemma 4.5 are strictly held in the simulation settings.

In Fig. 4.8, the average throughput per subchannel is plotted versus the number of SBSs which transmit the cooperative control packet for the spectrum detection. It can be observed that as the number of SBSs are optimal for a given cluster heads, the throughput is maximized. However, lower number of SBS will receive

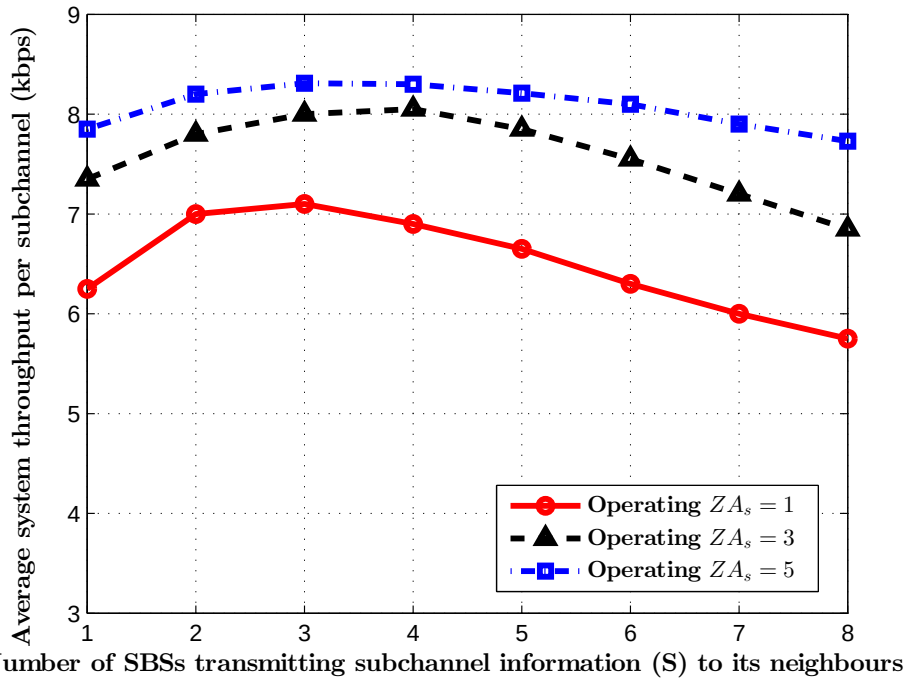

Figure 4.8: The average throughput per subchannel *vs.* number of SBS.

less information about the subchannel availability and, as a result, the throughput per subchannel decreases. In addition, when the number of signalling bits at the SBS increases, secondary system has to perform logical AND operation among large decision variables which results in detecting less opportunities to access the primary subchannel.

Furthermore the higher the number of ZAs, the higher is the accuracy of spectrum sensing. Therefore, the system throughput is increased accordingly. For a given simulation setup, the increment of ZAs from 1 to 3 significantly increases per subchannel throughput in comparison to increment from 3 to 5. As shown in Fig. 4.8, for a network setup of 3 SBSs, the subchannel throughput is achieved to be 7 kbps which can be increased to 8 kbps by increasing ZAs by 2 within a SBS region. However, further increase in ZAs to 5 does not improve the throughput at the same rate, i.e., it is just increased by 0.2 kbps by increasing ZAs to 5. It proves that finding the optimal number of SBSs and ZAs is more

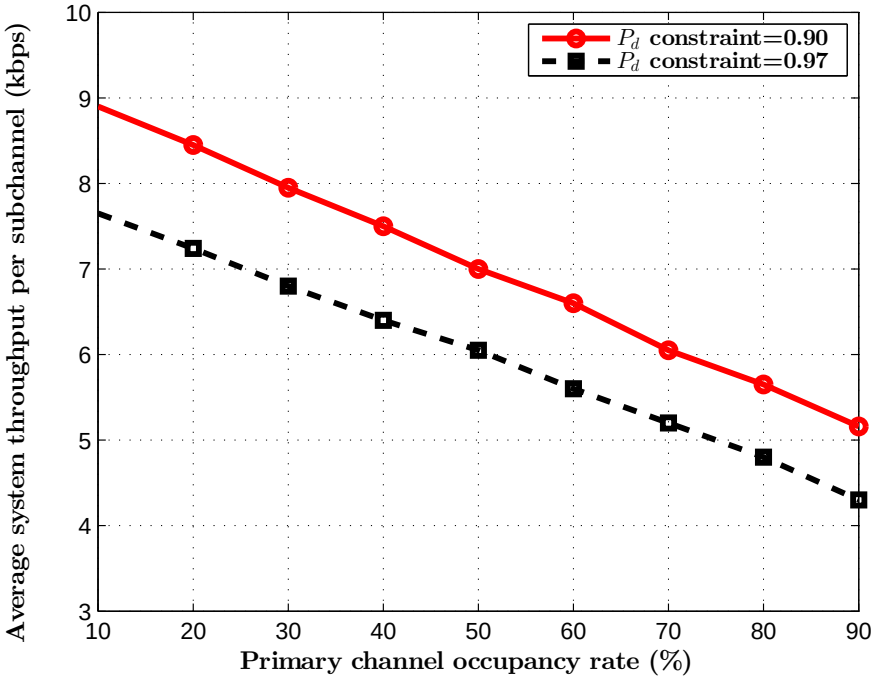

Figure 4.9: Average system throughput per subchannel *vs.* the primary subchannel activity for various detection probability constraints.

important then increasing their numbers which is also a feasible conclusion from the economic point of view on network design.

Fig. 4.9 shows average throughput per subchannel versus the primary channel occupancy rate. When the primary subchannels that can not be accessed by the secondary systems is lower, i.e., typically at 10%, the access constraint is relaxed and thus more subchannels are available to be shared among SUs. As a result, the system throughput is relatively higher at 7.7 kbps and 8.9 kbps when probability of detection is below 0.97 and 0.9, respectively. In contrast, when 90% of the subchannels are occupied, secondary system maintains a very tight constraint on subchannel selection as well as the protection of primary system. In this case, the subchannel throughput is achieved to be 4.2 kbps and 5.2 kbps, respectively. Therefore, it can be concluded that when the primary system has very strict rule

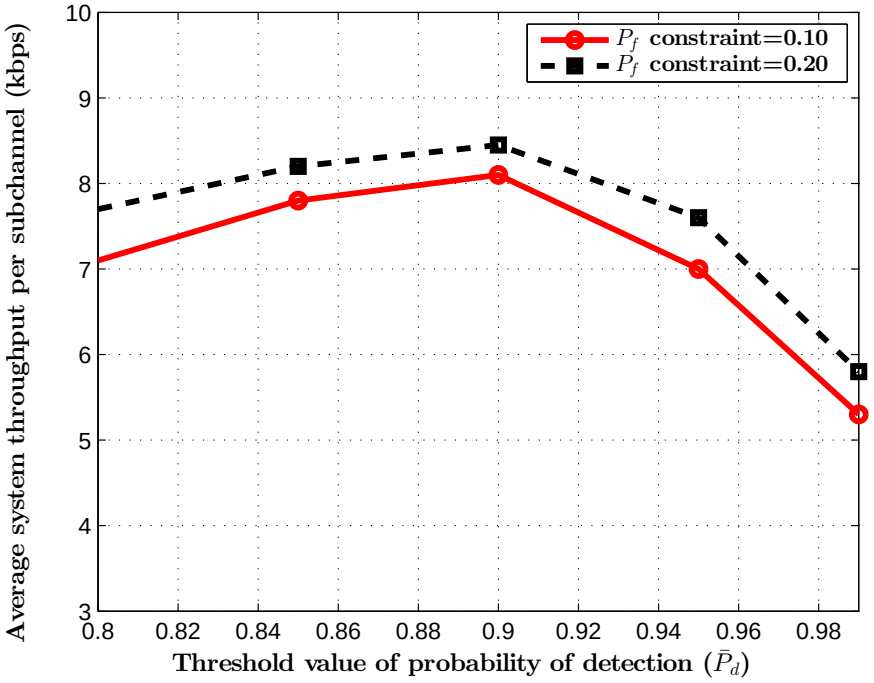

Figure 4.10: Average system throughput per subchannel *vs.* the probability of detection for various false alarm probability constraints.

of interference the secondary systems have to sacrifice a portion of throughput which can be compensated with the proposed spectrum sensing network.

On further analysis, it can be observed that when the probability of detection constraint is relaxed, for instance, from 0.97 to 0.9, there is a higher chance to access the subchannels. In both cases, the subchannel occupancy rate is linearly decreased with the increasing primary channel activities. Therefore, for a particular cellular network scenario, the secondary system throughout cannot be increased beyond a certain limit depending on nature of primary system.

The subchannel throughput versus the probability of detection constraint, i.e., $\overline{\mathcal{P}}_{\mathrm{d}}$, is given in Fig. 4.10 for various false alarm probabilities. When $\overline{\mathcal{P}}_{\mathrm{d}}$ is maintained at the lower value, e.g., at ≈ 0.8, there is higher chance of miss detection of the subchannel status and therefore the throughput is relatively lower than the

case where $\overline{\mathcal{P}}_{\mathrm{d}}$ is constrained at ≈ 0.9. However, by increasing $\overline{\mathcal{P}}_{\mathrm{d}}$ from 0.9 to 0.97, the throughput falls down quickly because the detection constraint becomes tight and smaller number of primary subchannels are available for secondary users. It has also been observed that as long as $\overline{\mathcal{P}}_{\mathrm{f}}$ remains within the maximum limit defined in the simulation setup for a given optimal $\overline{\mathcal{P}}_{\mathrm{d}}$, the throughput is not significantly degraded even if the false alarm constraint is relaxed from $\overline{\mathcal{P}}_{\mathrm{f}} = 0.1$ to 0.2. Therefore, along with selection of optimal detection threshold (ε), the optimal choices of $\overline{\mathcal{P}}_{\mathrm{d}}$ and $\overline{\mathcal{P}}_{\mathrm{f}}$ are always important for the accurate sensing of the subchannels and efficiently utilizing them. The proposed spectrum sensing network approach thus helps not only to enhance the performance but also to choose the accurate network parameters for cellular cognitive radio design and implementation.

4.6 Conclusions

In this chapter, a new method for multichannel spectrum sensing through an independent monitoring network has been presented in which the location of the sensor is partly incorporated into the subchannel allocation. It was also shown that the proposed zone-based cooperative spectrum sensing method increases the sensing accuracy which facilitates higher spectrum reusability. The detail description of spectrum sensing algorithms and signalling protocols which incorporate zone location information in the spectrum sensing has been also presented which enables the *micro-spectrum-reuse* and results in higher system throughput, lower signalling overhead, and thus the lower latency. It is obvious that the cost involved in designing overlaid spectrum sensing network is higher, however the advantages of spectrum sensing accuracy and subchannels reusability outnumbers the disadvantages.

An analytical framework is also developed with the objective function to maximize the secondary system throughput under various monitoring network scenarios subject to the spectrum sensing accuracy and maximum tolerable interference imposed at the primary system. Moreover, various required conditions have been identified and derived mathematically to achieve the optimal solution in the form

of detection threshold. The spectrum sensing accuracy has been derived for various configurations of ZAs and SBSs and shown that the optimization problem is convex under all possible configurations. As a result, a closed form solution for the optimal sensing threshold value has been successfully determined. Similarly, the obtained solutions would be linearly combined based on allocated weights to make the optimal detection threshold valid for possible configurations. It has been also shown that the proposed method outperforms many conventional cooperative sensing techniques in terms of sensing accuracy with the help of numerical analysis and simulations results.

Higher system throughput is partly due to the extra subchannel reusability created by exploiting location information of the spectrum sensors through the *micro-spectrum-reuse*. In addition, it provided the concept of spectrum sensing network collocated with the cellular CRN system and its design aspect for next generation network. Using simulations, the sensing accuracy and system throughput have been evaluated against various network parameters to prove the efficiency of the proposed method of spectrum sensing. The simulations also demonstrated the improvement on the spectrum sensing accuracy due to the proposed method with significantly lower latency and higher system throughput comparing to the cases without zoning. Furthermore, it is also shown that when the sensing duration is lowered as described in the proposed method, it is very important to find the optimal sensing threshold to improve the system throughput. In addition, there are always optimal numbers of sensing devices to be installed inside the cellular region in which maximum system throughput is achieved. The optimal choice of probabilities of miss detection and false alarm are equally important in the considered spectrum sensing method as described in this chapter.

This chapter dealt with the spectrum sensing techniques by deploying the spectrum sensing network to maximize the secondary system throughput. However, the issues that are frequently faced in CRN, such as modelling the primary user activity in the subchannels, are not considered in this model. As a matter of fact, such issue is equally important to be considered in the problem domain because the activity of primary users put the limitations on the cognitive radio network due to the imposed interference constraint as well as transmit power

constraint. In the next chapter, a detail mathematical modelling of primary user activity for the proposed optimal resource allocation techniques will be discussed. In addition, spectral efficiency and energy efficiency are important measures of CRN performance. The detail study of such parameters is lacking in this chapter, which are particularly considered in terms of primary user activity model in the next chapter. Also, few interesting analytical results and simulations will also be presented to validate the proposed resource allocation methods.

Chapter 5

Resource Allocation in Multicell Collaborative Cognitive Radio Networks

When the spectrum sensing is executed by the secondary system to obtain the channel availability information, they must be efficiently utilized with a minimum level of transmit power to achieve higher spectral and energy efficiencies. In cognitive radio enabled wireless communications, a secondary network, i.e., cognitive radio networks, opportunistically accesses the available spectrum initially licensed to the primary network. As mentioned in the previous chapters, cognitive radio technique is one of the solutions that has been considered to improve the spectral efficiency (SE), which is defined as the total capacity normalized by the available bandwidth measured in bps/Hz, in the cellular band [127]. However, the main challenge in spectrum sharing is to efficiently exploit the underutilized portions of the primary spectrum without compromising the QoS requirements in the primary system.

The level of underutilized radio resources available to the cognitive multicell networks depends on the nature of users communication activities in the primary system. Several spectrum sharing methods have been defined for the CRNs in-

cluding overlay, underlay and a combination of both [22],[128]. In the overlay spectrum sharing, the secondary system accesses the subchannel only when it is in idle state. In the underlay method, the secondary system simultaneously utilizes the subchannel subject to keeping the aggregated interference at the primary receiver below a predefined threshold. This threshold is a system parameter which depends on the primary system characteristics [29]. Ideally, to assure the QoS in the primary system, in overlay (underlay) access, accurate information of spectrum sensing (perfect channel state information for the channel between the secondary transmitters and the primary receivers) is a prerequisite. In practice however, attaining such parameters is very challenging because there is generally no or very limited resources for inter-system signalling.

On the other hand, the research on energy efficiency (EE) has attracted significant attention because of the environmental concern as well as the device requirements of longer battery life [129]. The impact of the proposed primary subchannel activity profile on the EE is further investigated on the considered multicell system. Here, EE measures how efficiently the available energy is utilized to maintain the QoS in the end-to-end communications [130]. The EE metric can take various forms such as energy-per-bit to noise power spectral density ratio, i.e., E_b/N_0, bit per Joule capacity, rate per energy, or Joule per bit, however they are essentially equivalent and mutually convertible [131]. Both EE and SE are required to study in a single framework because there is a very strict tradeoff exist between them such that improvement of one may deteriorate the other [132].

In the considered multicarrier multicell CRN, the coordination among the neighbouring secondary base stations plays a paramount role in efficient design of the network-wide optimal assignment of the scarce radio resources [133]. Network-wide resource allocation significantly reduces the impact of intra-system interference on the overall secondary system performance. It also enables the secondary system to exploit the temporal variations in the idle or underutilized spectrum due to the stochastic nature of primary system communication activity on the subchannels. Exploiting the real-time primary subchannel behaviour, which is temporal and nondeterministic, can enhance the performance of the radio resource allocation in the secondary system [94].

To characterize the primary users communication activity, Poisson Point Process (PPP) based models have been proposed in [134]. However, due to the dynamic but unpredictable nature of the primary traffic, such models often fail to apprehend instantaneous primary subchannel activity [86]. Other researchers propose schemes which are designed to exploit the primary service activity, however it is usually assumed that the activity information is available to the secondary system, either through signalling or a priori knowledge, see, e.g., [29]. Yet, this assumption may not always be valid in practical scenarios where multicell networks are considered.

In this chapter, the activity levels of primary users on the subchannels are incorporated into the transmission power allocation at SBS such that the maximum possible SE can be achieved. The higher signalling level is expected when subchannel activities are necessary to broadcast to the centralized system. However, the proposed method simplifies the power allocation method in CRN thereby significantly reducing the signalling overhead. Moreover, when the SE and subchannel activity profile are integrated, the objective function is characterized as a utility function.

On the other hand, the EE as an objective function depends directly on the level of accuracy of the channel state information (CSI), however such information may not be available to the SU transmitter [135]. The proposed method in this chapter addresses the problems due to the unknown channel gain by means of incorporating the estimated primary users' activity level on the subchannels with the minimum signalling overhead. An energy per received bits has been considered as a metric in [136] as the basis for a resource allocation approach that adopts the spectrum sharing along with soft-sensing information by adaptively setting the sensing threshold. Irrespective of the proposed method, the energy and spectral efficient design for CRN is studied in [137],[138] to optimize one of them at a time which remains valid for a frame duration.

The accurate prediction of the primary system activity on subchannels is a function of arrival and departure rate of the PUs in addition to the allocated transmitted power and channel gains, which are random in nature and very difficult to obtain, if not impossible, in practice. Instead, the *subchannel activity index* (SAI) as a new parameter is now defined, which indicates the level of communication

activity within the primary subchannels. Therefore, SAI is a probabilistic metric which is based on the sensing outcomes using energy detection by a limited number of spectrum decision makers. In this chapter, a novel scheme to evaluate the *aggregated SAI* (ASAI) among the SBSs will be presented. The ASAI parameter is then utilized in an optimal and efficient design of the SU's transmission power allocation strategy which maintains better achievable SE and EE such that the best possible scenario can be obtained from both energy and spectrum utilization perspectives.

The purpose of the SAI (or ASAI when all the neighbour cells are considered) is to address the signalling overhead issue in multicell CRN. When the subchannels are found to be underutilized, there is still room, subject to careful and controlled power allocation, to accommodate secondary users due to low primary system activity. In a secondary cell covered by a SBS, ASAI carries dual information, i.e., firstly, activity of the primary users located in that cell, and secondly, the primary users accessing the subchannels in the adjacent cells. A combination of both is utilized in this case to design the efficient resource allocation scheme. It is therefore proposed a simple, yet efficient, collaborative spectrum monitoring scheme with very low signalling overhead to estimate the ASAI based on one bit per subchannel feedback transmitted by the neighbour SBSs as a control packet.

Depending on the ASAI estimation, a very important tradeoff occurs which has a significant impact on the optimal subchannel and transmit power allocations. In cases where the SBS allocates a higher transmission power to the subchannels with a higher ASAI, the minimum QoS requirements to the primary services may be compromised along with significant degradation on EE. On the other hand, a low utilization of the available spectrum is achieved by allocating a lower power to a subchannel with a lower ASAI. To model this tradeoff, A notion of utility function is adopted [139],[140]. For each SU communicating over the subchannel, two utility functions are then formulated as a decreasing function of the ASAI and, first, increasing function of the achievable rate and, second, increasing function of EE for each cognitively utilized subchannel.

At first, optimal power allocation method is formulated in which the objective is to maximize the total SBS utility, in terms of the SE, subject to total available transmit power at the SBS and primary system collision probability constraints.

Secondly, under the same system settings, the optimal power allocation will be formulated with the objective of maximizing the total SBS utility, in terms of EE, subject to the similar constraints described above. The first optimization problem is non-convex, and the second case is a fractional optimization problem which can be approximated as quasi-convex under certain assumptions. The formulated problems are the instances of weighted sum-rate maximization which have been substantially studied in the related literature, see, e.g., [27],[133],[141],[142] although most of the previous works require accurate channel state information and/or spectrum sensing, thus need direct inter-system and heavy intra-system signalling. A unique feature of our proposed method is its very low signalling overhead which uses only one bit per sunchannel.

The detail comparison of the system performance is discussed in terms of EE against a cognitive cellular network when there is no signalling among the SBSs in which the SBS executes equal subchannel power allocation. The significant sum-rate improvement is confirmed by the simulation results. The sum-rate performance of the proposed method will also be compared with a scenario in which the combination of underlay and overlay access techniques are adopted, where perfect knowledge of interference channel state and spectrum sensing information are available at the SBS. Finally, the energy efficient CRN design under the similar network settings will be discussed and obtain the practical network scenario in which both EE and SE can be optimized. Simulation results also show that the proposed method closely follows the ideal spectrum access with a slightly lower achievable rate although the required signalling overhead is significantly reduced.

The major contributions of this chapter are summarised as following.

- The *subchannel activity index* is first defined and characterized as an indicator of activities level of the primary users in their corresponding subchannels. It is then followed by a simple yet efficient collaborative spectrum monitoring among the base stations to obtain the *aggregated SAI* (ASAI) for efficient transmit power allocation at the SBSs which also maintains a very low signalling overhead among the cellular systems.

- A utility function is defined to incorporate the ASAI into the corresponding spectral efficiency for all subchannels. The joint efficient transmit power

and subchannel allocation schemes are then formulated as an optimization problem in the SBS to maximize the total SBS utility function.

- The further investigation is presented to examine the impact of ASAI into the energy efficiency on the similar system settings. This case is also handled in a similar approach to that of the previous one by defining utility function in terms of energy efficiency to find the efficient transmission power profile. The obtained solutions can be easily extended to many practical cellular network scenarios with relevant modifications.

- Finally, a suboptimal subchannel and transmit power allocation schemes are studied considering both spectral and energy efficiencies using various mathematical and optimization tools. Moreover, the design technique to achieve the near optimal spectral and energy efficiencies based on ASAI by varying the spectrum sensing parameters will be elaborated. The obtained SE and EE relation based on ASAI in the proposed method is practically more efficient than the conventional EE and SE tradeoff which is, in most cases, based on the transmit power. The results are then validated through the extensive simulations.

In the next section, a brief description of the considered system model in this chapter will be presented.

5.1 System Model

The considered system includes a cellular CRN which is collocated with a legacy cellular primary system which is the same as presented in chapter 3 and chapter 4 with some add-on features which are described in this Section. A schematic of the considered network is presented in Fig. 5.1. In this system model however, the independent sensing network is optional and therefore the clusters are not presented. In addition, the subchannel activity information is shared among the base stations to achieve the parameter known as ASAI. Here, a B Hz frequency band is licensed to the primary system which serves primary users indexed by $j \in \{1, \ldots, J\}$. The spectrum of the primary system is shared with

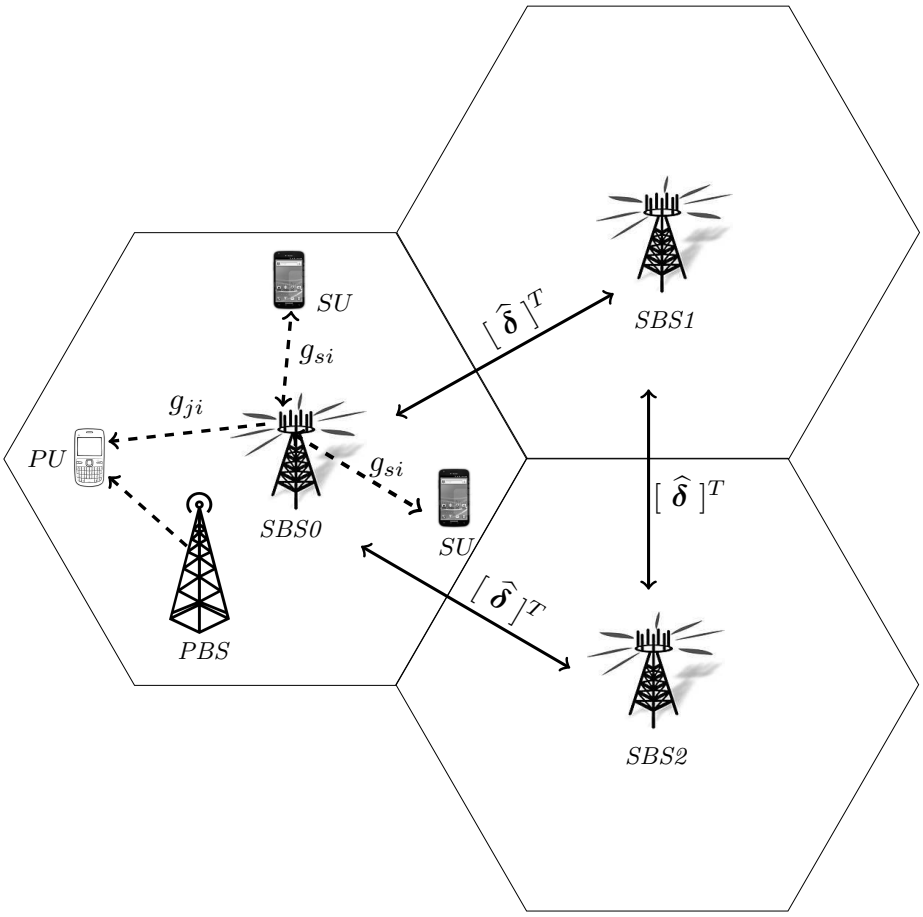

Figure 5.1: A schematic of the considered cognitive cellular network.

secondary system for downlink transmission. The CRN is a multi-cell network with M base stations. In the central cell, SBS serves secondary users indexed by $s \in \{1, \ldots, S\}$. The secondary system utilizes orthogonal frequency division multiple access (OFDMA), as mentioned in Section 3.2, where the radio spectrum is divided into N non-overlapping $B_i = B/N$ Hz subchannels which are indexed by $i \in \{1, \ldots, N\}$.

The communication link between the secondary transmitter to the secondary receivers and secondary transmitter to the primary receivers, for subchannel $i \in \{1, \ldots, N\}$, are referred to as secondary channel, and interference channel, and denoted by $g_{si}(\nu)$, and $g_{ji}(\nu)$, respectively. Parameter ν denotes the joint

fading state which is dropped hereafter for brevity. The value of g_{si} is updated through the measurement in each time frame by the CRN user. Making g_{ji} available at the secondary system is a challenging task because there is often no direct signalling between primary and secondary systems. Here, similar to [142], the basic assumption is that it is estimated through the aggregated interference received at the SUs due to the primary transmission.

In this setting, the spectral efficiency for SU, s, accessing subchannel i is:

$$r_{si} = \log_2(1 + P_{si}h_{si}) \text{ bps/Hz}, \tag{5.1}$$

where, h_{si} is the subchannel gain to interference plus noise ratio which is a random variable, and P_{si} is the allocated transmission power on subchannel i at the SBS corresponding to secondary user s. Here, $\mathbf{r}_s = [r_{s1} \dots r_{si} \dots r_{sN}]^T$ is defined as the rate vector for secondary user s, where $[.]^T$ indicates vector transpose operator. The optimal transmit power vector in the central SBS, $\mathbf{P}_i^* = [P_{1i}^* \dots P_{s,i}^* \dots P_{Si}^*]^T$, is directly related to the primary network communication activity on subchannel i as well as the associated constraints for protecting PU's QoS.

Time is slotted into frames and SBSs are synchronized in the frame level. There is no signalling between the primary system and the CRN. The secondary service either adopts underlay or overlay spectrum access technique based on each subchannel status. In underlay access the secondary service can always access to the subchannel subject to the interference constraint for the primary system. In overlay access, the secondary service senses the subchannel status and conducts transmission if the corresponding frequency band is idle. While implementing OFDMA in CRN, the inter-channel interference is negligible due to high spectral distance and sharp bandpass filter in the secondary system [29].

5.1.1 Spectrum Sensing

The energy detection based spectrum sensing has been described in detail in previous chapters, however a brief review is presented here. In the considered energy detector spectrum sensing technique, spectrum sensing is performed in each sensing slot at the SUs to determine whether the subchannel is idle or busy.

Therefore, when the subchannel status is estimated, it is either a correct estimation or embedded with a sensing errors. It is further assumed that subchannel i's status remains unchanged during a sensing slot, $T_{s,i}$. The actual state of the subchannel $i \in \{1 \dots N\}$ is represented by hypothesis $\{H_{0,i}, H_{1,i}\}$, where $H_{0,i}$ ($H_{1,i}$) indicates the idle (busy) state of the subchannel i. The probabilities of $H_{0,i}$, $H_{1,i}$ are denoted by P_{H0}, and P_{H1}, respectively.

In energy detection, the SUs receive $T_{s,i}f_s$ baseband complex samples during the sensing slot, $T_{s,i}$, where sampling rate is f_s. Let $y_i[k]$ denote the k^{th} sampled signals received at the SU during the sensing duration are

$$y_i[k] = \begin{cases} w_i[k], & : H_0, \\ g_i[k]x_i[k] + w_i[k], & : H_1, \end{cases} \tag{5.2}$$

where $x_i[k]$ is the received signal from PUs and $w_i[k]$ is the additive white Gaussian noise (AWGN) with variance $\sigma_w^2 = E[|w_i[k]|^2]$, and $g_i[k]$ is the channel gain which is assumed to be constant during the signalling duration. The test statistic of the received signal is thus obtained as

$$\mathscr{E}_i[\mathbf{y}] = \frac{1}{T_{s,i}f_s} \sum_{k=1}^{T_{s,i}f_s} |y_i[k]|^2. \tag{5.3}$$

For each subchannel i, the test statistic is then compared with the threshold energy level, ε_i, to locally obtain the status of subchannel i. In practice, ε_i is a system parameter which mainly depends on the primary system requirements, such as their interference suppression capability [27].

5.1.2 Subchannel Activity Index

For a subchannel $i \in \{1, \dots, N\}$, the outcomes of detection are: idle ($\mathscr{E}_i[\mathbf{y}] < \varepsilon_i|H_{0,i}$), busy ($\mathscr{E}_i[\mathbf{y}] \geq \varepsilon_i|H_{1,i}$), miss detection ($\mathscr{E}_i[\mathbf{y}] < \varepsilon_i|H_{1,i}$), and false alarm ($\mathscr{E}_i[\mathbf{y}] \geq \varepsilon_i|H_{0,i}$). A necessary condition for the SUs to access the subchannel i is $\Pr(idle) + \Pr(miss\ detection) > \Pr(busy) + \Pr(false\ alarm)$. Here for brevity equiprobable subchannels are generally assumed in which the probability of a subchannel being idle is equal to that of being busy as in [121]. The above

necessary condition for subchannel being available thus reduced to the following probability ratio.

$$\Psi_i \triangleq \frac{\Pr(\mathscr{E}_i[\mathbf{y}] < \varepsilon_i | H_{0,i}) + \Pr(\mathscr{E}_i[\mathbf{y}] < \varepsilon_i | H_{1,i})}{\Pr(\mathscr{E}_i[\mathbf{y}] \geq \varepsilon_i | H_{1,i}) + \Pr(\mathscr{E}_i[\mathbf{y}] \geq \varepsilon_i | H_{0,i})} > 1. \tag{5.4}$$

The parameter δ_i is now defined as a measure of the primary system activity as following.

$$\delta_i \triangleq \begin{cases} 1, & \text{if } \frac{\Pr(\mathscr{E}_i[\mathbf{y}]<\varepsilon_i|H_{0,i})+\Pr(\mathscr{E}_i[\mathbf{y}]<\varepsilon_i|H_{1,i})}{\Pr(\mathscr{E}_i[\mathbf{y}]\geq\varepsilon_i|H_{1,i})+\Pr(\mathscr{E}_i[\mathbf{y}]\geq\varepsilon_i|H_{0,i})} < 1, \\ 0, & \text{if } \frac{\Pr(\mathscr{E}_i[\mathbf{y}]<\varepsilon_i|H_{0,i})+\Pr(\mathscr{E}_i[\mathbf{y}]<\varepsilon_i|H_{1,i})}{\Pr(\mathscr{E}_i[\mathbf{y}]\geq\varepsilon_i|H_{1,i})+\Pr(\mathscr{E}_i[\mathbf{y}]\geq\varepsilon_i|H_{0,i})} > 1, \\ \text{either 0 or 1}, & \text{otherwise.} \end{cases} \tag{5.5}$$

It is straightforward to express Ψ_i in terms of miss detection and false alarm for the outcomes of subchannel detection method as $\Psi_i = \frac{1-\mathcal{P}_{\text{f,i}}+\mathcal{P}_{\text{m,i}}}{1+\mathcal{P}_{\text{f,i}}-\mathcal{P}_{\text{m,i}}}$, where for subchannel $i \in \{1, \ldots, N\}$, $\mathcal{P}_{\text{m,i}}$ and $\mathcal{P}_{\text{f,i}}$ are the probabilities of miss detection and false alarm, respectively.

In cases $\delta_i \triangleq 0$, the activity of primary system on subchannel i is most likely low. In such cases, the SUs can access subchannel i with a low risk of interference. Conversely, when $\delta_i \triangleq 1$, it is likely that the subchannel is in use by the primary system, and thus SUs are not allowed to access the subchannel without proper transmit power control mechanism.

When the probability ratio, Ψ_i in (5.4) is equal to 1, although it occurs with a low probability, δ_i randomly selects either 0 or 1, which is basically a decision deadlock situation. If this decision does not fall towards the correct state of the subchannel, the interference to the primary transmission system is likely to be unavoidable. This situation occurs if and only if $\Psi_i = 1$ thus $\mathcal{P}_{\text{m,i}} = \mathcal{P}_{\text{f,i}}, \forall i$. For a given energy detector, such cases are less likely which can be concluded from the complementary receiver operating characteristic (CROC) curve, i.e., the plot of $\mathcal{P}_{\text{m,i}}$ against $\mathcal{P}_{\text{f,i}}$ in a cognitive radio environment.

In the following, the cases $\delta_i = 0$ and $\delta_i = 1$ are further investigated to find the optimal resource allocation among users. In addition, $\Psi_i = 1$ is a less likely event and therefore further exploration is irrelevant for the considered system.

For the sensing duration, $T_{s,i}$, and sampling frequency, f_s, $\mathcal{P}_{\text{d,i}}$ for energy detection is [143]: $\mathrm{Q}\left(\left(\frac{\varepsilon_i}{\sigma_w^2} - \gamma_i - 1\right)\sqrt{\frac{T_i f_0}{2\gamma_i+1}}\right)$, where $\mathrm{Q}(z) := (1/\sqrt{2\pi})\int_z^{+\infty} e^{-(\tau^2/2)} d\tau$,

and ε_i, σ_w^2, and γ_i are energy detection threshold, variance of the additive white Gaussian noise at the spectrum sensors, and the average received signal to noise ratio (SNR) of primary system signal received at the spectrum sensors, respectively. The sensing parameters are assumed to be fixed during the sensing duration. Noting (5.4), $\Psi_i \gtrless 1$ reduces to $\mathcal{P}_{\mathrm{m,i}} \gtrless \mathcal{P}_{\mathrm{f,i}}$, thus

$$\mathcal{P}_{\mathrm{f,i}} \gtrless 1 - \mathrm{Q}\left(\left(\frac{\varepsilon_i}{\sigma_w^2} - \gamma_i - 1\right)\sqrt{\frac{T_i f_0}{2\gamma_i + 1}}\right), \ \forall i. \tag{5.6}$$

$\mathcal{P}_{\mathrm{f,i}}$ is thus obtained from (5.6) as

$$\frac{\mathrm{Q}^{-1}(1 - \bar{\mathcal{P}}_{\mathrm{f,i}})}{\sqrt{T_{s,i} f_s}} \gtrless \left(\frac{\varepsilon_i}{\sigma_w^2} - 1\right)\frac{1}{\sqrt{2\gamma_i + 1}} - \frac{\gamma_i}{\sqrt{2\gamma_i + 1}}, \ \forall i. \tag{5.7}$$

Setting $\Theta_{1i} = \frac{\varepsilon_i}{\sigma_w^2} - 1$, $\Theta_{2i} = \frac{\mathrm{Q}^{-1}(1-\bar{\mathcal{P}}_{\mathrm{f,i}})}{\sqrt{T_{s,i} f_s}}$, (5.7) is further reduced to

$$\gamma_i \gtrless \Theta_{1i} + \Theta_{2i}^2 \pm \Theta_{2i}\sqrt{\Theta_{2i}^2 + 2\Theta_{1i} + 1}, \ \forall i. \tag{5.8}$$

Using (5.7) as an equation, the maximum tolerable false alarm probability, i.e., $\bar{\mathcal{P}}_{\mathrm{f}}$, is obtained along with its corresponding received SNR, $\bar{\gamma}_i$. In Fig. 5.2, the $\mathcal{P}_{\mathrm{f,i}}$ is shown versus the received SNR. The SNR threshold is obtained at $\gamma_i = \bar{\gamma}_i$, where δ_i is randomly chosen, thereby introducing the interference due to imperfect decision. Here, $\bar{\gamma}_i$ is in fact the SNR threshold based on which the subchannel availability is detected. Furthermore, when the condition $\gamma_i > \bar{\gamma}_i$ ($\gamma_i < \bar{\gamma}_i$) is satisfied, the interference to the primary system due to the imperfect decision is very low. The plot in Fig. 5.2 is presented while other sensing parameters including sensing overhead, frame duration etc. are kept constant.

In cases where a lower $\bar{\mathcal{P}}_{\mathrm{f,i}}$ is set, which ultimately enhances the spectrum utilization, the subchannel is available only in high received SNR regime. However when the constraint is relaxed, the condition $\gamma_i > \bar{\gamma}_i$ is achieved even for lower SNR. Therefore, more subchannels become available to be accessed by the SUs. Note that in Fig. 5.2, $\mathcal{P}_{\mathrm{m,i}} = \mathcal{P}_{\mathrm{f,i}}$, or $\gamma = \bar{\gamma}$, is the region in CROC curve around which the maximum interference occurs because of the uncertainty in decision made on the availability of subchannel i. In the considered system, having $\gamma_i = \bar{\gamma}_i$ is however always less likely than $\gamma_i \gtrless \bar{\gamma}_i$. Therefore in the proposed method, the interference due to the random subchannel decision would be negligible.

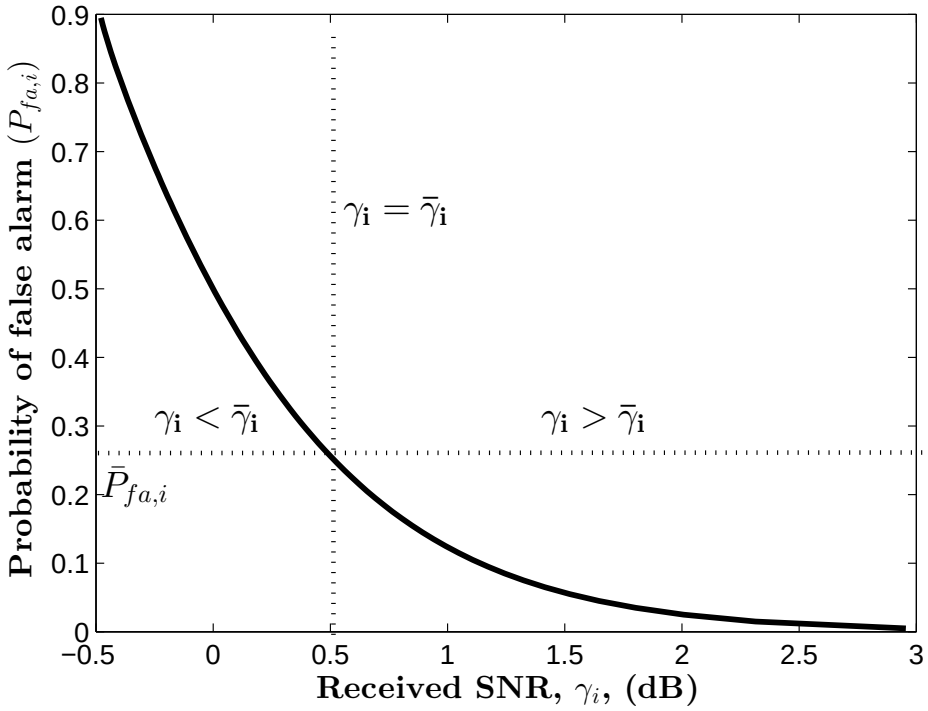

Figure 5.2: Probability of false alarm *vs.* the received SNR to estimate the idle (or busy) primary channels.

5.2 Inter-Cell Collaborative Spectrum Monitoring

The SBSs perform the spectrum sensing and estimate the status of the subchannels. Corresponding to subchannel i in SBS m, where $m = 1, \ldots, M$, spectrum sensing returns a decision variable $\delta_{m,i}$. If subchannel i is busy (idle), then $\delta_{m,i} = 1$ ($\delta_{m,i} = 0$). Sensing vector, $\boldsymbol{\delta}_m = [\delta_{m,1}, \ldots, \delta_{m,N}]^T$, indicates the status of the subchannels in SBS m.

The cooperative detection technique on $\delta_{m,i|\{m=1\ldots M,\ i\in\{1\ldots N\}\}}$ is then implemented among the SBSs to obtain the *aggregated SAI* (ASAI). The subchannel sensing however is not perfect, which results the subchannel status, e.g., idle or busy, is likely subject to sensing errors. Therefore, when the subchannel is busy

(idle), there are two possible statuses, i.e., either in the idle state or busy state in which only one of them is correct.

For subchannel i in a SBS with $M-1$ neighbouring SBSs, the ASAI is then obtained as following.

$$\hat{\delta}_i = \frac{1}{M}\sum_{m=1}^{M} w_m \delta_{m,i}, \quad \forall i, \tag{5.9}$$

where w_m is the weight associated with $\boldsymbol{\delta}_{m,i}$ provided by SBS $m \in \{1,\ldots,M\}$ which primarily depends on the priority given to the decision, e.g., depending on the distance of the neighbour SBSs. Here, we simply consider unit weights, $w_m = 1,\ m = 1,\ldots,M$ to ensure the equal contributions from all the SBSs. The weights could be also assigned based on the level of interference from the neighbouring SBSs, or depending on the nature of traffic in the neighbour base stations. The aggregated activity index vector for an SBS is then defined as following.

$$\hat{\boldsymbol{\delta}} = \left[\hat{\delta}_1,\ldots,\hat{\delta}_N\right]^T, \tag{5.10}$$

where according to (5.9), $0 \leq \hat{\delta}_i \leq 1$, $\forall i$.

To obtain ASAI, each SBS only needs to transmit 1-bit of information per subchannel to the neighbouring SBSs. In the proposed method, each SBS broadcasts its corresponding δ_i at the beginning of each time frame which is received and recognized by all its neighbouring SBSs. Therefore, in a SBS obtaining ASAI for all N subchannels in a SBS with $M-1$ neighbouring cells only requires $(M-1)\times N$ bits of feedback.

5.2.1 Collaborative Spectrum Access

In a given SBS, the availability of subchannel i is then evaluated based on the value of $\hat{\delta}_i$. The SBS then adopts an appropriate access technique for each subchannel based on its corresponding ASAI.

In this section, a power allocation scheme is proposed in which incorporating $\hat{\delta}_i$, the transmit power of the SBS is obtained to maximize the achievable rate of

Algorithm 2 Inter-Cell Collaborative Spectrum Monitoring Scheme at SBS0

1: Neighboring SBSs, feedback $\boldsymbol{\delta}_m = [\delta_{m1}, \ldots, \delta_{mN}]^T$, to SBS0,
2: **for** each subchannel i, **do**
3: SBS0, obtains $\hat{\delta}_i$, using (5.9)
4: **if** $\hat{\delta}_i = 1$, **then**
5: the subchannel is not allocated in SBS0.
6: **else if** $\hat{\delta}_i = 0$, **then**
7: overlay access is adopted by the SBS0 on subchannel i,
8: obtain optimal transmit power,$\mathbf{P}^*_{\mathbf{a}}$, and maximize spectral efficiency,
9: go to step (12),
10: **else if** $0 < \hat{\delta}_i < 1$, **then**
11: SBS0 adopts underlay access on subchannel i and allocates power based on scheme in Section III.D.
12: obtain optimal transmit power,$\mathbf{P}^*_{\mathbf{b}}$based on the scheme in Section IV.
13: **end if**
14: **end for**

the secondary system subject to the maximum SBS transmit power and the QoS constraints in the primary network. The proposed spectrum access method at the SBS based on ASAI is summarized in Algorithm 2.

There are three possible cases: *i*) $\hat{\delta}_i = 0$, *ii*) $\hat{\delta}_i = 1$, and *iii*) $0 < \hat{\delta}_i < 1$. For $\hat{\delta}_i = 0$, there is no PU transmission detected on subchannel i both within the SBS and in the neighbouring cells. Therefore, overlay spectrum access is adopted for transmission over subchannel i. In cases where $\hat{\delta}_i = 1$, subchannel i is busy both in the SBS and its neighbouring cells, therefore secondary transmission on this subchannel is not allowed. In cases where $0 < \hat{\delta}_i < 1$ which is most

likely to occur, underlay spectrum access technique is adopted by the secondary system. The larger the $\hat{\delta}_i$, the higher will be the chance of imposing interference on subchannel i, thus the transmit power at the SBS should be adjusted accordingly to protect the primary system communication activity. In the following section, the detail analytical solution of the proposed subchannel power allocation for the case $0 < \hat{\delta}_i < 1$ is presented.

5.2.2 Optimal Power Allocation for $0 < \hat{\delta}_i < 1$

Here, an analytical framework is proposed to obtain the optimal subchannel power allocation based on $\hat{\boldsymbol{\delta}}_i$. As it is seen in (5.1), the achievable rate for user s on subchannel i, r_{si}, is a function of h_{si}, where $h_{si} = |g_{si}|^2/(N_0 + I_{pi})$, N_0 is the power of AWGN at the secondary receiver, and I_{pi} is the aggregated interference due to simultaneous transmissions by the PUs. It is assumed that the primary transmitters follow a non-adaptive and constant transmission power. On the other hand, the higher the value of $\hat{\boldsymbol{\delta}}_i$, the higher is the activity of the primary system over subchannel i. Therefore, a higher P_{si} is required to keep r_{si} at the same level to maintain the QoS.

It is again considered that for a SU s, two subchannels i, k, provide the same achievable rate, $r_{si} = r_{sk}$. If $\hat{\delta}_i < \hat{\delta}_k$, then $I_{pi} < I_{pk}$. Therefore, according to (5.1) a higher transmit power is required to provide the same rate, i.e., $P_{si} < P_{sk}$. In other words, the "cost" of providing the same rate to user s on subchannel i is lower than that of subchannel k.

Since there are multiple network parameters in the objective function, one way to incorporate them in an optimization problem is by defining a utility function. Here the purpose is to quantify the impact of $\hat{\delta}_i$ on the system performance at the SBS when deciding for the access method, and the transmit power on subchannel i, P_{si}. Thus corresponding to SU s, transmitting on subchannel i, the utility function, u_{si}, is defined as following. The utility based resource allocation for OFDMA system has been considered in many previous work, see, e.g, [140].

$$u_{si} \triangleq \frac{r_{si}}{\hat{\delta}_i}\alpha_{si}, \tag{5.11}$$

where α_{si} is a weight parameter assigned by the secondary system for the user fairness and prioritize the traffic. The larger the value of u_{si}, the lower is the cost of transmission on subchannel i. Total secondary system utility, U_a, is then defined as

$$U_a = \sum_{s=1}^{S} \sum_{i=1}^{N} u_{si}. \tag{5.12}$$

If $0 < \hat{\delta}_i < 1$, the SBS adopt underlay spectrum access. Thus interference is introduced at the primary receivers. Transmission collision may then occur at the primary receiver if the inflicted interference by the secondary transmission, $I_{ji} = \sum_{s=1}^{S} P_{si}\, g_{ji}, \forall i, j$, which is the interference at primary user due to secondary transmission, gets higher than a predefined threshold $\beta_{ji}, \forall j, i$. To protect the QoS in the primary system, a radio resource allocation is devised so that the probability of collision in the primary system is kept below a threshold, η_{ji}, which is a primary system parameter related to the primary QoS [142]. The optimal radio resource allocation is then formulated as following.

$$\mathcal{A}_1 : \max_{\mathbf{P}} \; U_a, \tag{5.13a}$$

$$\text{s.t.} \quad \sum_{s=1}^{S} \sum_{i=1}^{N} P_{si} \leq P_T, \tag{5.13b}$$

$$\Pr\left\{ \sum_{s=1}^{S} P_{si}\, g_{ji} > \beta_{ji} \right\} \leq \eta_{ji}, \quad \forall j, i, \tag{5.13c}$$

where P_{si} is the allocated transmission power for SU s on subchannel i, $\mathbf{P}$ is a $S \times N$ matrix, $\mathbf{P} = [\mathbf{P}_1 | \ldots | \mathbf{P}_S]$, and $\mathbf{P}_s = [P_{s1}, \ldots, P_{sN}]^T$. Constraint in (5.13b) ensures that the total transmit power in the SBS is always smaller than its maximum transmit power, P_T. Furthermore, (5.13c) is to keep the collision probability for the primary users below η_{ji}. Hereafter, for brevity it is assumed that the same QoS requirements for all users and over all subchannels, thus $\beta_{ji} = \overline{\beta}$, and $\eta_{ji} = \overline{\eta}$.

The probabilistic constraint in (5.13c) is difficult to be handled analytically. Instead, similar to [142], the constraint is transformed into a convex approxima-

tion, assuming that the channel distribution information (CDI) of the interference channel, g_{ji}, is known to the SBS. The constraint in (5.13c) is then reduced to

$$\begin{aligned}\Pr\left\{g_{ji} > \frac{\overline{\beta}}{\sum_{s=1}^{S} P_{si}}\right\} &= 1 - \Pr\left\{g_{ji} \leq \frac{\overline{\beta}}{\sum_{s=1}^{S} P_{si}}\right\}, \\ &= 1 - F_{g_{ji}}\left[\frac{\overline{\beta}}{\sum_{s=1}^{S} P_{si}}\right], \\ &\leq \overline{\eta}, \quad \forall j, i, \end{aligned} \tag{5.14}$$

where, $F_X(x)$ represents the cumulative distribution function (CDF) of a random variable X.

5.2.2.1 Rayleigh Distributed Interference Link

If g_{ji} follows a Rayleigh distribution with parameter r, then (5.14) is further reduced as following.

$$\exp\left(\frac{-\overline{\beta}}{2r^2 \sum_{s=1}^{S} P_{si}}\right) \leq \overline{\eta}, \ \forall i. \tag{5.15}$$

For Rayleigh distributed g_{ji}, using (5.15), (5.13c) is then reduced to

$$\sum_{s=1}^{S} P_{si} \leq \frac{\overline{\beta}}{2r^2\left(\ln\frac{1}{\overline{\eta}}\right)}, \ \forall i. \tag{5.16}$$

Therefore, under Rayleigh fading interference channels, $\mathcal{A}_1$ is reduced to the following optimization problem.

$$\mathcal{A}_2 : \max_{\mathbf{P}} \quad \sum_{s=1}^{S}\sum_{i=1}^{N} \frac{r_{si}}{\hat{\delta}_i}\alpha_{si}, \tag{5.17a}$$

$$\text{s.t.} \quad \sum_{s=1}^{S}\sum_{i=1}^{N} P_{si} \leq P_T, \tag{5.17b}$$

$$\sum_{s=1}^{S} P_{si} \leq \frac{\overline{\beta}}{2r^2\left(\ln\frac{1}{\overline{\eta}}\right)}, \ \forall i. \tag{5.17c}$$

Hereafter, for brevity, we assume $\alpha_{si} = 1 \ \forall i, s$.

5.2.2.2 Optimal Power Allocation in SBS

It can be observed that the optimization problem $\mathcal{A}_2$ is non-convex due to its non-convex feasible power allocation set, $\mathbf{P}$. Here, the dual decomposition approach [125] is adopted to obtain a sub-optimal solutions. There is a duality gap between the obtained solutions which are obtained using the dual decomposition method and the actual optimal solutions. However, it is shown in [144] that if the number of subchannels is sufficiently large, the duality gap becomes very small. Note that the obtained U_a using dual decomposition is in fact a lower bound on the maximum achieved total secondary system utility.

Lagrange function, $\mathcal{L}$, corresponding to $\mathcal{A}_2$ is obtained as following.

$$\mathcal{L}(\mathbf{P},\lambda,\boldsymbol{\mu}) = \sum_{i=1}^{N} \frac{1}{\hat{\delta}_i} \sum_{s\in \mathrm{S}} \log_2\left(1+\frac{|g_{si}|^2 P_{si}(\hat{\delta}_i)}{N_0+I_{pi}}\right) + \lambda\left(\sum_{s=1}^{S}\sum_{i=1}^{N} P_{si} \le P_T\right) + \sum_{i=1}^{N} \boldsymbol{\mu}_i \left(\sum_{s=1}^{S} P_{si}(\hat{\delta}_i) \le \frac{\overline{\beta}}{2r^2\left(\ln\frac{1}{\overline{\eta}}\right)}\right), \quad (5.18)$$

where, $\lambda \ge 0$ is the Lagrangian multiplier associated with the constraint (5.17b), and $\boldsymbol{\mu} \ge 0$ is the Lagrangian vector associated with the constraints in (5.17c). Here, I_{pi} is the aggregated interference observed at secondary system. The dual function is accordingly defined as:

$$\mathcal{D}(\lambda,\boldsymbol{\mu}) = \max_{\mathbf{P}} \mathcal{L}_a(P,\lambda,\boldsymbol{\mu}). \quad (5.19)$$

Therefore, the corresponding dual function is:

$$\mathcal{D}(\lambda,\boldsymbol{\mu}) = \max_{\mathbf{P}} \sum_{i=1}^{N} \frac{1}{\hat{\delta}_i} \sum_{s\in \mathrm{S}} \log_2\left(1+\frac{|g_{si}|^2 P_{si}(\hat{\delta}_i)}{N_0+I_{pi}}\right) - \lambda\sum_{i=1}^{N}\sum_{s=1}^{S} P_{si}(\hat{\delta}_i) - \sum_{i=1}^{N} \boldsymbol{\mu}_i \sum_{s=1}^{S} P_{si}(\hat{\delta}_i), \quad (5.20)$$

and thus the corresponding dual optimization problem is

$$\begin{aligned} &\min \quad \mathcal{D}(\lambda, \boldsymbol{\mu}), \\ &\text{s.t. } \lambda \geq 0, \ \boldsymbol{\mu} \geq 0. \end{aligned} \tag{5.21}$$

The optimal transmission power obtained from (5.21) maximizes the total system utility, however it needs to adjust $\lambda, \boldsymbol{\mu}$, which are in fact the prices associated with the constraints in $\mathcal{A}_2$.

Here, the Lagrangian multipliers $(\lambda, \boldsymbol{\mu})$ are iteratively estimated using the sub-gradient method [145], where the suitable direction of $(\lambda, \boldsymbol{\mu})$ is obtained. This reduces the computational complexity of finding the solution of the optimization problem. The value of λ and $\boldsymbol{\mu}$ are calculated through the following iterations.

$$\lambda(l+1) = \left(\lambda_i(l) + \Delta_s(l) \left(P_T - \sum_{s=1}^{S} \sum_{i=1}^{N} P_{si} \right) \right)^+, \tag{5.22}$$

$$\mu_i(l+1) = \left(\mu_i(l) + \Delta_s(l) \left(\frac{\overline{\beta}}{2r^2 \left(\ln \frac{1}{\overline{\eta}} \right)} - \sum_{s=1}^{S} P_{si}(\hat{\delta}_i) \right) \right)^+, \tag{5.23}$$

where, $(a)^+ = \max\{0, a\}$ and $\Delta_s(l)$ is the step size at the l^{th} iteration. The step size is initialized as $\Delta_s(l) \geq 0$, where $\sum_{l=1}^{\infty} \Delta_s^2(l) < \infty$, and $\sum_{l=1}^{\infty} \Delta_s(l) \to \infty$.

The optimal power allocation for each subchannel which maximizes the total utility in the SBS is a classic water-filling problem [125], thus, after few mathematical manipulations, the transmit power profile is obtained as following.

$$P_{si}^* = \left(\frac{1/\ln(2)}{\hat{\delta}_i(\lambda + \sum_i \mu_i)} - \frac{N_0 + I_{pi}}{|g_{si}|^2} \right)^+. \tag{5.24}$$

As it is seen, (5.24) returns $P_{si}^* = 0$ for subchannel i if $\frac{N_0 + I_{pi}}{|g_{si}|^2} > \frac{1/\ln 2}{\hat{\delta}_i(\lambda + \sum_i \mu_i)}, \forall s$. Note that P_{si}^* is independent from $\overline{\eta}$ and $\overline{\beta}$. Therefore, the constraint in (5.17c) needs to be re-evaluated as a further requirement of optimum transmit power allocation.

In OFDMA based cognitive radio systems only one SU, s^*, accesses subchannel i , therefore the maximum transmission power for the case where there is a free

subchannel is calculated as the maximum value of the constraint in (5.17c) as following.

$$P^*_{s^*i} = \frac{\overline{\beta}}{2r^2\left(\ln\frac{1}{\overline{\eta}}\right)}. \tag{5.25}$$

Therefore, the optimum transmission power is

$$P^{opt}_{si} = \min\left\{\max(0, P^*_{si}), \max(P^*_{s^*i}, 0)\right\}, \forall s, i, \tag{5.26}$$

which maintains the collision probability requirement for all the PUs as well as the transmission power constraint for the SBSs. Here, (5.26) is in fact the minimum value of (5.24) and (5.25), which is considered as the optimal transmission power because this does not violate other constraints and also fulfils the QoS requirements of the primary system.

5.3 Energy Efficient Power Allocation

In this section, the efficient transmission power allocation method is investigated from the energy efficiency (EE) perspective. As mentioned in the previous section, the ASAI provided an extra degree of freedom in system design to achieve the optimal spectral efficiency. Here, the implication of $\hat{\delta}_i$ on the energy efficiency (EE) of the CRN is studied as a new design criteria. Furthermore, the concept of EE is extended and accordingly defined as the achievable utility per unit power consumption. Similar to the case of spectral efficiency, the total interference constraints is considered to guarantee the minimum QoS to the PUs. Therefore, a utility function U_b is further defined to characterize the energy efficiency of the system as following.

$$U_b = \frac{\sum_{i=1}^{N} \frac{1}{\hat{\delta}_i} \sum_{s\in \mathrm{S}} \log_2\left(1 + \frac{|g_{si}|^2 P_{si}(\hat{\delta}_i)}{N_0 + I_{pi}}\right)}{k_1 + k_2 \sum_{i=1}^{N}\sum_{s=1}^{S} P_{si}(\hat{\delta}_i)} \alpha_{si}, \tag{5.27}$$

where, k_1 and k_2 are the circuit operation power and power amplifier consumptions, respectively. For brevity, hereafter it is assumed that $\alpha_{si} = 1,\ \forall i, s$.

The maximum achievable EE is obtained through the following optimization problem.

$$\mathcal{A}_3 : \xi^* = \max_{\mathbf{P}} \quad \frac{\sum_{i=1}^{N} \frac{1}{\hat{\delta}_i} \sum_{s\in \mathrm{S}} \log_2 \left(1 + \frac{|g_{si}|^2 P_{si}(\hat{\delta}_i)}{N_0 + I_{pi}}\right)}{k_1 + k_2 \sum_{i=1}^{N} \sum_{s=1}^{S} P_{si}(\hat{\delta}_i)}, \tag{5.28a}$$

$$\text{s.t.} \quad \sum_{s=1}^{S} P_{si}\ g_{ji} < \beta_{ji}, \tag{5.28b}$$

$$P_{si} \geq 0 \quad \forall s, i. \tag{5.28c}$$

The optimization problem $\mathcal{A}_3$ needs to be approximated to be transformed into a convex optimization problem. Therefore, the fractional function in (5.28a) requires further analysis to show that it is quasi-concave. Since the global optimal and local optimal solutions match when it satisfied the KKT conditions, it can be concluded that $P^*_{s,i}(\hat{\delta}_i)$ is an optimal solution if it satisfies the KKT conditions, see, e.g., [136] and references therein.

The results in [146] can be used here in which it is shown that utilizing Charnes-Cooper Transformation (CCT), a quasi-concave fractional optimization can be further reduced to a concave optimization problem. Therefore, to further simplify $\mathcal{A}_3$, here $\mathbf{y} = t\mathbf{P}$ is set, i.e., $\mathbf{P} = \frac{\mathbf{y}}{t}$, where $t = \frac{1}{k_1 + k_2 \sum_{i=1}^{N} \sum_{s=1}^{S} P_{si}(\hat{\boldsymbol{\delta}}_i)}$, and $\mathbf{y} \triangleq \{y_{si}\}_{\{s=1\ldots S,\ i=1\ldots N\}}$.

By following further analytical manipulation, $\mathcal{A}_3$ is then reduced to

$$\mathcal{A}_4 : \max_{\mathbf{y}, t>0} t \sum_{i=1}^{N} \frac{1}{\hat{\delta}_i} \sum_{s\in \mathrm{S}} \log_2 \left(1 + \frac{\mathbf{y}}{t} \frac{|g_{si}|^2}{N_0 + I_{pi}}\right), \tag{5.29a}$$

$$\text{s.t.} \quad \sum_{s=1}^{S} y_{si}\ g_{ji} - \overline{\beta}\ t \leq 0, \tag{5.29b}$$

$$t \left(k_1 + k_2 \sum_{i=1}^{N} \sum_{s=1}^{S} y_{si}(\hat{\delta}_i)\right) = 1, \tag{5.29c}$$

$$y_{si} \geq 0 \quad \forall s, i. \tag{5.29d}$$

$\mathcal{A}_4$ can be further reduced as following.

$$\mathcal{A}_5 : \max_{\mathbf{y},t>0} \sum_{i=1}^{N} t\frac{1}{\hat{\delta}_i}\sum_{s\in \mathrm{S}} \log_2\left(1+\frac{\mathbf{y}}{t}\frac{|g_{si}|^2}{N_0+I_{pi}}\right) - \sum_{s=1}^{S} t\log_2(t), \tag{5.30a}$$

$$\text{s.t. } (5.29b), (5.29c), (5.29d), \tag{5.30b}$$

which has been now converted to the convex optimization problem. The Lagrangian function corresponding to $\mathcal{A}_5$ is then obtained as:

$$\begin{aligned}\mathcal{L}(\mathbf{y},t,\lambda,\mu,\phi,\upsilon) = &\sum_{i=1}^{N} t\frac{1}{\hat{\delta}_i}\sum_{s\in \mathrm{S}} \log_2\left(1+\frac{\mathbf{y}}{t}\frac{|g_{si}|^2}{N_0+I_{pi}}\right) - \\ &\sum_{s=1}^{S} t\cdot\log_2(t) - \sum_{i=1}^{N}\lambda_i\left(\sum_{s=1}^{S} y_{si}\ g_{ji} - \overline{\beta}\ t\right) - \\ &\mu\left(t\cdot k_1 + k_2\sum_{i=1}^{N}\sum_{s=1}^{S} y_{si}(\hat{\delta}_i) - 1\right) + \sum_{s=1}^{S}\phi_s y_s + \upsilon\cdot t,\end{aligned} \tag{5.31}$$

where λ, μ, ϕ and υ are Lagrangian coefficients associated with the corresponding constraints in $\mathcal{A}_5$. In addition, ξ can also be defined as EE and we find optimal transmission power profile which maximizes ξ. Following the same line of arguments as in the chapter 4, by taking the complimentary slackness of KKT condition and noting that $0 \le \mathbf{P} \le P_T$, the optimal transmission power is obtained as $P^* = \frac{y^*}{t^*}$ which ultimately is reduced as following.

$$P_{si}^* = \min\left\{\left[\frac{\frac{1}{\ln(2)}}{\hat{\delta}_i\left(\sum_i \lambda_i g_{ji} + \mu\right)} - \frac{N_0+I_{pi}}{|g_{si}|^2}\right]^+, P_T\right\}. \tag{5.32}$$

A new optimization problem can also be obtained by adding a new constraint to the total transmission power in $\mathcal{A}_5$. The closed form solution of the optimal transmission power can be obtained similar to (5.32). Therefore, P_T has been considered as maximum range of P_{si}^* which is similar analysis as in [147] and references therein.

For further observation, fractional utility function, U_b, in (5.27) can be written as $\xi = \frac{X_{\mathcal{N}}(\mathbf{P},\hat{\delta}_i)}{X_{\mathcal{D}}(\mathbf{P},\hat{\delta}_i)}$. Dinkenlbach's theorem [148], [149] is then utilized to obtain the optimal ξ and transmit power as shown in Theorem 5.1.

Algorithm 3 Iterative power allocation algorithm and EE optimization

Input: error tolerance: $\epsilon > 0$, maximum iterations: I_{max}, iteration index: n, $\lambda^{(0)} = \lambda_{(0)}$, $\mu^{(0)} = \mu_{(0)}$, initial EE: $\xi^{(0)} = \xi_{(0)}$

Output: ϵ-optimal power profile: $\mathbf{P}^*$, optimal EE: ξ^*

1: **while** ($n \leq I_{max}$ AND $X_{\mathcal{N}}(\mathbf{P}^*, \hat{\delta}_i) - \xi^* X_{\mathcal{D}}(\mathbf{P}^*, \hat{\delta}_i) \geq 0$) **do**

2: obtain $\mathbf{P}^{(n)}$ from (5.32) for a given (or obtained) $\xi^{(n)}$

3: obtain $\lambda^{(n)}$, and $\mu^{(n)}$ using subgradient method

4: set $n = n + 1$, and $\xi^{(n)} = \frac{X_{\mathcal{N}}(\mathbf{P}^*, \hat{\delta}_i)}{X_{\mathcal{D}}(\mathbf{P}^*, \hat{\delta}_i)}$

5: **end while**

6: **return** the ϵ-optimal power allocation profile $\mathbf{P}^* = \mathbf{P}^{(n)}$, and $\xi^* = \xi^{(n)}$.

Theorem 5.1. *The optimal energy efficiency, ξ^*, is achieved in $\mathcal{A}_3$ when the condition $\max_{\mathbf{P}} X_{\mathcal{N}}(\mathbf{P}, \hat{\delta}_i) - \xi^* X_{\mathcal{D}}(\mathbf{P}, \hat{\delta}_i) = X_{\mathcal{N}}(\mathbf{P}^*, \hat{\delta}_i) - \xi^* X_{\mathcal{D}}(\mathbf{P}^*, \hat{\delta}_i) = 0$ is satisfied for $X_{\mathcal{N}}(\mathbf{P}, \hat{\delta}_i) \geq 0$ and $X_{\mathcal{D}}(\mathbf{P}, \hat{\delta}_i) > 0$.*

The iterative power allocation algorithm is adopted to obtain the optimal power allocation profile, $\mathbf{P}^*$ based on (5.32), to resolve the EE optimization problem. According to Theorem 5.1, the iteratively calculated transmission power profile is optimal if and only if, in Algorithm 3, $X_{\mathcal{N}}(\mathbf{P}^*, \hat{\delta}_i) - \xi^* X_{\mathcal{D}}(\mathbf{P}^*, \hat{\delta}_i)$ becomes equal to zero after n iterations. In other cases, the ϵ-optimal transmission power and energy efficiency, $X_{\mathcal{N}}(\mathbf{P}^*, \hat{\delta}_i) - \xi^* X_{\mathcal{D}}(\mathbf{P}^*, \hat{\delta}_i) < \epsilon$ is achieved, where $\epsilon > 0$ is an error tolerance which is a very small positive number. The convergence of Algorithm 3 depends on the associated constraints, channel gain information, error tolerance factors etc.

5.4 Simulation Results

In this Section, the analytical results of the proposed techniques are simulated and then compared against the reference models for validation.

5.4.1 Simulation Settings

Table 5.1: Simulation Parameters

Channel Model	Rayleigh with $r = 1$.
Number of Subchannels (N)	32
Subchannel Bandwidth (B_i)	125 KHz
Number of The Secondary Users (S)	6
Interference Threshold ($\overline{\beta}$)	0.15
Collision Probability Threshold ($\overline{\eta}$)	0.1-0.6
Maximum SBS Transmit Power (P_T)	10-30 dBm
Probability of Idle Subchannel (P_{H0})	0.5
Noise Spectral Density (N_0)	-174 dBm/Hz[1]
Location of SUs	Random around SBS0 (origin)

In this Section, the simulation is performed considering an OFDMA based cellular cognitive radio network, where primary system is collocated with the secondary system, as shown in Fig. 5.1. Firstly, one secondary base station is considered, e.g., SBS0, which implements the proposed Algorithm 2 presented in Section 5.2. Both primary and secondary users are randomly dispersed within the transmission range of SBS0. In each time frame, ASAI, i.e., $0 < \hat{\delta}_i \leq 1$, where $i \in \{1, \ldots, N\}$, is estimated using the low complexity collaborative spectrum sensing approach. As mentioned in the previous sections, ASAI in all subchannels are independently estimated through the energy detection method. The simulation parameters are shown in Table 5.1, unless otherwise stated.

At first, the investigation results on the impact of system parameters on the performance of the proposed method is presented which will be briefly discussed later in this Section. The system performance of the proposed method is then compared against two benchmark system models. Various schemes have been

[1]The noise power in the considered subchannel is 4.976×10^{-13} mW.

proposed in literature to measure the performance of channel and power allocation technique, e.g., [29], [47], [150], [151]. Based on them, several benchmark models have been developed for comparison, therefore they will be referenced in this chapter as well. The concepts of equal power allocation, perfect channel utilization, and bursty primary traffic are some of the designs from the previous works for comparison purpose in this chapter.

The first one is branded as *Equal Power Allocation* (EPA). Here, EPA is the scenario under which standalone SBS0 with no signalling among the adjacent SBSs is considered. As a result, the base station does not have a priori knowledge of ASAI which ultimately forces to allocate equal transmit power in all the subchannels. Therefore, in such cases, the SBS has to allocate the equal transmit power to users even when the channel gain is measured to be the lower bound. Moreover, *Perfect Channel Utilization* (PCU) is considered as a second reference model for comparison. This ideal scenario is the upper-bound benchmark, which may not be generally available in practice. Here, PCU is a scenario in which an ideal spectrum sharing system is considered, where both accurate spectrum sensing information and perfect interference channel state are available on the secondary system. Therefore, depending on the subchannel access rate, PCU utilizes overlay spectrum sharing for idle subchannels, and underlay spectrum sharing method for underutilized subchannels.

For underlay spectrum access method, the secondary system utility is maximized for a proposed power allocation method subject to aggregated interference constraint and maximum SBS transmit power constraint. Moreover, EPA can be considered as a worst case scenario due to the lack of knowledge about primary user activity and interference channel status, whereas PCU is considered as the best case scenario due to the availability of interference channel and primary user activity information. The investigated performance metric is the total achievable spectral efficiency defined as $\sum_{s=1}^{S}\sum_{i=1}^{N} r_{si}$ which is the sum-rate normalized over the system bandwidth.

5.4.2 Impact of Maximum Transmit Power

Here, it is examined how primary traffic load and total transmit power constraint at SBS affect the total achievable spectral efficiency of secondary system. When the PUs are more active by accessing subchannels more frequently, i.e., higher $\hat{\delta}_i$, the achievable rate at SBS is decreased as shown in Fig. 5.3. Interestingly however, it is observed that when the rate of PUs accessing their subchannel is less frequent, e.g., $\hat{\delta}_i < 0.5$, increasing P_T does not significantly help to achieve better system throughput. As it can be further observed that the increase in P_T from 10 dBm to 30 dBm, the maximum SE achievement is below 1 bps/Hz. This is due to the fact that, for lower $\hat{\boldsymbol{\delta}}$ where a large number of subchannels are available for secondary systems, even by allocating a higher P_T, the transmit power per subchannel at SBS remains almost constant due to the imposed interference constraint.

5.4.3 Impact of Collision Probability Constraint

The total achievable spectral efficiency at the SBS versus the interference constraint at the primary system ($\overline{\eta}$) is plotted in Fig. 5.4 for the proposed power allocation scheme as well as the system settings for PCU. As it can be observed, allocating a higher maximum transmission power results in a higher spectral efficiency which can be considered as an obvious case. However, it is further observed that increasing P_T from 10 to 30 dBm results in an improvement of 1 bps/Hz on the spectral efficiency mostly in all considered interference constraints from 0.01 to 0.12. Corresponding to a larger P_T, a relatively greater throughput improvement is observed for larger values of $\overline{\eta}$. Since a primary system with a larger $\overline{\eta}$ demonstrates a higher tolerance against the secondary interference, the SBS is able to allocate a higher transmission power, thus achieves a higher spectral efficiency.

Fig. 5.4 further indicates that the spectral efficiency performance of the proposed method closely follows the scenario of PCU where the underlay and overlay method of cognitive radio channel access is implemented. Note that comparing to PCU, the proposed method requires a significantly lower signalling overhead.

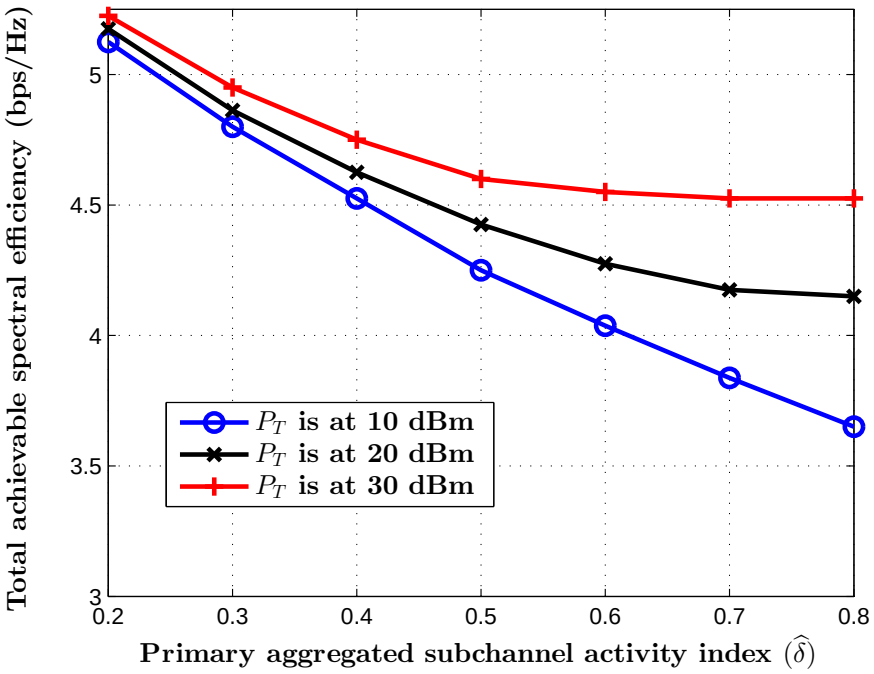

Figure 5.3: Total achievable spectral efficiency at the secondary system *vs.* aggregated subchannel activity index for various transmit power constraints.

In other words, the lower level of required signalling in the proposed method is associated with a reasonable cost on throughput.

5.4.4 Impact of Primary Network Activity

In this Section, the total achievable spectral efficiency obtained through the proposed method for two distinct primary network load conditions are compared. The first scenario is the case in which the primary service transmitter has very limited amount of data to transmit. This situation is modelled by setting very low duty cycle which apparently simulates the low traffic intensity at primary transmitter. This will result in a very low ASAI which is typically obtained with average value of $\hat{\boldsymbol{\delta}} = 0.001$. The next is a case when moderately loaded primary service is considered, where subchannel activity index is achieved to be $\hat{\boldsymbol{\delta}} = 0.6$.

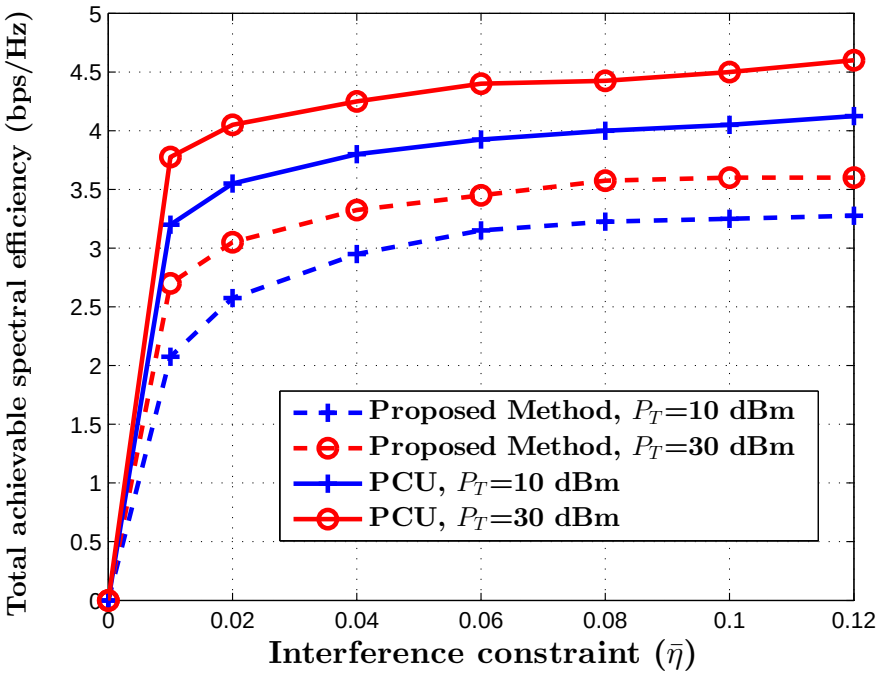

Figure 5.4: Total achievable spectral efficiency of SBS *vs.* collision probability threshold for $P_T = 10, 30$ dBm for the proposed method and the PCU for $\hat{\boldsymbol{\delta}} = 0.6$.

When the network scenario is set such that $\hat{\boldsymbol{\delta}}$ is achieved to be 0.001, the power allocation in Section 5.2 acts very approximately to an overlay method of spectrum access. Therefore, the comparison presented here indicates how efficient is the proposed power allocation scheme in exploiting the load variations in the primary network.

The total achievable spectral efficiency at the secondary system is plotted in Fig. 5.5 when the number of SUs (S) varies in the range of 4 to 10, and total transmit power (P_T) varies from 10 to 30 dBm. Also the network scenario is maintained such that ASAI is achieved to be at $\hat{\boldsymbol{\delta}} = 0.001, 0.6, 0.999$ to simulate three different network load conditions and $\overline{\eta}$ is set to be 0.05. As it is observed in Fig. 5.5, when the ASAI ($\hat{\delta}_i$) in the primary network is increased, the achievable spectral efficiency at secondary system simultaneously decreases. Surprisingly however, the achievable spectral efficiency of the proposed method is very close

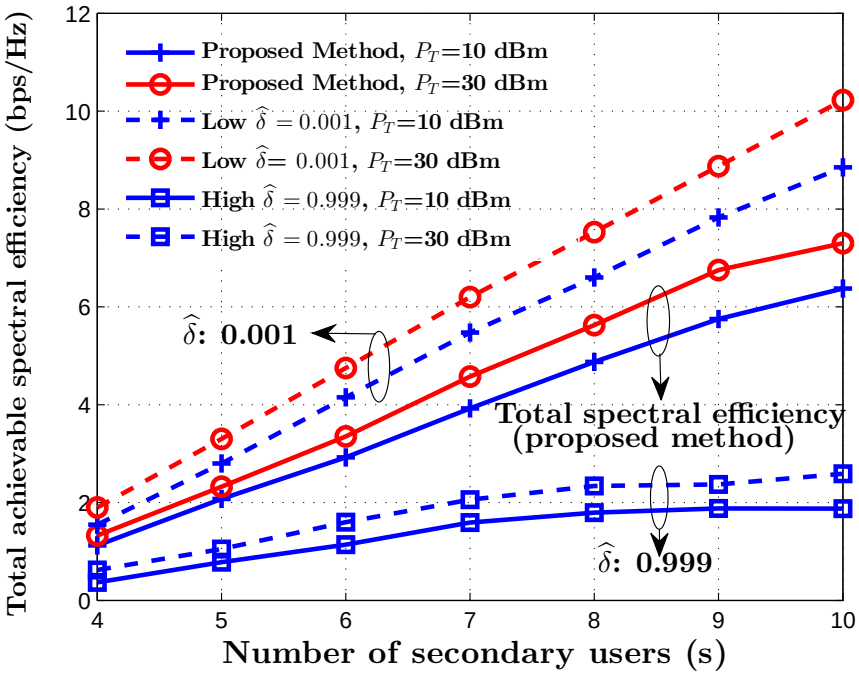

Figure 5.5: The total achievable spectral efficiency of the SBS *vs.* the number of SUs, S, for $P_T = 10$, 30 dBm, $\hat{\boldsymbol{\delta}} = 0.001, 0.6$ and $\overline{\eta} = 0.05$.

to that of the overlay access for a low to moderate secondary network load. It is also observed in Fig. 5.5 that for $P_T = 10$ dBm, 30 dBm, the spectral efficiency does not increase with the same rate due to the imposed collision probability constraint while formulating the optimization problem. This apparently suggests that the proposed method achieves the total spectral efficiency very close to the when there is very low traffic load on the primary network with the lower signalling complexity.

5.4.5 Comparison with EPA and PCU

The spectral efficiency of the proposed system along with its comparison against two benchmark power allocation settings, i.e., EPA and PCU, are presented in Fig. 5.6. The variations in traffic demand in the secondary system represented

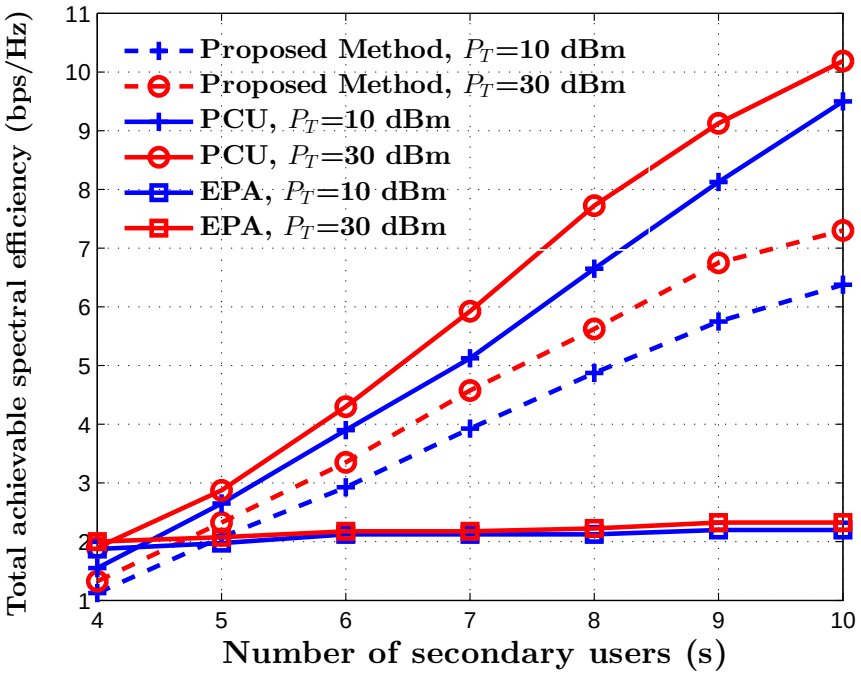

Figure 5.6: Total achievable spectral efficiency of the secondary system *vs.* the total number of the secondary users for different scenarios and P_T values.

by the number of secondary users, S, when maximum transmit power is kept at 10 dBm, 30 dBm. As expected, PCU achieves the highest system utility due to ideally utilizing the subchannels, whereas EPA has the lowest due to the absence of subchannel activity profile at the primary system which enforces system to allocate equal transmit power. The proposed resource allocation scheme however achieves a significantly higher spectral efficiency than that of the EPA. This is due to the fact that the primary system activity provided by incorporating ASAI is exploited in the subchannel power allocation. It is further observed that the proposed method closely follows the ideal subchannel access, i.e., PCA with a slightly lower spectral efficiency but significantly lower signalling overhead among the secondary base stations.

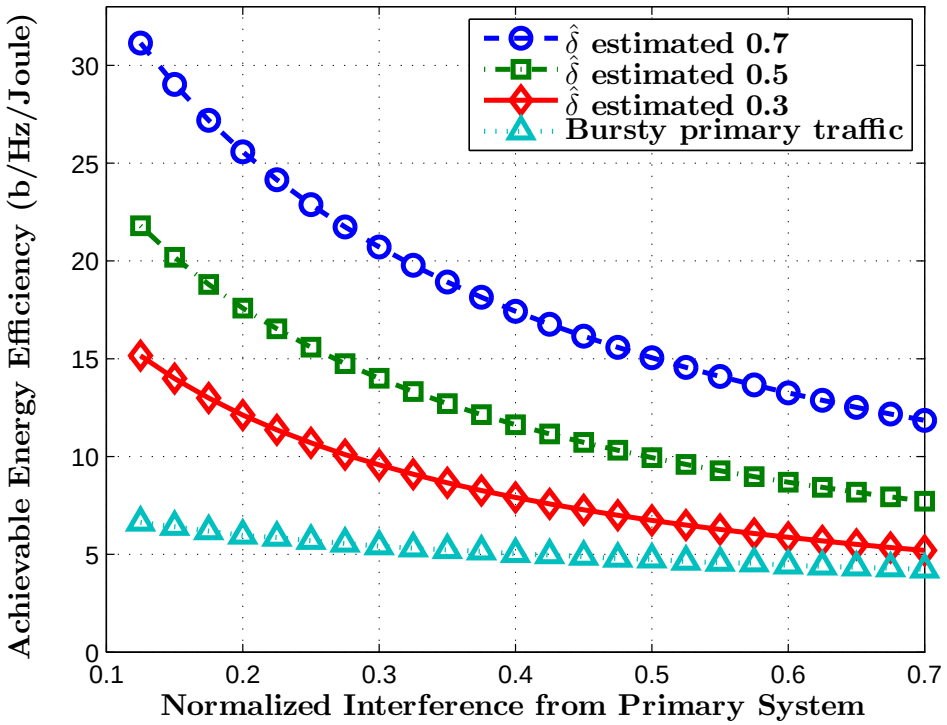

Figure 5.7: Energy efficiency *vs.* normalized interference from primary system for various primary network traffic.

5.4.6 Impact of Primary Network Traffic on Energy Efficiency

The performance of the proposed method in terms of energy efficiency is investigated against the case when the ASAI is not estimated. When the impact of interference from primary system increases, the achievable energy efficiency deteriorates due to the higher transmit power requirement at the secondary system to suppress the interference. The lowest energy efficiency is achieved when the primary network traffic is of bursty nature in which the variation of $\hat{\delta}$ becomes high. Therefore, even in the lower interference regime, the energy efficiency is not significantly higher. For instance, energy efficiency is achieved to be four times higher ($\approx$ 20 b/Hz/Joule) when $\hat{\delta} = 0.7$ than the case of bursty primary network

traffic ($\approx$ 5 b/Hz/Joule). Therefore, it can be concluded that the $\hat{\delta}$ estimation enables the improved resource allocation to achieve higher energy efficiency as shown in Fig. 5.7. Moreover, when the primary users activity is higher and is considered to be accurately estimated, there are more opportunities available to access the subchannels such that the system energy is significantly utilized for data transmission to achieve improved energy efficiency. However when the interference from the primary system is higher, energy efficiency cannot be significantly improved in the same way. For instance, at the normalized interference of 0.6, the energy efficiency is improved just from 4 to 6 b/Hz/Joule, in cases of bursty primary traffic and $\hat{\delta}_i = 0.3$, respectively.

5.4.7 Energy Efficiency and Total Spectral Efficiency

Here, further analysis is presented regarding the optimal energy and spectral efficiencies as a unified model for the real-time measurement of the subchannel activity index, $\hat{\boldsymbol{\delta}}$, since both EE and SE depend on optimal transmit power and QoS requirements imposed by the primary system. In addition, the ASAI is used in the proposed analytical models to design the optimal transmit power allocation. Such an articulated analysis is possible to design due to the proposed system model and utility functions presented in previous sections.

The optimal spectral efficiency and energy efficiency as a function of $\hat{\delta}_i$ for the proposed method, for a range of total transmit power, is shown in Fig. 5.8. The proposed methods improve the performance in various range of ASAI, i.e., $\hat{\delta}_i$. It is shown in Fig. 5.8, for instance, that when subchannels are busy, as indicated by $\hat{\delta}_i$ in the range of $[0.65, 0.9]$, the transmission power is controlled in such a way that the EE is improved whereas the SE does not degrade significantly when maximum P_T is 30 dBm. Also in the lower ASAI, as indicated by $\hat{\delta}_i$ in the range of $[0.1, 0.3]$, EE remains in the same level of around 15 b/Hz/Joule without significant decrease in the spectral efficiency. Moreover, when the primary subchannels are moderately occupied, i.e., $\hat{\delta}_i$ in the range of $[0.4, 0.6]$, the secondary system can achieve acceptable levels of both EE and SE simultaneously. In this case, the maximum P_T does not play a vital role on the system performance.

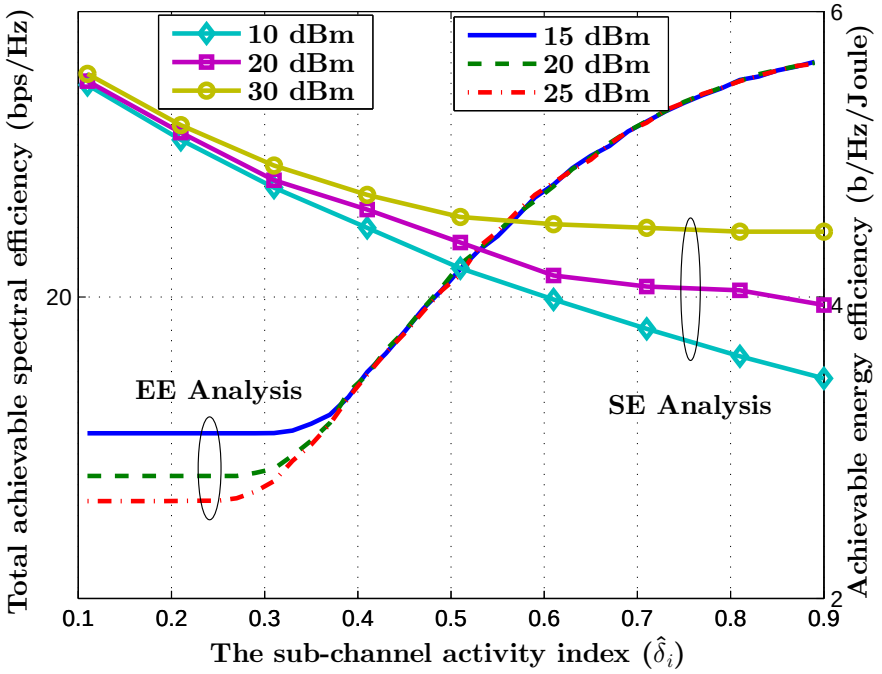

Figure 5.8: Achievable spectral and energy efficiency *vs.* primary user activity index for various total power constraints.

In a conventional EE and SE optimization, the improvement in EE as well as SE is obtained either by considering a linear combination of EE and SE objectives [129], or defining an objective function based on the transmit power as discussed in [138]. In such cases, when the transmit power is increased, improved SE is obtained with the sacrifice on the EE and vice-versa. The major concern in such models of CRN design is that there is a limited range of transmit power for SUs due to the interference constraints imposed by primary system. For instance, the higher the transmit power, larger will be the interference to the primary system which puts the limitations on the secondary system. In the proposed model however, by relaxing (or tightening) the constraint in (5.8), larger (or smaller) number of subchannels could be available for SUs such that $\hat{\delta}_i$ slightly moves to the higher (or lower) range. Therefore, depending on the requirements, i.e., either better EE or better SE is anticipated, system parameters can be optimized to

achieve the target without compromising the primary system QoS in the proposed method.

Therefore, the proposed method provides an entirely new perspective on cognitive radio and communication system design where the operating point in terms of ASAI, as shown in x-axis in the Fig. 5.8, can be dynamically obtained by adjusting the sensing parameters, e.g., sensing duration, sensing threshold, and detection probability threshold.

5.5 Conclusions

At the beginning of this chapter, the reference system model with the add-on features considered for the proposed method of resource allocation has been presented. In addition, the essentials of energy detection method for spectrum sensing and the associated hypothesis testing are reviewed. Based on the conditional probabilities of hypotheses tests, the decisions parameters are identified which ultimately provides information about the primary subchannels. This resulted the parameter *subchannel activity index* which has been defined and characterized to incorporate the communication activity associated with the PUs in efficient resource allocation. Moreover, a simple yet efficient intercell collaborative spectrum monitoring scheme has been proposed with very low signalling overhead to evaluate the activities level of users in the subchannels, i.e., *aggregated subchannel activity index*, as an indicator of network wide activities level of PUs on the subchannels.

The efficient power allocation profile is then obtained at the SBS with the objective of maximizing total SBS utility and total primary users interference constraint as well as the total transmit power constraint. The SBS utility has been defined based on ASAI and system throughput. In addition, the impact of ASAI into the energy efficiency is also investigated by defining the utility function and obtained the efficient transmit power profile with the associated constraints. In the cognitive radio network, the energy and spectral efficiencies contradict each other due to the fact that both cannot be maximized at the same time. A general practice is that one of them is maximized keeping another at

a certain level. However in the proposed method, a novel and practically viable design between spectral and energy efficiencies has been successfully achieved considering the primary communication activity on the allocated subchannels.

The simulation results have further confirmed that the proposed scheme exploits the variations in the primary system communication activity to improve the secondary system achievable rate. It is also confirmed the slight decrease of the rate comparing to the ideal case in which both underlay and overlay methods of spectrum sensing are implemented, however it is greater than the case when no optimal power allocation algorithm is implemented, i.e., the equal power allocation method. Further investigation has been executed to measure the impact of ASAI into the energy efficiency and concluded that the proposed method is a better design approach to obtain the optimal energy efficiency and/or spectral efficiency concurrently by adjusting the spectrum sensing parameters at the secondary system.

Chapter 6

Conclusions and Future Works

6.1 Summary of the Thesis

In **Chapter 1**, the very beginning picture of cognitive radio networks has been discussed. The requirements of cognitive radio is basically due to the current convergence of various wireless communication technologies, the exponential growth of user densities and the data-hungry applications. In addition, the requirements for M2M and Internet-of-Everything also demanded more data transmission through the wireless channel. On this context, software-defined network and cognitive radio communication have been studied for last one and half decade. A detail study of cognitive cycle to enable the cognitive radio concept has also been discussed in this chapter. The journey of cognitive radio networks has come long way to make it worldwide acceptable by industry, government and academia. Various organizations, for instance the IEEE, have worked together to make a global standard for cognitive radio, such as IEEE 802.22 to be used in TV band, in this period. The journey of cognitive radio has been briefly described in this chapter. Since the research domain of cognitive radio networks is very wide, there are even many challenges to implement them in practice. Such research challenges in terms of spectrum sensing, resource allocation, energy efficiency etc. have also been described along with the relevant examples. The factors that motivated

to conduct this research, which apparently produced this Thesis, have also been included in this chapter.

In **Chapter 2**, a brief description of various spectrum sensing techniques proposed for cognitive radio networks has been presented. The spectrum sensing task is obviously one of the first requirements to enable the cognitive radio communication in current cellular network architecture. Therefore, based on the outcome of sensing technique, an efficient resource allocation method could be designed, i.e., higher the spectrum sensing accuracy, better will be the resource allocation strategy. Nevertheless, a very important tradeoff between sensing duration and transmission duration do exist in cognitive radio communication. Such issues have been clearly identified and described in this chapter. Moreover, various spectrum sensing methods have been described that are available in the literature as a foundation of the proposed spectrum sensing methods proposed in this Thesis. Specifically, the cooperative and non-cooperative spectrum sensing also have been described with their respective advantages and disadvantages. In a cooperative spectrum sensing method where local information about the subchannel availability is diffused at a centralized system, soft combining and hard combining methods are, in general, used in such cases. The benefit have been described in this chapter, such as the hard combining method has less complexity with lower accuracy on the spectrum sensing results. The challenges of spectrum sensing methods for cognitive radio have been briefly discussed. At last but not the least, the spectrum sensing results obtained from the specially designed spectrum sensors for TV band and GSM band, i.e., 500 MHz, 800 MHz and 1600 MHz have been collected in the Lancaster City area to show the nature of spectrum availability in real network. The rest of the chapters discussed to exploit the available spectrum as shown on the obtained spectrum sensing results.

In **Chapter 3**, a brief introduction of the considered system model has been presented. The concepts of multi-cellular and multi-carrier system with primary and secondary service providers collocated in the same geographical region for spectrum sharing have been discussed with the appropriate network diagrams. The concept of subchannels, orthogonal frequency division multiple access (OFDMA) as an optimal modulation scheme for cognitive radio in addition to the interference models have also been described to justify their usage in the

considered system of spectrum sensing and resource management. Furthermore, the channel models, frame structure where spectrum sensing and transmission durations are embedded have also been discussed. The features presented in this chapter is the basis for the follow-up chapters with some add-on features when they are needed. The last part of the chapter discussed one of the available cognitive radio standards for the TV band, i.e, IEEE 802.22 standard, to explain the strict requirements to implement cognitive radio in practice. The purpose of this subsection is that the rest of the proposed methods would follow such requirements to choose the appropriate cognitive radio parameters.

In **Chapter 4**, the proposed low-latency zone-based cooperative spectrum sensing scheme in a multicell network has been exclusively described. It was basically the sensor-enabled cognitive radio system where the dedicated sensing devices took control the spectrum sensing task from the secondary system. In conventional cognitive radio however, the secondary users have to consume the precise resource of time frame in terms of the sensing duration. As a result of the proposed methods, the secondary users can have more frame duration to transmit the data packets which apparently improves the system throughout. In addition, the proposed method significantly improves the power consumption in the secondary system due to skipping the bulky spectrum sensing task. This chapter also presented the design criteria of sensing devices such that the trade-off among the sensing accuracy, system throughput and sensing network cost can be explained both mathematically and through the simulation results. The detail communication protocol among secondary system and the sensing devices have also been presented. However offloading the sensing task to an independent network is a good idea, the design of such a network is equally a challenging task. In this chapter, various combination of spectrum sensing devices and base stations have been considered and it has been shown mathematically that the optimization problem is a convex optimization problem under some specific network parameters. Such conditions have been explained and solved the problem to find the optimal design of such network. Finally, the simulation results demonstrated the improved sensing accuracy and thus the system throughput in the proposed network scenarios.

In **Chapter 5**, the proposed method of subchannels and transmit power allocation have been presented. It is obvious to believe that the communication activities of primary users on the subchannels highly affect the resource allocation strategy in secondary system. As a result, a reliable method of estimating the activities of primary users on the subchannels was explained by defining a parameter called the *subchannel activity index*. This parameter was later obtained in the multiple cell scenario such that the aggregated version is obtained by incorporating such decision vectors from the neighbouring cells. This parameter literally indicates the best possible subchannel in the vicinity of the cell at a particular time and location. Furthermore, the transmit power allocation problem is defined as an optimization problem with the primary system interference constraint and total transmit power constraint. The problem was then solved using dual decomposition method to find the optimal transmit power profile. While formulating the optimization problem, both spectral efficiency and energy efficiency have been considered. Therefore, the energy efficiency also has been defined as a utility function in terms of the *subchannel activity index*. The fractional optimization problem has been defined with the similar constraints mentioned above. Later in the chapter, the obtained results from the optimization problem have been analysed together which concluded that the proposed method maintains a better system design approach to maintain the balanced between energy efficiency and spectral efficiency by changing the sensing parameters in the secondary system.

Finally, in this **Chapter 6**, the summary and contributions of this Thesis have been presented. Based on the recent research activities, the future directions of radio resource allocation in cognitive radio in terms of the requirements of 5G are also discussed.

6.2 Future Research

It is in fact too early to predict the features of 5G telecommunication system. Nevertheless, the early prediction shows that the data volume has to be 1000 times higher per area with up to 100 times higher data rate and 10 times longer

battery life of devices [152]. Such services must be available with the milliseconds of end-to-end delay. Therefore, it can be anticipated that a single technology alone cannot fulfil such a vibrant requirements. Therefore, there must be diverse technologies which converge together with appropriate protocols to achieve the targets. Some of the recently proposed technologies for 5G are mmWave, NOMA, heterogeneous network (HetNet), massive MIMO etc. [153]. The cognitive radio enabled M2M communication has gained huge attention recently to solve spectrum scarcity and energy efficiency issues in M2M communications [154]. However it is needless to say that one of the highly celebrated and matured technologies in 5G and beyond is cognitive radio network. It is due to the fact that the scarcity of spectrum will be the key challenge to provide the services in 5G and cognitive radio is capable of tackling such issues. Therefore, a further research work is to obtain the reliable and robust spectrum sensing and radio resource allocation methods to make cognitive radio as one of the inevitable candidate technologies of 5G. One of the solutions to solve the spectrum scarcity problem is to use mmWave in 35 GHz or 70 GHz where huge amount of bandwidth is available. However, it is too immature to expect mmWave communication in near future because the early stage of channel modelling has just been undertaken. Also, microwave band is very attractive for wireless communication among service providers because it travels longer distance and its channel properties are well understood. As a result, more effort should be devoted to make cognitive radio an important technology at early stage of 5G and beyond.

Since cellular mobile communication system from 1G to 4G were basically human oriented, such as they carry audio, video and data generated by users. On the other hand, in case of 5G, the things oriented communication system is considered to be enabled [155]. The recent research and development efforts in D2D and M2M to enable IoT are the early signs of future wireless communication system [156],[157]. These are the short range radio communication systems where peer devices are close to each other with line-of-sight (LOS) or non-LOS communication range. In such cases, the cognitive radio technique could be implemented using the underlay access mode such that they do not interfere, or with minimum interference, to the primary system. Therefore, finding the appropriate

protocols and techniques for such communication systems is another important future research.

The important milestone of cognitive radio to make it commercially available is by drifting the IEEE 802.22 standard in TV bands to solve connectivity issue such as in the rural broadband services. The recent announcement by FCC and Ofcom to enable spectrum occupancy database temporarily solves the spectrum sensing requirements, so the key issues now have to do with cognitive networks, particularly of the integration of space-time-spectrum databases into cognitive networks. A further research is needed to make such database to be useful in real-time as well as enabled with context-aware functionality. One of the important issue in this approach is the security in the database system. Although some recent research provides the theory on how a cognitive radio can be inherently secure, including smart enough to examine uploads to accept trustable updates from the local spectrum sensors and to reject that are potentially malicious, the foundations have yet to be embraced by the cognitive radio community. Similarly, the access mechanism to such spectrum database by the authentic users is another unsolved research problem which needs further research to propose the robust solution.

The concept of NOMA at the first hand emerged from the concept of dynamic spectrum access in cognitive radio, such as the underlay spectrum sharing scheme between secondary and primary systems. In NOMA, distinct power levels are allocated among the multiple users depending on the channel gain, where communication takes place at the same time frame and frequency subchannels [158]. This concept is similar to the concept of underlay spectrum access where the secondary users transmit even when primary system is using subchannels with the constraint of interference to the primary system is below threshold. Therefore, it can be argued that the advancement in cognitive radio not only improves the spectrum utilization but also assists to initiate new technologies which ultimately enforce to achieve the target of 5G. Further research must be conducted in NOMA implying the similar concepts proposed for CRN.

There are also various research issues to make CRN as an enabling technology for next generation networks. The instances are LTE over CRN to improve the QoS of LTE users and the spectrum handoff mechanism [159] to minimize the

switching delay when secondary system has to communicate (or terminate) on the next available subchannel. Furthermore, the accurate and real-time estimation of primary user activities such that opportunities are not missed by secondary users. The concept of Kalman filter is also considered to be a future work to evaluate the temporal characteristics in the cognitive network, for instance, the primary users activities, for optimal resource allocation. Nevertheless, the future research direction is not only limited to the above mentioned areas but also to explore further as an multi-disciplinary research area.

Appendix A

Proof of Lemma 4.1

Proof. In this proof, equiprobable hypotheses, i.e., the probability of the channel being in idle or busy states are equal, is being considered. Therefore, the probability of accurate channel sensing in the sensing devices is,

$$\mathcal{P}_{cs,i}(\varepsilon_i, T_{s,i}) \triangleq 1 - \left\{ \mathcal{P}_{\mathrm{m,i}}(\varepsilon_i, T_{s,i}) + \mathcal{P}_{\mathrm{f,i}}(\varepsilon_i, T_{s,i}) \right\}, \forall i. \tag{A.1}$$

The cases with no sensing errors, i.e., $\mathcal{P}_{\mathrm{f,i}}(\varepsilon_i, T_{s,i}) = 0$, and $\mathcal{P}_{\mathrm{m,i}}(\varepsilon_i, T_{s,i}) = 0$, are referred to as perfect channel sensing, in such cases $\mathcal{P}_{cs,i}(\varepsilon_i, T_{s,i}) = 1$. However, practically $\mathcal{P}_{cs,i}(\varepsilon_i, T_{s,i}) \in [0, 1]$ which can be obtained by varying the operating points in ROC curve within the range, $\mathcal{P}_{\mathrm{m}}(\varepsilon_i, T_{s,i}) \leq 0.5$, and $\mathcal{P}_{\mathrm{f}}(\varepsilon_i, T_{s,i}) \leq 0.5$, which is also described in detail in (4.7c), (5.17a), and Lemmas 4.6-4.4. In the maximally inaccurate sensing case, i.e., $\mathcal{P}_{\mathrm{m}}(\varepsilon_i, T_{s,i}) = 0.5$, (or $\mathcal{P}_{\mathrm{d}}(\varepsilon_i, T_{s,i}) = 0.5$), and $\mathcal{P}_{\mathrm{f}}(\varepsilon_i, T_{s,i}) = 0.5$, we get $\mathcal{P}_{cs,i}(\varepsilon_i, T_{s,i}) = 0$. Similarly in the perfect sensing case, i.e., $\mathcal{P}_{\mathrm{m}}(\varepsilon_i, T_{s,i}) = 0$, (or $\mathcal{P}_{\mathrm{d}}(\varepsilon_i, T_{s,i}) = 1$), and $\mathcal{P}_{\mathrm{f}}(\varepsilon_i, T_{s,i}) = 0$, we get $\mathcal{P}_{cs,i}(\varepsilon_i, T_{s,i}) = 1$.

The logical AND rule is implemented in the ZAs, based on the sensing information collected from sensing devices. Therefore, the aggregated information is

$\mathcal{P}_{\text{ag,i}} = \prod_{i=1}^{N} \mathcal{P}_{\text{x,i}}$, where $\mathcal{P}_{\text{x,i}}$ is either miss detection or false alarm probability. Therefore, for any channel i,

$$\mathcal{P}_{cs,i}^{(ZA)}(\varepsilon_i, T_{s,i}) = 1 - \left\{ \prod_{z=1}^{Z} \mathcal{P}_{\text{m,i}}(\varepsilon_i, T_{s,i}) + \prod_{z=1}^{Z} \mathcal{P}_{\text{f,i}}(\varepsilon_i, T_{s,i}) \right\}. \tag{A.2}$$

The ZAs then make the spectrum sensing decision for each channel in its corresponding zone based on applying AND rule on the sensing decisions provided by the sensor in their corresponding zone. The obtained information is combined at the SBS such that one channel can be utilized by multiple users within the transmission range of SBS but no adjacent zones are permitted to access the same channels.

Therefore, for possible *micro-spectrum-reuse*, the aggregate information is $\mathcal{P}_{\text{ag,i}} = 1 - \prod_{i=1}^{N}(1 - \mathcal{P}_{\text{y,i}})$, where $\mathcal{P}_{\text{y,i}}$ is either miss detection or false alarm probability for channel i. Consequently, $\mathcal{P}_{\text{ag,i}} = 0$ for $\mathcal{P}_{\text{y,i}} = 0$, $\forall i$ thus (A.2) is written as

$$\mathcal{P}_{cs,i}^{(SBS)} = 1 - \prod_{m=1}^{M} 1 - \left[1 - \prod_{z=1}^{Z} \mathcal{P}_{\text{m,i}}(\varepsilon_i, T_{s,i}) - \prod_{z=1}^{Z} \mathcal{P}_{\text{f,i}}(\varepsilon_i, T_{s,i}) \right]. \tag{A.3}$$

Straightforward mathematical manipulations for independent decisions from ZAs result in the following

$$\mathcal{P}_{cs,i}^{(SBS)} = 1 - \left[\left\{ 1 - \mathcal{P}_{\text{d}}(\varepsilon_i, T_{s,i}) \right\}^{Z} + \left\{ \mathcal{P}_{\text{f}}(\varepsilon_i, T_{s,i}) \right\}^{Z} \right]^{M}, \forall i \tag{A.4}$$

which completes the proof.

Appendix B

Proof of Lemma 4.2

Proof. Starting from $\mathcal{P}_{\mathrm{f}}(\varepsilon_i, T_{s,i}) \leq 0.5$ along with (4.2), we write:

$$\left(\frac{\varepsilon_i}{\sigma_w^2} - 1\right)\sqrt{T_{s,i} f_s} \geq \mathrm{Q}^{-1}(0.5) = 0. \tag{B.1}$$

Since $T_{s,i} f_s > 0$, then $\frac{\varepsilon_i}{\sigma_w^2} - 1 \geq 0$, therefore, $\varepsilon_i \geq \sigma_w^2$.

Similarly, substituting (4.3) in $\mathcal{P}_{\mathrm{m}}(\varepsilon_i, T_{s,i}) \leq 0.5$, results in:

$$\left(\frac{\varepsilon_i}{\sigma_w^2} - \gamma_i - 1\right)\sqrt{\frac{T_{s,i} f_s}{2\gamma_i + 1}} \leq \mathrm{Q}^{-1}(0.5) = 0. \tag{B.2}$$

Since $\frac{T_{s,i} f_s}{2\gamma_i + 1} > 0$, then $\frac{\varepsilon_i}{\sigma_w^2} - \gamma_i - 1 \leq 0$. Therefore, $\varepsilon_i \leq (1 + \gamma_i)\sigma_w^2$.

Appendix C

Proof of Lemma 4.3

Proof. Starting from (4.2), the first derivative of $\mathcal{P}_{\mathrm{f}}(\varepsilon_i, T_{s,i})$ is

$$\frac{\partial \mathcal{P}_{\mathrm{f}}(\varepsilon_i, T_{s,i})}{\partial \varepsilon_i} = -\frac{\sqrt{T_{s,i} f_s}}{\sqrt{2\pi}\sigma_w^2} \exp\left(-\left(\frac{\varepsilon_i}{\sigma_w^2} - 1\right)^2 \frac{T_{s,i} f_s}{2}\right), \tag{C.1}$$

which is always negative; thus, $\mathcal{P}_{\mathrm{f}}(\varepsilon_i, T_{s,i})$ is a decreasing function of ε_i. The second derivative of $\mathcal{P}_{\mathrm{f}}(\varepsilon_i, T_{s,i})$ is

$$\frac{\partial^2 \mathcal{P}_{\mathrm{f}}(\varepsilon_i, T_{s,i})}{\partial^2 \varepsilon_i} = \frac{T_{s,i} f_s}{\sqrt{2\pi}\sigma_w^4} \exp\left(-C_1^2 \frac{T_{s,i} f_s}{2}\right)\left(\frac{\varepsilon_i}{\sigma_w^2} - 1\right), \tag{C.2}$$

where $C_1 = \frac{\varepsilon_i}{\sigma_w^2} - 1$. Since $\sigma_w^2 \leq \varepsilon_i$, the second derivation is always positive; therefore, $\mathcal{P}_{\mathrm{f}}(\varepsilon_i, T_{s,i})$ is a convex function of ε_i.

Appendix D

Proof of Lemma 4.4

Proof. Starting from (4.3), the first derivative of $\mathcal{P}_{\mathrm{d}}(\varepsilon_i, T_{s,i})$ is

$$\frac{\partial \mathcal{P}_{\mathrm{d}}(\varepsilon_i, T_{s,i})}{\partial \varepsilon_i} = -\sqrt{\frac{T_{s,i} f_s}{2\pi(2\gamma_i + 1)}} \frac{1}{\sigma_w^2} \exp\left(-C_2 \frac{T_{s,i} f_s}{2}\right), \tag{D.1}$$

where, $C_2 = \left(\frac{\varepsilon_i}{\sigma_w^2} - \gamma_i - 1\right)^2$. Since $\frac{\partial \mathcal{P}_{\mathrm{d}}(\varepsilon_i, T_{s,i})}{\partial \varepsilon_i} < 0$, and $\mathcal{P}_{\mathrm{m}}(\varepsilon_i, T_{s,i}) = 1 - \mathcal{P}_{\mathrm{d}}(\varepsilon_i, T_{s,i})$, it can be shown by substitution that $\frac{\partial \mathcal{P}_{\mathrm{m}}(\varepsilon_i, T_{s,i})}{\partial \varepsilon_i} > 0$. This also shows that $\mathcal{P}_{\mathrm{m}}(\varepsilon_i, T_{s,i})$ is an increasing function of ε_i.

The second derivative of $\mathcal{P}_{\mathrm{d}}(\varepsilon_i, T_{s,i})$ is

$$\frac{\partial^2 \mathcal{P}_{\mathrm{d}}(\varepsilon_i, T_{s,i})}{\partial^2 \varepsilon_i} = \sqrt{\frac{T_{s,i} f_s}{2\pi(2\gamma_i + 1)}} \frac{1}{\sigma_w^4} \exp\left(-C_3\right) \left(\frac{\varepsilon_i}{\sigma_w^2} - \gamma_i - 1\right), \tag{D.2}$$

where, $C_3 = \left(\frac{\varepsilon_i}{\sigma_w^2} - \gamma_i - 1\right)^2 \frac{T_{s,i} f_s}{2}$. Here, all the terms are positive except $\frac{\varepsilon_i}{\sigma_w^2} - \gamma_i - 1$. However, the inequality $\frac{\varepsilon_i}{\sigma_w^2} - \gamma_i - 1 \leq 0$ holds under the condition $\varepsilon_i \leq (1 + \gamma_i)\sigma_w^2$. Therefore, $\frac{\partial^2 \mathcal{P}_{\mathrm{d}}(\varepsilon_i, T_{s,i})}{\partial^2 \varepsilon_i} < 0$ holds and $\mathcal{P}_{\mathrm{m}}(\varepsilon_i, T_{s,i}) = 1 - \mathcal{P}_{\mathrm{d}}(\varepsilon_i, T_{s,i})$ proves that $\frac{\partial^2 \mathcal{P}_{\mathrm{m}}(\varepsilon_i, T_{s,i})}{\partial^2 \varepsilon_i} > 0$. Consequently, $\mathcal{P}_{\mathrm{m}}(\varepsilon_i, T_{s,i})$ is an increasing and convex function of ε_i. This completes the proof.

Appendix E

Proof of Corollary 4.1

Proof. To prove Corollary 4.1, the probability of channel accurate sensing in (4.10a) is shown to be concave. We start with the scenario, where $Z = M = 1$.

Scenario 1: For $Z = 1$, $M = 1$, and a fixed signalling duration, $\overline{T}_{s,i}$, and frame duration, T, under the stated conditions in Lemma 4.6-Lemma 4.4, the probability of accurate sensing of channel i is a concave function of ε_i.

In this scenario, $\mathcal{P}_{\text{cs,i}}(\varepsilon_i) = 1 - ((1 - \mathcal{P}_{\text{d}}(\varepsilon_i)) + \mathcal{P}_{\text{f}}(\varepsilon_i))$. The second derivative of $\mathcal{P}_{\text{cs,i}}$ is

$$\frac{\partial^2 \mathcal{P}_{\text{cs,i}}(\varepsilon_i, \overline{T}_{s,i})}{\partial^2 \varepsilon_i} = -\frac{\partial^2 \mathcal{P}_{\text{m}}(\varepsilon_i, \overline{T}_{s,i})}{\partial^2 \varepsilon_i} - \frac{\partial^2 \mathcal{P}_{\text{f}}(\varepsilon_i, \overline{T}_{s,i})}{\partial^2 \varepsilon_i}. \tag{E.1}$$

It was already shown that $\frac{\partial^2 \mathcal{P}_{\text{m}}(\varepsilon_i, \overline{T}_{s,i})}{\partial^2 \varepsilon_i} > 0$, and $\frac{\partial^2 \mathcal{P}_{\text{f}}(\varepsilon_i, \overline{T}_{s,i})}{\partial^2 \varepsilon_i} > 0$, therefore $\frac{\partial^2 \mathcal{P}_{\text{cs,i}}(\varepsilon_i, \overline{T}_{s,i})}{\partial^2 \varepsilon_i} < 0$.

Therefore, the second derivative of $\mathcal{P}_{\text{cs,i}}$ is negative $\forall i$, thus it is a concave function of ε_i for which the maximum occurs at optimal detection threshold, ε_i^*.

Scenario 2: Following the same line of argument as in Scenario 1, the probability of accurate sensing of channel i is a concave function of ε_i, for $Z = 2$ and

$M = 1$.

In this scenario, $\mathcal{P}_{\text{cs,i}}(\varepsilon_i) = 1 - ((1 - \mathcal{P}^2_{\text{d}}(\varepsilon_i)) + \mathcal{P}^2_{\text{f}}(\varepsilon_i))$. The second derivative of $\mathcal{P}_{\text{cs,i}}$ is

$$\frac{\partial^2 \mathcal{P}_{\text{cs,i}}(\varepsilon_i, \overline{T}_{s,i})}{\partial^2 \varepsilon_i} = -\frac{\partial^2 \mathcal{P}^2_{\text{m}}(\varepsilon_i, \overline{T}_{s,i})}{\partial^2 \varepsilon_i} - \frac{\partial^2 \mathcal{P}^2_{\text{f}}(\varepsilon_i, \overline{T}_{s,i})}{\partial^2 \varepsilon_i}. \tag{E.2}$$

Now the second derivative of $\mathcal{P}^2_{\text{f,i}}(\varepsilon_i)$ is

$$\begin{aligned}\frac{\partial^2 \mathcal{P}^2_{\text{f}}(\varepsilon_i, T_{s,i})}{\partial \varepsilon_i^2} = &- 2\frac{\sqrt{T_{s,i} f_s}}{\sqrt{2\pi}\sigma_w^2}\left[\exp\left(\frac{-A}{2}\right)\frac{\partial \mathcal{P}_{\text{f}}(\varepsilon_i, T_{s,i})}{\partial \varepsilon_i}\right. \\ &\left. + \overline{\mathcal{P}}_{\text{f}}\frac{\partial}{\partial \varepsilon_i}\left(\exp\left(\frac{-A}{2}\right)\right)\right],\end{aligned} \tag{E.3}$$

where $A = T_{s,i} f_s \left(\frac{\varepsilon_i}{\sigma_w^2} - 1\right)^2$. According to Lemma 4.3, $\frac{\partial \mathcal{P}_{\text{f}}(\varepsilon_i, T_{s,i})}{\partial \varepsilon_i} < 0$; we further notice that for $\overline{\mathcal{P}}_f > 0$ and any $x \neq 0$, $\frac{\partial e^{-x}}{\partial x} < 0$. Using (E.3), we conclude that $\frac{\partial^2 \mathcal{P}^2_f(\varepsilon_i, T_{s,i})}{\partial \varepsilon_i^2} > 0$.

Following the same line of argument as in (E.3), it is straightforward to show that $\frac{\partial^2 \mathcal{P}^2_{\text{d}}(\varepsilon_i, T_{s,i})}{\partial \varepsilon_i^2} > 0$. Substituting $\mathcal{P}^2_{\text{d,i}}(\varepsilon_i) = (1 - \mathcal{P}_{\text{m,i}}(\varepsilon_i))^2$, we then get:

$$\frac{\partial^2 \mathcal{P}^2_{\text{d}}(\varepsilon_i, T_{s,i})}{\partial \varepsilon_i^2} = \left(-2\frac{\partial^2 \mathcal{P}_{\text{m}}(\varepsilon_i, T_{s,i})}{\partial \varepsilon_i^2} + \frac{\partial^2 \mathcal{P}^2_{\text{m}}(\varepsilon_i, T_{s,i})}{\partial \varepsilon_i^2}\right) > 0. \tag{E.4}$$

According to Lemma 4.4, we also have $\frac{\partial^2 \mathcal{P}_{\text{m}}(\varepsilon_i, T_{s,i})}{\partial \varepsilon_i^2} > 0$, therefore we conclude $\frac{\partial^2 \mathcal{P}^2_{\text{m}}(\varepsilon_i, T_{s,i})}{\partial \varepsilon_i^2} > 0$.

From (E.3) and noting that the positive sum of two concave functions is also a concave function, one can conclude that $\frac{\partial^2 \mathcal{P}_{\text{cs,i}}(\varepsilon_i, T_{s,i})}{\partial \varepsilon_i^2} < 0$. It means the probability of accurate sensing is a concave and decreasing function of ε_i.

Scenario 3: Similar to Scenario 1 and 2, the probability of accurate sensing of channel i is concave for $Z = 1$ and $M = 2$. In this case, the probability of

accurate sensing is calculated as below.

$$\begin{aligned}\mathcal{P}_{\mathrm{cs,i}}(\varepsilon_i) &= 1 - \Big[\mathcal{P}_{\mathrm{m}}(\varepsilon_i) + \mathcal{P}_{\mathrm{f}}(\varepsilon_i)\Big]^2 \\ &= 1 - \mathcal{P}^2_{\mathrm{m}}(\varepsilon_1) - 2\mathcal{P}_{\mathrm{m}}(\varepsilon_1)\mathcal{P}_{\mathrm{f}}(\varepsilon_1) - \mathcal{P}^2_{\mathrm{f}}(\varepsilon_1).\end{aligned} \tag{E.5}$$

The second order derivative of (E.5) is

$$\begin{aligned}\frac{\partial^2 \mathcal{P}^2_{\mathrm{cs,i}}(\varepsilon_i)}{\partial \varepsilon_i^2} = &- \frac{\partial^2 \mathcal{P}^2_{\mathrm{m}}(\varepsilon_i)}{\partial \varepsilon_i^2} - 2\overline{\mathcal{P}}_{\mathrm{m}} \frac{\partial^2 \mathcal{P}_{\mathrm{f}}(\varepsilon_i)}{\partial \varepsilon_i^2} \\ &- 2\overline{\mathcal{P}}_{\mathrm{f}} \frac{\partial^2 \mathcal{P}_{\mathrm{m}}(\varepsilon_i)}{\partial \varepsilon_i^2} - \frac{\partial^2 \mathcal{P}^2_{\mathrm{f}}(\varepsilon_i)}{\partial \varepsilon_i^2}.\end{aligned} \tag{E.6}$$

For a fixed signalling duration $\overline{T}_{s,i}$, we already showed that $\frac{\partial^2 \mathcal{P}_{\mathrm{f}}(\varepsilon_i)}{\partial \varepsilon_i^2} > 0$ in Lemma 4.3, $\frac{\partial^2 \mathcal{P}_{\mathrm{m}}(\varepsilon_i)}{\partial \varepsilon_i^2} > 0$ in Lemma 4.4, and $\frac{\partial^2 \mathcal{P}^2_{\mathrm{m}}(\varepsilon_i)}{\partial \varepsilon_i^2} > 0$, and $\frac{\partial^2 \mathcal{P}^2_{\mathrm{f}}(\varepsilon_i)}{\partial \varepsilon_i^2} > 0$ in Scenario 2. Moreover, we note that the maximum acceptable probability of miss detection, and false alarm are bounded as $0 \leq \overline{\mathcal{P}}_{\mathrm{f}} \leq 0.5$, and $0 \leq \overline{\mathcal{P}}_{\mathrm{m}} \leq 0.5$, respectively. Therefore, we can conclude that $\frac{\partial^2 \mathcal{P}^2_{\mathrm{cs,i}}(\varepsilon_i)}{\partial \varepsilon_i^2} < 0$ and is concave function of ε_i, and the maximum value occurs at $\varepsilon_i = \varepsilon_i^*$ which has been obtained in Section 4.4.4.

Scenario 4: Following the same line of argument as in Scenarios 1-3, the probability of accurate sensing of channel i is a concave function of ε_i for $Z = 1$, $M = 3$, as well as $Z = 3$, $M = 1$.

We then argue that the function is concave for the combination of ZAs, i.e., $n_1 = 2$ and $n_2 = n_1 + 1$ and SBSs, i.e., $n_3 = 2$ and $n_4 = n_3 + 1$ and it also holds for $n_1 = 1$ and $n_3 = 1$. It means that it must be also true for any possible combination of natural numbers of ZAs and SBSs according to the principal of mathematical induction.

References

[1] A. Al-Fuqaha, M. Guizani, M. Mohammadi, M. Aledhari, and M. Ayyash, "Internet of things: A survey on enabling technologies, protocols, and applications," *IEEE Communications Surveys Tutorials*, vol. 17, no. 4, pp. 2347–2376, Fourthquarter 2015. (Page 1).

[2] M. Weyrich, J. P. Schmidt, and C. Ebert, "Machine-to-machine communication," *IEEE Software*, vol. 31, no. 4, pp. 19–23, July 2014. (Page 1).

[3] Cisco Inc., "Cisco virtual networking index," *White Paper at www.cisco.com*, Feb 2014. (Pages 1, 4).

[4] W. H. Chin, Z. Fan, and R. Haines, "Emerging technologies and research challenges for 5G wireless networks," *IEEE Wireless Communications*, vol. 21, no. 2, pp. 106–112, April 2014. (Page 1).

[5] J. G. Andrews, S. Buzzi, W. Choi, S. V. Hanly, A. Lozano, A. C. K. Soong, and J. C. Zhang, "What will 5G be?" *IEEE Journal on Selected Areas in Communications*, vol. 32, no. 6, pp. 1065–1082, June 2014. (Page 1).

[6] F. Boccardi, R. W. Heath, A. Lozano, T. L. Marzetta, and P. Popovski, "Five disruptive technology directions for 5G," *IEEE Communications Magazine*, vol. 52, no. 2, pp. 74–80, February 2014. (Page 2).

[7] V. Jungnickel, K. Manolakis, W. Zirwas, B. Panzner, V. Braun, M. Lossow, M. Sternad, R. Apelfrojd, and T. Svensson, "The role of small cells, coordinated multipoint, and massive MIMO in 5G," *IEEE Communications Magazine*, vol. 52, no. 5, pp. 44–51, May 2014. (Page 2).

[8] E. Hossain, M. Rasti, H. Tabassum, and A. Abdelnasser, "Evolution toward 5G multi-tier cellular wireless networks: An interference management perspective," *IEEE Wireless Communications*, vol. 21, no. 3, pp. 118–127, 2014. (Page 2).

[9] T. 3rd Generation Partnership Project, "Lte-advanced," *Release-11*, 2013, (Accessed on: April-2014). [Online]. Available: http://www.3gpp.org/technologies/keywords-acronyms/97-lte-advanced (Page 2).

[10] A. A. Atayero, O. I. Adu, and A. A. Alatishe, "Self organizing networks for 3GPP LTE," in *International Conference on Computational Science and Its Applications*. Springer, 2014, pp. 242–254. (Page 2).

[11] S. Sun, Q. Gao, Y. Peng, Y. Wang, and L. Song, "Interference management through CoMP in 3GPP LTE-advanced networks," *IEEE Wireless Communications*, vol. 20, no. 1, pp. 59–66, February 2013. (Page 3).

[12] Qualcomm Inc., "LTE MTC: Optimizing LTE Advanced for machine-type communications," *White Paper at www.qualcom.com*, Feb 2014, (Accessed on: 10-Dec-2015). [Online]. Available: https://www.qualcomm.com/documents/lte-mtc-optimizing-lte-advanced-machine-type-communications (Page 3).

[13] C. S. Park, L. Sundstrm, A. Walln, and A. Khayrallah, "Carrier aggregation for LTE-advanced: design challenges of terminals," *IEEE Communications Magazine*, vol. 51, no. 12, pp. 76–84, December 2013. (Page 3).

[14] Qualcomm Inc., "LTE advanced carrier aggregation," *White Paper at www.qualcom.com*, 2016, (Accessed on: 24-Mar-2016). [Online]. Available: https://www.qualcomm.com/invention/technologies/lte/lte-carrier-aggregation (Page 3).

[15] Federal Communications Commission, "Spectrum policy task force report," *FCC 02-155*, 2002. (Pages 4, 8).

[16] Q. Zhao and B. M. Sadler, "A survey of dynamic spectrum access," *IEEE signal processing magazine*, vol. 24, no. 3, pp. 79–89, 2007. (Page 4).

[17] S. Haykin, "Cognitive radio: brain-empowered wireless communications," *IEEE Journal on Selected Areas in Communications*, vol. 23, no. 2, pp. 201–220, 2005. (Pages 4, 8).

[18] FCC ET, "Docket no 03-222 notice of proposed rule making and order," 2003. (Pages 4, 8).

[19] R. Menon, R. Buehrer, and J. Reed, "On the impact of dynamic spectrum sharing techniques on legacy radio systems," *IEEE Transactions on Wireless Communications*, vol. 7, no. 11, pp. 4198–4207, 2008. (Page 5).

[20] A. Ghasemi and E. Sousa, "Fundamental limits of spectrum-sharing in fading environments," *IEEE Transactions on Wireless Communications*, vol. 6, no. 2, pp. 649–658, 2007. (Page 5).

[21] X. Kang, R. Zhang, Y.-C. Liang, and H. K. Garg, "Optimal power allocation strategies for fading cognitive radio channels with primary user outage constraint," *IEEE Journal on Selected Areas in Communications*, vol. 29, no. 2, pp. 374–383, 2011. (Page 5).

[22] M. Khoshkholgh, K. Navaie, and H. Yanikomeroglu, "Access strategies for spectrum sharing in fading environment: Overlay, underlay, and mixed," *IEEE Transactions on Mobile Computing*, vol. 9, no. 12, pp. 1780–1793, 2010. (Pages 5, 46, 55, 88).

[23] M. T. Masonta, M. Mzyece, and N. Ntlatlapa, "Spectrum decision in cognitive radio networks: A survey," *IEEE Communications Surveys & Tutorials*, vol. 15, no. 3, pp. 1088–1107, 2013. (Page 5).

[24] T. Yucek and H. Arslan, "A survey of spectrum sensing algorithms for cognitive radio applications," *IEEE Communications Suevey & Tutorials*, vol. 11, no. 1, pp. 116–130, 2009. (Pages 5, 20).

[25] I. F. Akyildiz, W.-Y. Lee, M. C. Vuran, and S. Mohanty, "Next generation/dynamic spectrum access/cognitive radio wireless networks: A survey," *Computer Networks*, vol. 50, no. 13, pp. 2127 – 2159, 2006. [Online]. Available: http://www.sciencedirect.com/science/article/pii/S1389128606001009 (Page 6).

[26] D. T. Ngo, C. Tellambura, and H. H. Nguyen, "Resource allocation for OFDMA-based cognitive radio multicast networks with primary user activity consideration," *IEEE Transactions on Vehicular Technology*, vol. 59, no. 4, pp. 1668–1679, May 2010. (Page 6).

[27] L. Zhang, Y. Xin, Y.-C. Liang, and H. Poor, "Cognitive multiple access channels: optimal power allocation for weighted sum rate maximization," *IEEE Transactions on Communications*, vol. 57, no. 9, pp. 2754–2762, 2009. (Pages 6, 11, 91, 95).

[28] D. Xu, E. Jung, and X. Liu, "Efficient and fair bandwidth allocation in multichannel cognitive radio networks," *IEEE Transactions on Mobile Computing*, vol. 11, no. 8, pp. 1372–1385, 2012. (Page 6).

[29] G. Bansal, M. Hossain, V. Bhargava, and T. Le-Ngoc, "Subcarrier and power allocation for ofdma-based cognitive radio systems with joint overlay and underlay spectrum access mechanism," *IEEE Transactions on Vehicular Technology*, vol. 62, no. 3, pp. 1111–1122, 2013. (Pages 6, 88, 89, 94, 111).

[30] F. Sheikholeslami, M. Nasiri-Kenari, and F. Ashtiani, "Optimal probabilistic initial and target channel selection for spectrum handoff in cognitive radio networks," *IEEE Transactions on Wireless Communications*, vol. 14, no. 1, pp. 570–584, 2015. (Pages 6, 11).

[31] L. C. Wang, C. W. Wang, and C. J. Chang, "Optimal target channel sequence design for multiple spectrum handoffs in cognitive radio networks," *IEEE Transactions on Communications*, vol. 60, no. 9, pp. 2444–2455, September 2012. (Page 6).

[32] J. Mitola and G. Q. Maguire, "Cognitive radio: making software radios more personal," *IEEE Personal Communications*, vol. 6, no. 4, pp. 13–18, Aug 1999. (Page 7).

[33] J. Mitola, "Cognitive radio-an integrated agent architecture for software defined radio," *Royal Institute of Technology (KTH)*, 2000. (Page 7).

[34] M. Nekovee, "A survey of cognitive radio access to TV white spaces," in *2009 International Conference on Ultra Modern Telecommunications Workshops*, Oct 2009, pp. 1–8. (Page 9).

[35] "IEEE 802.22 WRAN WG," http://www.ieee802.org/22/, 2012, (Accessed on: October-2013). (Pages 9, 57, 58, 60, 63, 65, 74).

[36] X. Hong, J. Wang, C. X. Wang, and J. Shi, "Cognitive radio in 5G: a perspective on energy-spectral efficiency trade-off," *IEEE Communications Magazine*, vol. 52, no. 7, pp. 46–53, July 2014. (Page 9).

[37] A. Ghasemi and E. S. Sousa, "Spectrum sensing in cognitive radio networks: requirements, challenges and design trade-offs," *IEEE Communications Magazine*, vol. 46, no. 4, pp. 32–39, April 2008. (Page 10).

[38] A. B. Flores, R. E. Guerra, E. W. Knightly, P. Ecclesine, and S. Pandey, "Ieee 802.11af: a standard for tv white space spectrum sharing," *IEEE Communications Magazine*, vol. 51, no. 10, pp. 92–100, October 2013. (Page 10).

[39] P. Paysarvi-Hoseini and N. Beaulieu, "On the benefits of multichannel/wideband spectrum sensing with non-uniform channel sensing durations for cognitive radio networks," *IEEE Transactions on Communications*, vol. 60, no. 9, pp. 2434–2443, September 2012. (Page 10).

[40] E. Axell, G. Leus, E. G. Larsson, and H. V. Poor, "Spectrum sensing for cognitive radio: State-of-the-art and recent advances," *IEEE Signal Processing Magazine*, vol. 29, no. 3, pp. 101–116, 2012. (Pages 10, 21, 31).

[41] E. Peh, Y.-C. Liang, Y. L. Guan, and Y. Zeng, "Cooperative spectrum sensing in cognitive radio networks with weighted decision fusion schemes," *IEEE Transactions on Wireless Communications*, vol. 9, no. 12, pp. 3838–3847, December 2010. (Pages 10, 47).

[42] D. Xue, E. Ekici, and M. C. Vuran, "Cooperative spectrum sensing in cognitive radio networks using multidimensional correlations," *IEEE Transactions on Wireless Communications*, vol. 13, no. 4, pp. 1832–1843, April 2014. (Pages 10, 47, 47).

[43] Y.-C. Liang, Y. Zeng, E. Peh, and A. T. Hoang, "Sensing-throughput tradeoff for cognitive radio networks," *IEEE Transactions on Wireless Communications*, vol. 7, no. 4, pp. 1326–1337, 2008. (Pages 10, 46, 47, 55, 60, 62).

[44] K. W. Choi and E. Hossain, "Estimation of primary user parameters in cognitive radio systems via hidden markov model," *IEEE Transactions on Signal Processing*, vol. 61, no. 3, pp. 782–795, 2013. (Page 11).

[45] B. Canberk, I. Akyildiz, and S. Oktug, "Primary user activity modeling using first-difference filter clustering and correlation in cognitive radio networks," *IEEE/ACM Transactions of Networking*, vol. 19, no. 1, pp. 170–183, 2011. (Page 11).

[46] M. Ashour, A. A. El-Sherif, T. ElBatt, and A. Mohamed, "Cognitive radio networks with probabilistic relaying: stable throughput and delay tradeoffs," *IEEE Transactions on Communications*, vol. 63, no. 11, pp. 4002–4014, 2015. (Pages 11, 29).

[47] Y. Wang, P. Ren, F. Gao, and Z. Su, "A hybrid underlay/overlay transmission mode for cognitive radio networks with statistical quality-of-service provisioning," *IEEE Transactions on Communications*, vol. 13, no. 3, pp. 1482–1498, March 2014. (Pages 11, 111).

[48] H. ElSawy, E. Hossain, and M. Haenggi, "Stochastic geometry for modeling, analysis, and design of multi-tier and cognitive cellular wireless networks:

A survey," *IEEE Communications Surveys & Tutorials*, vol. 15, no. 3, pp. 996–1019, 2013. (Page 11).

[49] I. Macaluso, D. Finn, B. Ozgul, and L. A. DaSilva, "Complexity of spectrum activity and benefits of reinforcement learning for dynamic channel selection," *IEEE Journal on Selected Areas in Communications*, vol. 31, no. 11, pp. 2237–2248, November 2013. (Page 11).

[50] E. E. Yaacoub and Z. Dawy, "Centralized multicell scheduling with interference mitigation," *Resource Allocation in Uplink OFDMA Wireless Systems: Optimal Solutions and Practical Impl.*, pp. 173–201, 2012. (Page 11).

[51] F. Haider, C.-X. Wang, H. Haas, E. Hepsaydir, X. Ge, and D. Yuan, "Spectral and energy efficiency analysis for cognitive radio networks," *IEEE Transactions on Wireless Communications*, vol. 14, no. 6, pp. 2969–2980, 2015. (Page 11).

[52] F. Zhou, N. C. Beaulieu, Z. Li, J. Si, and P. Qi, "Energy-efficient optimal power allocation for fading cognitive radio channels: Ergodic capacity, outage capacity, and minimum-rate capacity," *IEEE Transactions on Wireless Communications*, vol. 15, no. 4, pp. 2741–2755, 2016. (Page 11).

[53] S. Stotas and A. Nallanathan, "Optimal sensing time and power allocation in multiband cognitive radio networks," *IEEE Transactions on Communications*, vol. 59, no. 1, pp. 226–235, 2011. (Pages 11, 41, 46, 62).

[54] Ofcom, "Digital dividend: cognitive access statement on licence-exempting cognitive devices using interleaved spectrum," *Ofcom Statement*, July 2009, (Accessed on: July-2013). [Online]. Available: http://stakeholders.ofcom.org.uk/binaries/consultations/cognitive/statement/statement.pdf (Page 13).

[55] ——, "TV white spaces: A consultation on white space device requirements," *Ofcom Statement*, November 2012, (Accessed on: August-2013). [Online]. Available: http://stakeholders.ofcom.org.uk/binaries/consultations/whitespaces/summary/condoc.pdf (Page 14).

[56] Huawei Inc., "Mitigating interference between LTE and GSM/UMTS networks," *Huawei Report*, 2012, (Accessed on: 10-Nov-2013). [Online]. Available: http://www1.huawei.com/enapp/198/hw-079474.htm (Page 14).

[57] H. N. Tran, K. Ishizu, and F. Kojima, "Evaluation of channel availability for mobile device by using a TV white space database qualified by the ofcom," in *2015 IEEE 81st Vehicular Technology Conference (VTC Spring)*, May 2015, pp. 1–6. (Page 21).

[58] H. Urkowitz, "Energy detection of unknown deterministic signals," *Proceedings of the IEEE*, vol. 55, no. 4, pp. 523–531, 1967. (Page 22).

[59] D. Cabric, S. M. Mishra, and R. W. Brodersen, "Implementation issues in spectrum sensing for cognitive radios," in *Signals, systems and computers, 2004. Conference record of the thirty-eighth Asilomar conference on*, vol. 1. IEEE, 2004, pp. 772–776. (Pages 22, 26).

[60] E. Axell and E. G. Larsson, "Optimal and sub-optimal spectrum sensing of OFDM signals in known and unknown noise variance," *IEEE Journal on Selected Areas in Communications*, vol. 29, no. 2, pp. 290–304, 2011. (Page 22).

[61] R. Tandra and A. Sahai, "SNR walls for signal detection," *IEEE Journal of selected topics in Signal Processing*, vol. 2, no. 1, pp. 4–17, 2008. (Pages 23, 25).

[62] F. Salahdine, H. E. Ghazi, N. Kaabouch, and W. F. Fihri, "Matched filter detection with dynamic threshold for cognitive radio networks," in *Wireless Networks and Mobile Communications (WINCOM), 2015 International Conference on*, Oct 2015, pp. 1–6. (Page 25).

[63] X. Zhang, F. Gao, R. Chai, and T. Jiang, "Matched filter based spectrum sensing when primary user has multiple power levels," *China Communications*, vol. 12, no. 2, pp. 21–31, Feb 2015. (Page 25).

[64] R. Tandra and A. Sahai, "Fundamental limits on detection in low SNR under noise uncertainty," in *2005 International Conference on Wireless Networks, Communications and Mobile Computing*, vol. 1. IEEE, 2005, pp. 464–469. (Page 25).

[65] P. D. Sutton, J. Lotze, K. E. Nolan, and L. E. Doyle, "Cyclostationary signature detection in multipath rayleigh fading environments," in *2007 2nd International Conference on Cognitive Radio Oriented Wireless Networks and Communications*. IEEE, 2007, pp. 408–413. (Page 26).

[66] J. Lundén, V. Koivunen, A. Huttunen, and H. V. Poor, "Collaborative cyclostationary spectrum sensing for cognitive radio systems," *IEEE Transactions on Signal Processing*, vol. 57, no. 11, pp. 4182–4195, 2009. (Page 26).

[67] J. K. Tugnait and G. Huang, "Cyclic autocorrelation based spectrum sensing in colored gaussian noise," in *2012 IEEE Wireless Communications and Networking Conference (WCNC)*, April 2012, pp. 731–736. (Page 26).

[68] W. A. Gardner, "Exploitation of spectral redundancy in cyclostationary signals," *IEEE Signal Processing Magazine*, vol. 8, no. 2, pp. 14–36, 1991. (Page 26).

[69] M. Feng, T. Jiang, D. Chen, and S. Mao, "Cooperative small cell networks: High capacity for hotspots with interference mitigation," *IEEE Wireless Communications*, vol. 21, no. 6, pp. 108–116, 2014. (Page 27).

[70] J. Shen, S. Liu, L. Zeng, G. Xie, J. Gao, and Y. Liu, "Optimisation of cooperative spectrum sensing in cognitive radio network," *IET communications*, vol. 3, no. 7, pp. 1170–1178, 2009. (Page 27).

[71] D. Cabric, A. Tkachenko, and R. W. Brodersen, "Spectrum sensing measurements of pilot, energy, and collaborative detection," in *MILCOM 2006-2006 IEEE Military Communications conference*. IEEE, 2006, pp. 1–7. (Page 27).

[72] C. Sun, W. Zhang, and K. B. Letaief, "Cluster-based cooperative spectrum sensing in cognitive radio systems," in *2007 IEEE International Conference on Communications*. IEEE, 2007, pp. 2511–2515. (Page 29).

[73] R. Gao, Z. Li, P. Qi, and H. Li, "A robust cooperative spectrum sensing method in cognitive radio networks," *IEEE Communications Letters*, vol. 18, no. 11, pp. 1987–1990, 2014. (Page 29).

[74] D. Teguig, B. Scheers, and V. L. Nir, "Data fusion schemes for cooperative spectrum sensing in cognitive radio networks," in *Communications and Information Systems Conference (MCC), 2012 Military*, Oct 2012, pp. 1–7. (Page 30).

[75] D. M. S. Bhatti and H. Nam, "Correlation based soft combining scheme for cooperative spectrum sensing in cognitive radio networks," in *2014 IEEE 79th Vehicular Technology Conference (VTC Spring)*, May 2014, pp. 1–5. (Page 30).

[76] S. M. Mishra, A. Sahai, and R. W. Brodersen, "Cooperative sensing among cognitive radios," in *2006 IEEE International Conference on Communications*, vol. 4, June 2006, pp. 1658–1663. (Page 30).

[77] L. Lu, X. Zhou, U. Onunkwo, and G. Y. Li, "Ten years of research in spectrum sensing and sharing in cognitive radio," *EURASIP Journal on Wireless Communications and Networking*, vol. 2012, no. 1, p. 1, 2012. (Page 31).

[78] Q. Wu, G. Ding, J. Wang, X. Li, and Y. Huang, "Consensus-based decentralized clustering for cooperative spectrum sensing in cognitive radio networks," *Chinese Science Bulletin*, vol. 57, no. 28, pp. 3677–3683, 2012. [Online]. Available: http://dx.doi.org/10.1007/s11434-012-5074-6 (Page 31).

[79] B. Wang and K. J. R. Liu, "Advances in cognitive radio networks: A survey," *IEEE Journal of Selected Topics in Signal Processing*, vol. 5, no. 1, pp. 5–23, Feb 2011. (Page 32).

[80] W.-Y. Lee and I. Akyildiz, "Optimal spectrum sensing framework for cognitive radio networks," *IEEE Transactions on Wireless Communications*, vol. 7, no. 10, pp. 3845–3857, 2008. (Page 33).

[81] W. Han, J. Li, Z. Tian, and Y. Zhang, "Dynamic sensing strategies for efficient spectrum utilization in cognitive radio networks," *IEEE Transactions on Wireless Communications*, vol. 10, no. 11, pp. 3644–3655, 2011. (Page 33).

[82] Y. Pei, Y.-C. Liang, K. Teh, and K. H. Li, "How much time is needed for wideband spectrum sensing?" *IEEE Transactions on Wireless Communications*, vol. 8, no. 11, pp. 5466–5471, 2009. (Pages 33, 41).

[83] Y. Chen, "Analytical performance of collaborative spectrum sensing using censored energy detection," *IEEE Transactions on Wireless Communications*, vol. 9, no. 12, pp. 3856–3865, 2010. (Page 33).

[84] S. Maleki, A. Pandharipande, and G. Leus, "Energy-efficient distributed spectrum sensing for cognitive sensor networks," *IEEE Sensors Journal*, vol. 11, no. 3, pp. 565–573, 2011. (Pages 33, 54).

[85] E. Pei, H. Han, Z. Sun, B. Shen, and T. Zhang, "LEAUCH: low-energy adaptive uneven clustering hierarchy for cognitive radio sensor network," *EURASIP Journal on Wireless Communications and Networking*, vol. 2015, no. 1, pp. 1–8, 2015. (Page 33).

[86] D. Willkomm, S. Machiraju, J. Bolot, and A. Wolisz, "Primary users in cellular networks: A large-scale measurement study," in *New frontiers in dynamic spectrum access networks, 2008. DySPAN 2008. 3rd IEEE symposium on*. IEEE, 2008, pp. 1–11. (Pages 35, 89).

[87] B. Golkar and E. S. Sousa, "Resource allocation in autonomous cellular networks," *IEEE Transactions on Wireless Communications*, vol. 12, no. 11, pp. 5572–5583, 2013. (Page 36).

[88] M. Monemi, M. Rasti, and E. Hossain, "On joint power and admission control in underlay cellular cognitive radio networks," *IEEE Transactions on Wireless Communications*, vol. 14, no. 1, pp. 265–278, 2015. (Page 36).

[89] H. A. Mahmoud, T. Yucek, and H. Arslan, "OFDM for cognitive radio: merits and challenges," *IEEE wireless communications*, vol. 16, no. 2, pp. 6–15, 2009. (Page 38).

[90] J. Mao, G. Xie, J. Gao, and Y. Liu, "Energy efficiency optimization for OFDM-based cognitive radio systems: A water-filling factor aided search method," *IEEE Transactions on Wireless Communications*, vol. 12, no. 5, pp. 2366–2375, 2013. (Page 38).

[91] K. G. M. Thilina, E. Hossain, and M. Moghadari, "Cellular ofdma cognitive radio networks: Generalized spectral footprint minimization," *IEEE Transactions on Vehicular Technology*, vol. 64, no. 7, pp. 3190–3204, July 2015. (Page 38).

[92] M. E. Sahin, I. Guvenc, and H. Arslan, "Opportunity detection for ofdma-based cognitive radio systems with timing misalignment," *IEEE Transactions on Wireless Communications*, vol. 8, no. 10, pp. 5300–5313, October 2009. (Page 38).

[93] Z. Wang, L. Jiang, and C. He, "Optimal price-based power control algorithm in cognitive radio networks," *IEEE Transactions on Wireless Communications*, vol. 13, no. 11, pp. 5909–5920, 2014. (Page 39).

[94] J. Zou, H. Xiong, D. Wang, and C. W. Chen, "Optimal power allocation for hybrid overlay/underlay spectrum sharing in multiband cognitive radio networks," *IEEE Transactions on Vehicular Technology*, vol. 62, no. 4, pp. 1827–1837, 2013. (Pages 41, 88).

[95] H. Shi, R. V. Prasad, V. S. Rao, I. Niemegeers, and M. Xu, "Spectrum-and energy-efficient D2DWRAN," *IEEE Communications Magazine*, vol. 52, no. 7, pp. 38–45, 2014. (Page 42).

[96] C.-S. Sum, G. P. Villardi, M. A. Rahman, T. Baykas, H. N. Tran, Z. Lan, C. Sun, Y. Alemseged, J. Wang, C. Song *et al.*, "Cognitive communication in TV white spaces: An overview of regulations, standards, and technology [accepted from open call]," *IEEE Communications Magazine*, vol. 51, no. 7, pp. 138–145, 2013. (Page 42).

[97] H. B. Yilmaz, T. Tugcu, F. Alagz, and S. Bayhan, "Radio environment map as enabler for practical cognitive radio networks," *IEEE Communications Magazine*, vol. 51, no. 12, pp. 162–169, December 2013. (Page 44).

[98] M. Caleffi and A. S. Cacciapuoti, "Database access strategy for TV white space cognitive radio networks," in *Sensing, Communication, and Networking Workshops (SECON Workshops), 2014 Eleventh Annual IEEE International Conference on*, June 2014, pp. 34–38. (Page 44).

[99] ——, "Optimal database access for TV white space," *IEEE Transactions on Communications*, vol. 64, no. 1, pp. 83–93, 2016. (Page 44).

[100] M. Khoshkholgh, K. Navaie, and H. Yanikomeroglu, "Optimal design of the spectrum sensing parameters in the overlay spectrum sharing," *IEEE Transactions on Mobile Computing*, vol. PP, no. 99, pp. 1–1, 2013. (Page 47, 47).

[101] A. Ghasemi and E. Sousa, "Collaborative spectrum sensing for opportunistic access in fading environments," in *New Frontiers in Dynamic Spectrum Access Networks, 2005. DySPAN 2005. 2005 First IEEE International Symposium on*, Nov 2005, pp. 131–136. (Pages 47, 48).

[102] H. Zhuang, Z. Luo, J. Zhang, and Y. Li, "Cooperative sensor solution to enhancing the performance of spectrum sensing," in *Communications and Networking in China (CHINACOM), 2010 5th International ICST Conf. on*, Aug 2010, pp. 1–6. (Page 47).

[103] H. Yu, W. Tang, and S. Li, "Optimization of multiple-channel cooperative spectrum sensing with data fusion rule in cognitive radio networks," *Journal of Electronics (China)*, vol. 29, no. 6, pp. 515–522, 2012. (Page 47, 47).

[104] Y. Abdi and T. Ristaniemi, "Joint local quantization and linear cooperation in spectrum sensing for cognitive radio networks," *IEEE Transactions on Signal Processing*, vol. 62, no. 17, pp. 4349–4362, Sept 2014. (Page 47).

[105] I. F. Akyildiz, B. F. Lo, and R. Balakrishnan, "Cooperative spectrum sensing in cognitive radio networks: A survey," *Physical Communication*, vol. 4, no. 1, pp. 40–62, Mar. 2011. (Pages 47, 48).

[106] W. Lin, Y. Wang, and W. Ni, "Cluster-based cooperative spectrum sensing in two-layer hierarchical cognitive radio networks," in *Global Comm. Conf. (GLOBECOM), 2013 IEEE*, Dec 2013, pp. 1082–1087. (Page 47).

[107] W. Zhang, Y. Yang, and C. K. Yeo, "Cluster-based cooperative spectrum sensing assignment strategy for heterogeneous cognitive radio network," *IEEE Transactions on Vehicular Technology*, vol. 64, no. 6, pp. 2637–2647, June 2015. (Page 47).

[108] C. G. Tsinos and K. Berberidis, "Decentralized adaptive eigenvalue-based spectrum sensing for multiantenna cognitive radio systems," *IEEE Transactions on Wireless Communications*, vol. 14, no. 3, pp. 1703–1715, March 2015. (Page 48).

[109] Y. Han, S. H. Ting, and A. Pandharipande, "Cooperative spectrum sharing protocol with secondary user selection," *IEEE Transactions on Wireless Communications*, vol. 9, no. 9, pp. 2914–2923, September 2010. (Page 48, 48).

[110] J. Lai, E. Dutkiewicz, R. Liu, and R. Vesilo, "Opportunistic spectrum access with two channel sensing in cognitive radio networks," *IEEE Transactions on Mobile Computing*, vol. PP, no. 99, pp. 1–1, 2013. (Page 48).

[111] I. Nevat, G. W. Peters, and I. B. Collings, "Location-aware cooperative spectrum sensing via gaussian processes," in *Communications Theory Workshop (AusCTW), 2012 Australian*, Jan 2012, pp. 19–24. (Page 48).

[112] M. Monemian and M. Mahdavi, "Analysis of a new energy-based sensor selection method for cooperative spectrum sensing in cognitive radio networks," *IEEE Sensors Journal*, vol. 14, no. 9, pp. 3021–3032, Sept 2014. (Page 49).

[113] Y. Selen, H. Tullberg, and J. Kronander, "Sensor selection for cooperative spectrum sensing," in *New Frontiers in Dynamic Spectrum Access Networks, DySPAN 2008. 3rd IEEE Symposium on*, Oct 2008, pp. 1–11. (Page 49).

[114] Y. Li, K. K. Chai, Y. Chen, and J. Loo, "Duty cycle control with joint optimisation of delay and energy efficiency for capillary machine-to-machine networks in 5G communication system," *Transactions on Emerging Telecomm. Tech.*, vol. 26, no. 1, pp. 56–69, 2015. (Page 49).

[115] B. Mercier, V. Fodor, R. Thobaben, M. Skoglund, V. Koivunen, S. Lindfors, J. Ryynänen, E. G. Larsson, C. PetriolI, G. Bongiovanni *et al.*, "Sensor networks for cognitive radio: Theory and system design," *ICT mobile summit*, 2008. (Page 49, 49).

[116] O. Grondalen, M. Lahteenoja, and P. Gronsund, "Evaluation of business cases for a cognitive radio network based on wireless sensor network," in *New Frontiers in Dynamic Spectrum Access Networks (DySPAN), 2011 IEEE Symposium on*, May 2011, pp. 242–253. (Page 49).

[117] N. Hasan, W. Ejaz, S. Lee, and H. Kim, "Knapsack-based energy-efficient node selection scheme for cooperative spectrum sensing in cognitive radio sensor networks," *IET Communications*, vol. 6, no. 17, pp. 2998–3005, November 2012. (Page 49).

[118] K. Letaief and W. Zhang, "Cooperative communications for cognitive radio networks," *Proceedings of the IEEE*, vol. 97, no. 5, pp. 878–893, May 2009. (Page 54).

[119] H. Cramér, *Mathematical methods of statistics*. Princeton university press, 1999, vol. 9. (Page 55).

[120] S. Atapattu, C. Tellambura, and H. Jiang, "Analysis of area under the ROC curve of energy detection," *IEEE Transactions on Wireless Communications*, vol. 9, no. 3, pp. 1216–1225, March 2010. (Page 56).

[121] A. Singh, M. Bhatnagar, and R. Mallik, "Cooperative spectrum sensing in multiple antenna based cognitive radio network using an improved energy detector," *IEEE Communications Letters*, vol. 16, no. 1, pp. 64–67, 2012. (Pages 61, 62, 95).

[122] P. Paysarvi-Hoseini and N. Beaulieu, "Optimal wideband spectrum sensing framework for cognitive radio systems," *IEEE Transactions on Signal Processing*, vol. 59, no. 3, pp. 1170–1182, March 2011. (Pages 63, 67).

[123] R. Fan and H. Jiang, "Optimal multi-channel cooperative sensing in cognitive radio networks," *IEEE Transactions on Wireless Communications*, vol. 9, no. 3, pp. 1128–1138, March 2010. (Page 64).

[124] Z.-Q. Luo and W. Yu, "An introduction to convex optimization for communications and signal processing," *IEEE Journal on Selected Areas in Communications*, vol. 24, no. 8, pp. 1426–1438, Aug 2006. (Page 66).

[125] S. P. Boyd and L. Vandenberghe, *Convex optimization*. Cambridge university press, 2004. (Pages 66, 66, 67, 104, 105).

[126] W. Wang, B. Kasiri, J. Cai, and A. S. Alfa, "Channel assignment schemes for cooperative spectrum sensing in multi-channel cognitive radio networks," *Wireless Communications and Mobile Computing*, vol. 15, no. 10, pp. 1471–1484, 2015. (Page 76).

[127] M. Khoshkholgh, K. Navaie, and H. Yanikomeroglu, "Achievable capacity in hybrid DS-CDMA/OFDM spectrum-sharing," *IEEE Transactions on Mobile Computing*, vol. 9, no. 6, pp. 765–777, June 2010. (Page 87).

[128] K. Shashika Manosha, N. Rajatheva, and M. Latva-aho, "Overlay/underlay spectrum sharing for multi-operator environment in cognitive radio networks," in *Vehicular Technology Conference (VTC Spring), 2011 IEEE 73rd*, 2011, pp. 1–5. (Page 88).

[129] H. Hu, H. Zhang, and Y. Liang, "On the spectrum- and energy-efficiency tradeoff in cognitive radio networks," *IEEE Transactions on Communications*, vol. 64, no. 2, pp. 490–501, Feb 2016. (Pages 88, 119).

[130] C. Han, T. Harrold, S. Armour, I. Krikidis, S. Videv, P. M. Grant, H. Haas, J. Thompson, I. Ku, C.-X. Wang, T. A. Le, M. Nakhai, J. Zhang, and L. Hanzo, "Green radio: radio techniques to enable energy-efficient wireless networks," *IEEE Transactions on Communications*, vol. 49, no. 6, pp. 46–54, June 2011. (Page 88).

[131] X. Hong, J. Wang, C. X. Wang, and J. Shi, "Cognitive radio in 5G: a perspective on energy-spectral efficiency trade-off," *IEEE Transactions on Communications*, vol. 52, no. 7, pp. 46–53, July 2014. (Page 88).

[132] R. Amin, J. Martin, J. Deaton, L. A. DaSilva, A. Hussien, and A. Eltawil, "Balancing spectral efficiency, energy consumption, and fairness in future heterogeneous wireless systems with reconfigurable devices," *IEEE Journal on Selected Areas in Communications*, vol. 31, no. 5, pp. 969–980, 2013. (Page 88).

[133] L. Liu, R. Zhang, and K.-C. Chua, "Achieving global optimality for weighted sum-rate maximization in the K-user gaussian interference channel with multiple antennas," *IEEE Transactions on Wireless Communications*, vol. 11, no. 5, pp. 1933–1945, 2012. (Pages 88, 91).

[134] X. Tan, H. Zhang, and J. Hu, "Achievable transmission rate of the secondary user in cognitive radio networks with hybrid spectrum access strategy," *IEEE Communications Letters*, vol. 17, no. 11, pp. 2088–2091, 2013. (Page 89).

[135] L. Wang, M. Sheng, Y. Zhang, X. Wang, and C. Xu, "Robust energy efficiency maximization in cognitive radio networks: The worst-case optimization approach," *IEEE Transactions on Communications*, vol. 63, no. 1, pp. 51–65, Jan 2015. (Page 89).

[136] A. Alabbasi, Z. Rezki, and B. Shihada, "Energy efficient resource allocation for cognitive radios: A generalized sensing analysis," *IEEE Transactions on Wireless Communications*, vol. 14, no. 5, pp. 2455–2469, May 2015. (Pages 89, 107).

[137] S. Wang, W. Shi, and C. Wang, "Energy-efficient resource management in OFDM-based cognitive radio networks under channel uncertainty," *IEEE Transactions on Communications*, vol. 63, no. 9, pp. 3092–3102, Sept 2015. (Page 89).

[138] W. Zhang, C. Wang, D. Chen, and H. Xiong, "Energy-spectral efficiency tradeoff in cognitive radio networks," *IEEE Transactions on Vehicular Technologies*, vol. PP, no. 99, pp. 1–1, 2015. (Pages 89, 119).

[139] F. Kelly, "Charging and rate control for elastic traffic," *European Transactions on Telecommunication*, vol. 8, no. 1, pp. 33–37, 1997. (Page 90).

[140] M. Katoozian, K. Navaie, and H. Yanikomeroglu, "Utility-based adaptive radio resource allocation in OFDM wireless networks with traffic prioritization," *IEEE Transactions on Wireless Communications*, vol. 8, no. 1, pp. 66–71, Jan 2009. (Pages 90, 101).

[141] J. Kaleva, A. Tolli, and M. Juntti, "Weighted sum rate maximization for interfering broadcast channel via successive convex approximation," in *Proc. IEEE GLOBECOM 2012*, 2012, pp. 3838–3843. (Page 91).

[142] N. Mokari, K. Navaie, and M. Khoshkholgh, "Downlink radio resource allocation in ofdma spectrum sharing environment with partial channel state information," *IEEE Transactions on Wireless Communications*, vol. 10, no. 10, pp. 3482–3495, 2011. (Pages 91, 94, 102, 102).

[143] W. Zhang, C. K. Yeo, and Y. Li, "A MAC sensing protocol design for data transmission with more protection to primary users," *IEEE Transactions on Mobile Computing*, vol. 12, no. 4, pp. 621–632, April 2013. (Page 96).

[144] W. Yu and R. Lui, "Dual methods for nonconvex spectrum optimization of multicarrier systems," *IEEE Transactions on Communications*, vol. 54, no. 7, pp. 1310–1322, July 2006. (Page 104).

[145] D. Palomar and M. Chiang, "A tutorial on decomposition methods for network utility maximization," *IEEE Journal on Selected Areas in Communications*, vol. 24, no. 8, pp. 1439–1451, 2006. (Page 105).

[146] A. Charnes and W. W. Cooper, "Programming with linear fractional functionals," *Naval Research Logistics Quarterly*, vol. 9, no. 3-4, pp. 181–186, 1962. [Online]. Available: http://dx.doi.org/10.1002/nav.3800090303 (Page 107).

[147] L. Wang, M. Sheng, X. Wang, Y. Zhang, and X. Ma, "Mean energy efficiency maximization in cognitive radio channels with PU outage constraint," *IEEE Communications Letters*, vol. 19, no. 2, pp. 287–290, Feb 2015. (Page 108).

[148] D. Ng, E. Lo, and R. Schober, "Energy-efficient resource allocation in multicell OFDMA systems with limited backhaul capacity," *IEEE Transactions on Wireless Communications*, vol. 11, no. 10, pp. 3618–3631, October 2012. (Page 108).

[149] W. Dinkelbach, "On nonlinear fractional programming," *Management Science*, vol. 13, no. 7, pp. pp. 492–498, 1967. [Online]. Available: http://www.jstor.org/stable/2627691 (Page 108).

[150] H. Peng and T. Fujii, "Hybrid overlay/underlay resource allocation for cognitive radio networks in user mobility environment," in *Vehicular Technology Conference (VTC Fall), 2013 IEEE 78th*, Sept 2013, pp. 1–6. (Page 111).

[151] S. Senthuran, A. Anpalagan, and O. Das, "Throughput analysis of opportunistic access strategies in hybrid underlay/overlay cognitive radio networks," *IEEE Transactions on Communications*, vol. 11, no. 6, pp. 2024–2035, June 2012. (Page 111).

[152] Q. C. Li, H. Niu, A. T. Papathanassiou, and G. Wu, "5G network capacity: key elements and technologies," *IEEE Vehicular Technology Magazine*, vol. 9, no. 1, pp. 71–78, 2014. (Page 126).

[153] C. X. Wang, F. Haider, X. Gao, X. H. You, Y. Yang, D. Yuan, H. M. Aggoune, H. Haas, S. Fletcher, and E. Hepsaydir, "Cellular architecture and key technologies for 5G wireless communication networks," *IEEE Communications Magazine*, vol. 52, no. 2, pp. 122–130, February 2014. (Page 126).

[154] A. Aijaz and A. H. Aghvami, "Cognitive machine-to-machine communications for internet-of-things: A protocol stack perspective," *IEEE Internet of Things Journal*, vol. 2, no. 2, pp. 103–112, April 2015. (Page 126).

[155] Z. Ma, Z. Zhang, Z. Ding, P. Fan, and H. Li, "Key techniques for 5G wireless communications: network architecture, physical layer, and MAC layer perspectives," *Science China Information Sciences*, vol. 58, no. 4, pp. 1–20, 2015. (Page 126).

[156] M. N. Tehrani, M. Uysal, and H. Yanikomeroglu, "Device-to-device communication in 5G cellular networks: challenges, solutions, and future directions," *IEEE Communications Magazine*, vol. 52, no. 5, pp. 86–92, 2014. (Page 126).

[157] A. Alexiou, "Wireless World 2020: Radio interface challenges and technology enablers," *IEEE Vehicular Technology Magazine*, vol. 9, no. 1, pp. 46–53, 2014. (Page 126).

[158] H. Tabassum, M. S. Ali, E. Hossain, M. Hossain, D. I. Kim *et al.*, "Non-orthogonal multiple access (NOMA) in cellular uplink and downlink: Challenges and enabling techniques," *arXiv preprint arXiv:1608.05783*, 2016. (Page 127).

[159] C. Zhang and K. G. Shin, "What should secondary users do upon incumbents' return?" *IEEE Journal on Selected Areas in Communications*, vol. 31, no. 3, pp. 417–428, 2013. (Page 127).